Christina Gleixner, BSc

Methionine restriction in life and death leads to higher vacuolar acidification levels in *Saccharomyces cerevisiae*

MASTERARBEIT

zur Erlangung des akademischen Grades

Master of Science

Masterstudium Molekulare Mikrobiologie

eingereicht an der

Technischen Universität Graz

Betreuer

Univ.-Prof. Dr.rer.nat. Kai-Uwe Fröhlich

Institut für Molekulare Biowissenschaften

Mag. Dr.rer.nat. Rudolf-Christoph Ruckenstuhl

Graz, Mai 2014

Der Fortgang der wissenschaftlichen Entwicklung ist im Endeffekt eine ständige Flucht vor dem Staunen.

Albert Einstein

Für meine Eltern

EIDESSTATTLICHE ERKLÄRUNG
AFFIDAVIT

Ich erkläre an Eides statt, dass ich die vorliegende Arbeit selbstständig verfasst, andere als die angegebenen Quellen/Hilfsmittel nicht benutzt, und die den benutzten Quellen wörtlich und inhaltlich entnommenen Stellen als solche kenntlich gemacht habe. Das in TUGRAZonline hochgeladene Textdokument ist mit der vorliegenden Masterarbeit identisch.

I declare that I have authored this thesis independently, that I have not used other than the declared sources/resources, and that I have explicitly indicated all material which has been quoted either literally or by content from the sources used. The text document uploaded to TUGRAZonline is identical to the present master's thesis.

Graz, 25.05.2014
Datum / Date

Christina Gleissner, BSc
Unterschrift / Signature

Danksagung

Zuerst möchte ich mich bei Univ.-Prof. Dr. rer. nat. Kai-Uwe Fröhlich für die Möglichkeit in seiner Arbeitsgruppe zu arbeiten bedanken. Ein weiteres Dankeschön auch für die gemeinsamen Kuchenrunden, die für mich immer sehr lustig, unterhaltsam und fröhlich waren.

Einen ganz großen Dank auch an Dr. rer. nat. Christoph Ruckenstuhl für die tolle Betreuung im Labor. Danke für deine Geduld, Unterstützung und Motivation.

Ein weiteres herzliches Dankschön auch an Ulli, Silvia, Lydia und Gertrude, die mir viele gute Tipps gegeben haben und von denen ich auch viel lernen durfte. Im Besonderen möchte ich mich bei Silvia für die Hilfe bei den Überlebensplattierungen bedanken.

Danke auch an alle Kollegen aus dem Erdgeschoß für das gute Arbeitsklima, die lustigen Pokerrunden und Pizzaabenden. Ein großes Danke an die Perlen: Steffi, Steffi, Jelena, Marion und Kathi für die gemeinsamen Salatrunden, die die Zeit im Labor eindeutig verschönert haben. Zusätzlich möchte ich mich bei Kathi bedanken: Du hast mir die Zeit im Studium eindeutig zur besten Zeit meines Lebens gemacht! Danke für die lustigen Mädelsabende und die langen Fortgehnächte. Danke auch, dass du mir während des ganzen Studiums unterstützend zur Seite gestanden bist!

Vielen Dank auch meinem Patrick! Du hast mich während meines ganzen Studiums unterstützt. Danke, dass du während des ganzen letzten Jahres, insbesondere in den letzten zwei Monaten meine Gefühlsschwankungen ausgehalten hast. Ohne dich wäre mein Laptop bestimmt irgendwann aus dem Fenster geflogen. Ich bin sehr froh, dass ich dich habe!

Der größte Dank gilt aber meinen Eltern. Mama, Papa, danke für eure Unterstützung, euer Verständnis und euren Rückhalt. Ihr seit immer für mich da und habt auch immer ein offenes Ohr für mich. Ihr habt immer an mich und meine Träume geglaubt. Einen großen Dank dafür! Ich hab euch lieb!

Abstract

The sulphur-containing proteinogenic amino acid methionine is one of the most important amino acids in different cellular processes in eukaryotic and prokaryotic cells. These processes include protein biosynthesis, the synthesis of glutathione, spermine, and spermidine as well as methylation reactions. It has been already reported that methionine restriction, a reduced supply of methionine, leads to life span extension in different species. The results of this master thesis support the hypothesis, that methionine restriction promotes longevity in *Saccharomyces cerevisiae* depending on an autophagy initiated vacuolar acidification. The methionine auxotrophic yeast strain *Bya MET15 Δmet2* shows more cells with an acidic vacuole in media without methionine compared to cells growing in media with 3 mg/l or 30 mg/l methionine. This effect is autophagy dependent as a deletion of *ATG5* decreases the rate of cells with an acidic vacuole. Further, an overexpression of the genes *VMA1* and *VPH2* of the vacuolar proton pump (v-ATPase) leads to an enhanced vacuolar acidification. However, autophagy mediated acidification of the vacuole might not only promote life span extension. Presumably, too high levels of autophagy trigger a specific type of cell death when under complete methionine restriction, in which the cells display high acidification throughout the whole cell. Further it seems that in this cell death mechanism protein phosphatase 2A (PP2A) and *SCH9* are involved, but not classical ER stress response mechanisms.

Kurzzusammenfassung

Die schwefelhaltige proteinogene Aminosäure Methionin ist eine der wichtigsten Aminosäuren bei verschiedenen zellulären Prozessen in eukaryotischen und prokaryotischen Zellen. Zu diesen Prozessen zählen die Proteinbiosynthese, die Synthese von Glutathion, Spermin und Spermidin sowie Methylierungsreaktionen. Es wurde bereits beschrieben, dass eine reduzierte Methioninzufuhr (Methioninrestriktion), einen lebensverlängernden Effekt auf verschiedene Spezies hat. Die Ergebnisse dieser Masterarbeit zeigen, dass Methioninrestriktion das Leben von *Saccharomyces cerevisiae* in Abhängigkeit von einer durch Autophagie ausgelösten vakuolären Azidität verlängert. Der Methionin auxotrophe Bäckerhefestamm *Bya MET15 Δmet2* zeigt im Medium ohne Methionin mehr Zellen mit einer sauren Vakuole, als *Bya MET15 Δmet2* Zellen, die im Medium mit 3 mg/l oder 30 mg/l Methionin wachsen. Dieser Effekt ist abhängig von Autophagie, da es durch Deletion von *ATG5* zu einer Reduzierung der Zellen mit saurer Vakuole kommt. Weiters führt eine Überexpression der Gene, *VMA1* und *VPH2*, der vakuolären Protonenpumpen (v-ATPasen) zu einer Erhöhung der vakuolären Azidität. Allerdings ist die durch Autophagie hervorgerufene Ansäuerung der Vakuole nicht nur lebensverlängernd. Zu hohe Level an Autophagie lösen unter kompletter Methioninrestriktion einen spezifischen Zelltod aus. Die Ursache dafür ist eine Übersäuerung der Zelle. Außerdem scheint es, dass an diesem Zelltod die Protein Phosphatase 2A (PP2A) und *SCH9* beteiligt sind. Allerdings kann eine Beteiligung von ER Stress nicht nachgewiesen werden.

TABLE OF CONTENTS

1. Introduction

1.1 Yeast as a model organism

The unicellular eukaryotic organism *Saccharomyces cerevisiae* possess a 12 MB genome, which is encoded by 6000 genes. 1996 it was sequenced by Goffeau et al. There are several databases about budding yeast obtainable, which include information about the genome and proteins, protein-protein interaction, genetic interactions, protein functions and predicted orthologous in other organisms.

S. cerevisiae is easy to cultivate and research on yeast is relatively cheap. This yeast strain can proliferate in diploid and haploid state.
Biochemical and genetic manipulations in yeast are easy and quick, as *S. cerevisiae* possess a doubling time of 90 minutes on rich media. Further genetically manipulations such as gene deletion, yeast transformation and homologous recombination for the integration of genes from other organisms are easy to perform.

There are many orthologous between several mechanisms and biological pathways between higher eukaryotes and yeast like cell cycle, intracellular transport or cellular control systems. There are basic mechanisms and pathways for example in neurodegenerations (like mitochondrial dysfunction, trafficking defects, proteasomal dysfunction or transcriptional dysregulation) or in apoptosis (such as ROS generation, chromatin condensation or phosphatidylserine externalisation) that are conserved between yeast and humans. Therefore budding yeast is effectively used for studying fundamental cell processes of higher eukaryotes. However, there are also some cellular components missing in *S. cerevisiae* and therefore it is required to validate the observations in yeast in other model organisms such as flies, worms or mice. (Gershon et al. 2000; Miller-Fleming et al. 2008)

1.2 Autophagy

Autophagy is the molecular process of self-degradation, which is important for survival, development, differentiation and homeostasis (balance between synthesis and degradation of protein, ribosomes, organelles and nucleic acids) of cells. Autophagy possesses a dual role in cell survival and death.

During starvation and under stress (like growth factor depletion, hypoxia or ER-stress) autophagy is enhanced. Autophagy plays a critical role in maintaining molecular synthesis, ATP production and protein and fatty acid synthesis. Further autophagy is involved in processes during intracellular stress such as accumulation of abnormal protein aggregates, damage or superfluous and intracellular pathogenesis. Autophagy eliminates damaged proteins during oxidative stress.

Autophagic cell death appears for example during developmental periods that requires massive cell elimination.

To high levels of autophagy lead to diseases such as neurodegenerative disorder. In contrast to this to low level of autophagy causes diseases like cancer.

There are different types of autophagy (see Figure 1.1): macroautophagy, microautophagy, chaperone-mediated autophagy (does not occur in yeast), mitophagy (mitochondria mediated autophagy), pexophagy (peroxisome mediated autophagy) and reticulophagy (ER mediated autophagy). They differ in the way, how the proteins and organelles are transported into the lysosome/vacuole. (Kourtis et al. 2008; Suzuki et al. 2007; Tsujimoto et al. 2005)

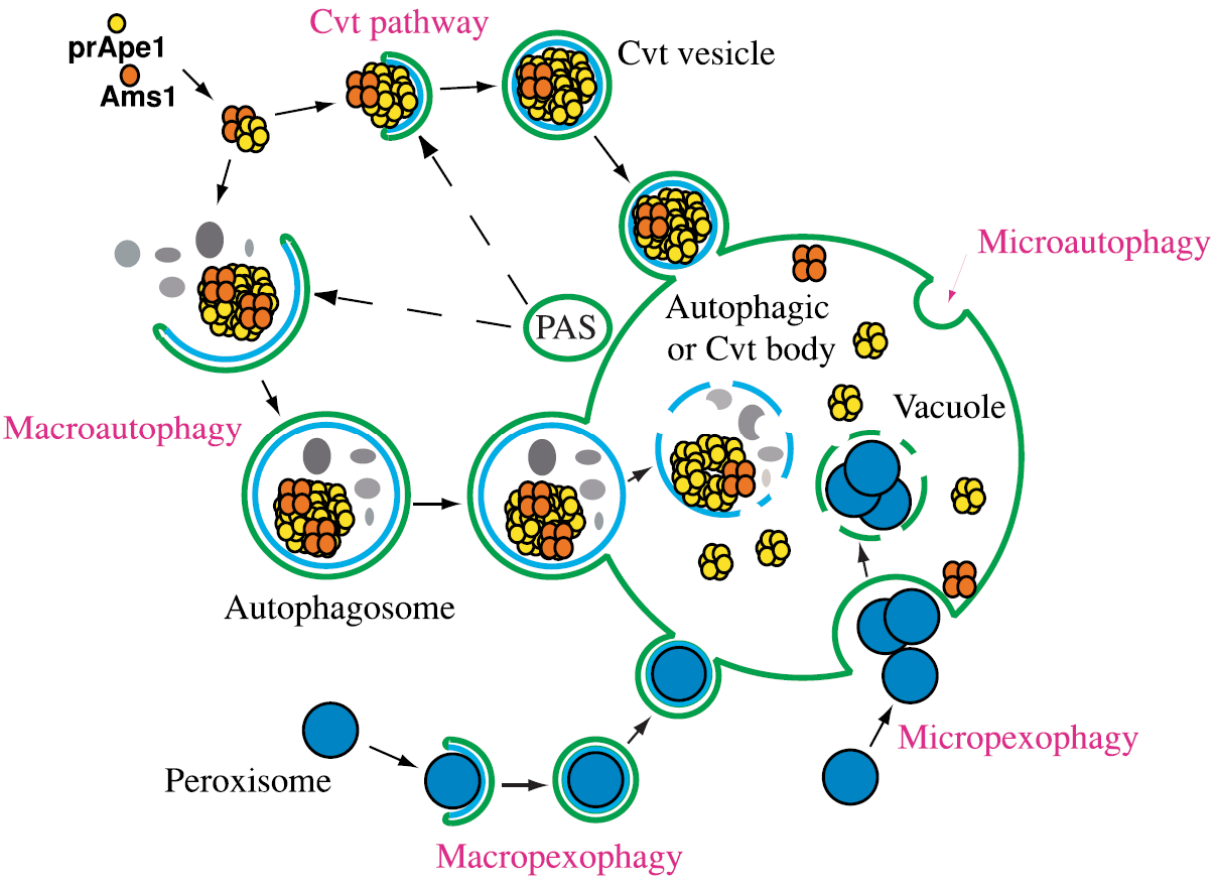

Figure 1.1: Different pathways of autophagy. For the formation of Cvt (cytoplasm-to-vacuole targeting) vesicles and the autophagosome the PAS (pre-autophagosomal structure) are required. Autophagosomes are formed by macroautophagy during nutrient starvation. Both the autophagosome and the Cvt vesicles fuse with the membrane of the lysosome/vacuole and release their content into the lumen. During microautophagy and micorpexophagy (peroxisome mediated autophagy) the lysosome/vacuole includes their aim directly through a contraction of the membrane. Macropexophagy, which is another type of peroxisome mediated autophagy, occurs after a shift from peroxisome including conditions to a preferred carbon source. (Huang et al. 2002)

1.2.1 Macroautophagy

Macroautophagy, which is often referred as autophagy, can be divided into eight steps. Autophagy occurs through detecting starvation signals. In the next step these signals are transmitted to the autophagosome generating apparatus, the PAS (pre-autophagosomal structure). From the PAS an isolation membrane (IM) is generated. The IM is expanded and the ends of the membrane fuse for the formation of the autophagosome. The outer membrane of the lysosome/vacuole and the outer membrane of the autophagosome fuses and the autophagic body is released into the lumen of the lysosome/vacuole. The autophagic body is generated from the inner membrane of the autophagosome. Next the autophagic bodies are decomposed and the vacuolar hydrolases degrade its content. In the last step the resulting amino acids

and lipids are transported into the cytoplasm, where they are used for novel protein synthesis. (Suzuki et al. 2007)
In these step several *ATG* (autophagy-related) genes are involved. (see Figure 1.2) One of the central regulators of autophagy is the serine/threonine kinase TOR (target of rapamycin). Under nutrient rich conditions TOR is active and hyperphosphorylates Atg13p. During starvation TOR is inactive and Atg13p is dephosphorylated. The dephosphorylated Atg13p binds to Atg1p, a serine/threonine kinase, and forms an Atg1p-Atg13p-Atg17p complex. Together with Atg17p this complex leads to the induction of autophagy.

The autophagosome formation is initiated at the PAS. The vesicle nucleation is performed by the PI3K (phosphatidylinositol 3-kinase) complex, which is composed of Atg6p, protein kinase Vps15p and phosphatidylinositol 3-kinase Vsp34. This complex is necessary for the formation of the phosphoinositol-3-phosphat, which recruits Atg proteins to the PAS. The association of these Atg proteins to the PAS leads to the formation of the phagophore, the initial autophagosomal vesicle.
The membrane is expanded around the material, which has to be degraded. Therefore PE (phosphatidyl ethanolamine) is added to the ubiquitin-like protein Atg8. The C-terminus of Atg8p is proteolytically processed by Atg4p and lapidated by Atg3p and Atg7p. Atg8p-PE binds to the outer and inner membrane of the autophagosome, which depends on the Atg12p-Atg5p conjugate. The conjugation of the ubiquitin-like protein Atg12p to Atg5p is generated by Atg7p and Atg10p. Next the Atg12p-Atg5p-Atg16p complex is formed.

After the conclusion of the outer membrane of the autophagosome, Atg8p is removed of the surface of the autophagosome by the protease Atg4p. Atg8p of the inner membrane is degradated in the vacuole. Further the Atg12p-Atg5p-Atg16p complex, which is localized on the surface of the autophagosome, is recycled to the PAS. The integral membrane protein Atg9 is recycled to the PAS too. This reaction is generated by Atg1p, Atg2p and Atg18p.

For the fusion of the outer membrane of the autophagosome with the vacuolar membrane the SNARE proteins (Vam3, Vam7, Vti1 and Ykt6), the class C Vps proteins

complex, known as HOPS complex (homotypic fusion and vacuole protein sorting), and the GTPase Ypt7 are required.
After the fusion of the outer membrane of the autophagosome with the membrane of the vacuole, the autophagic body and its content are degraded by Cvt17/Atg15p, the proteinase A and B and vacuolar hydrolases. The resulting amino acids and lipids are released into the cytoplasm, where they are used for the novel protein biosynthesis.
(He et al. 2009; Huang et al.2002; Nair et al. 2005; Suzuki et al. 2007; Tang et al. 2008; Todde et al. 2009)

1.2.2 Cvt pathway

The cytoplasm-to-vacuole targeting (Cvt) pathway (see Figure 1.2) occurs under nutrient rich conditions. At the moment it is not known to exist in other organisms than in yeast. The vacuolar hydrolases, aminopeptidase 1 (Ape1) and the α-mannosidase (Ams1) are necessary in this pathway, as they are sequestered into the Cvt vesicle. Although the autophagosome and the Cvt vesicle originate from the PAS and possess a similar morphology, there are differences in the size between these vesicles. The Cvt vesicles are much smaller than the autophagosome.

The precursor of the Ape1, the preApe1, is synthesized in the cytosol, where it forms a dodecamer. The dodecamer forms an oligomere, the Ape1 complex. The receptor protein Atg19 binds to both, the Ape1 and the Ams1. This complex is sequestered within the Cvt vesicle. Atg11p binds the C-terminus of Atg19p. The complex of preApe1, Atg11p and Atg19p is required for the formation of the PAS. Atg19p interacts with Atg8p-PE at the PAS. The Atg19p-Atg8p-PE complex leads to the formation of the mature Cvt vesicle. Afterwards the vesicle is transported to the vacuole, where the outer membrane of the vesicle fuses with the membrane of the vacuole. Next the inner membrane of the Cvt vesicle and its cargo is released into the lumen of the vacuole. However, Atg11p is recycled and not delivered into the vacuole. Further Atg8p-PE from the surface of the outer membrane of the vesicle is recycled too by a cleavage via Atg4p. In contrast Atg8p-PE of the inner membrane and the Atg19p are degraded in the vacuole.
Under nutrient rich conditions TOR is active and inhibits autophagy, as Atg13p is hyperphosphorylated and the affinity of Atg13p for Atg1p is reduced. The interaction between Atg1p and Atg13p seems to be important for the switch from the Cvt path-

way and autophagy. Under nutrient rich conditions, the kinase activity of Atg1p is enhanced and the cargos are degraded via the Cvt pathway.

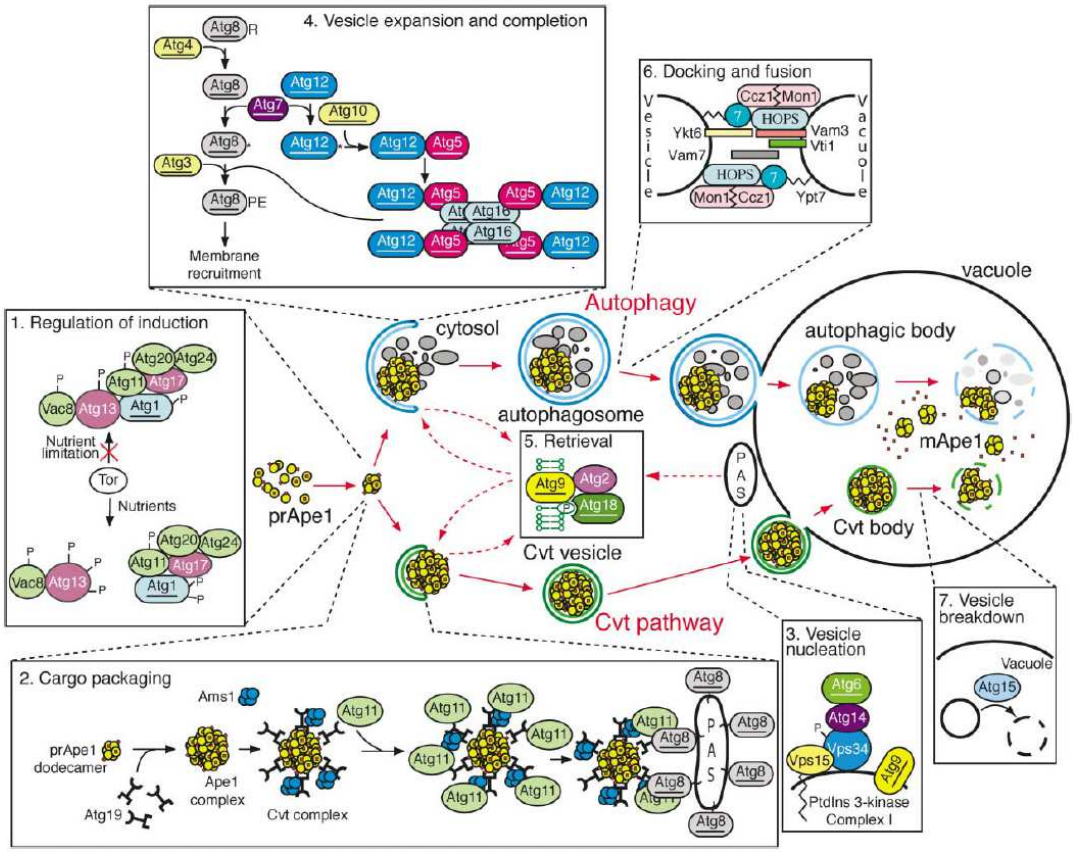

Figure 1.2: Macroautophagy and the Cvt pathway with their involved proteins. Some of the molecular mechanisms are overlapping in these two pathways. Atg1p is involved in both pathways. However, it interacts with different factors. The most important steps during autophagy and the Cvt pathway are: **1. Regulation of induction.** TOR is the main regulator of these two pathways. Under nutrient rich conditions TOR is active and hyperphosphorylates Atg13p, which leads to a decreased affinity for the kinase Atg1p (inhibition of autophagy and active Cvt pathway). In both pathways Atg1p acts with different proteins. **2. Cargo packaging.** During the Cvt pathway the preApe1 dodecamers forms oligomers, which interacts with the receptor Atg19p. Next this complex binds Atg11p. The preApe1-Atg19p-Atg11p complex transports the cargo together with the Atg8p-PE to the PAS. **3. Vesicle nucleation.** The PI3K (Vps34) forms the complex I, which is required for both, autophagy and the Cvt pathway. This complex is necessary to generate phosphatidylinositol-3-phosphat at the PAS. **4. Vesicle expansion.** During autophagy the ubiquitin-like Atg8p, which is activated by Atg7p, conjugates to PE. This complex recruits to the PAS membrane. Further Atg7p activates the ubiquitin-like Atg12p, which next conjugates to Atg5p. The Atg12p-Atg5p complex binds Atg16p. As Atg16p forms an oligomer, which then forms a multimeric complex. Atg3p and Atg10p are conjugation enzymes and Atg4p is a protease. **5. Retrieval.** To complete the autophagosome or the Cvt vesicle Atg8p is required. During the process of vesicle formation, proteins cycle on and off the membrane. However, for the removal of the integral membrane protein Atg9p, Atg2p and Atg19p are essential. **6. Docking and fusion.** For the fusion of the autophagosome and the Cvt vesicle with the vacuole several components are required. For example Ccz1 and Mon1 are essential for the docking of the vesicle to the vacuole. **7. Vesicle breakdown.** Once the autophagic body and the Cvt vesicle are transported into the lumen of the vacuole, the lipase Atg15p is required for the breakdown of the Cvt vesicle and the autophagic body. (Levine et al. 2004)

1.3 Regulation of autophagy

Autophagy in *S. cerevisiae* as well as in higher eukaryotes is regulated by stress response, such as nutrient starvation, hypoxia, inflammation, heat response as well as high salt concentrations. *TOR*, *SCH9* (homologue to the mammalian *PKB* (protein kinase B)), *PP2A* (protein phosphatase 2A), *PKA* (protein kinase A) and *Snf1* (sucrose non-fermenting; homologue of the mammalian *AMPK* (AMP activated kinase)) are all part of the signalling pathways, which are involved in the autophagy regulation (see Figure 1.3). (Fontana et al. 2010; Hedbacker et al. 2009; Kapahi et al. 2010; Mc Ewan et al. 2011; Wullschleger et al. 2006)

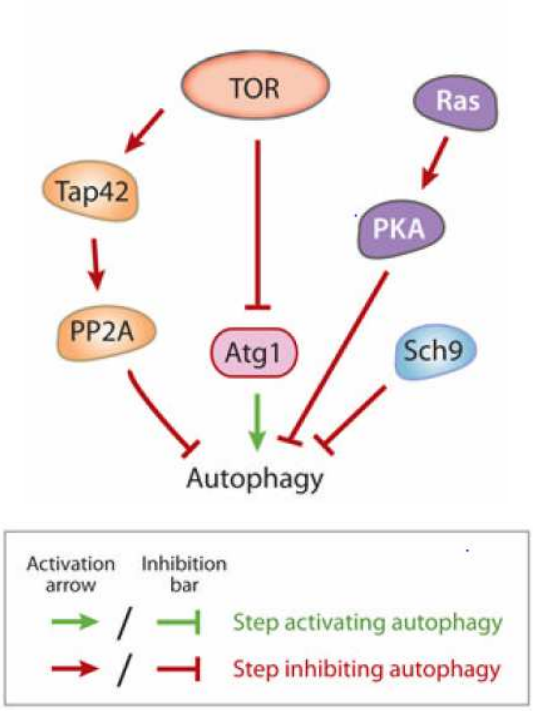

Figure 1.3: Signalling pathways of autophagy in yeast. *TOR, RAS/PKA* and *SCH9* are negative regulators of autophagy. Under nutrient rich conditions *TOR* and *RAS* are active. *TOR* negatively regulates autophagy via the inhibition of Atg1p and by activating *Tap42*. *Tap42* binds to *PP2A*, which further inhibits autophagy. In contrast to *TOR*, *RAS* activates *PKA*. The activated *PKA* negatively regulates autophagy. The third negative regulator of autophagy is *SCH9*, which is active under nutrient rich conditions too. (He et al. 2009)

The target of rapamycin (*TOR*), which is a serine/threonine kinase, is a negative regulator of autophagy, as it phosphorylates Atg13p, which reduces its affinity to Atg1p. TOR is a nutrient sensor kinase that regulates cell growth and proliferation via protein synthesis. In *S. cerevisiae TOR* consists out of two complexes, the *TOR* complex 1 (*TORC1*) and the *TOR* complex 2 (*TORC2*). *TORC1* is known to affect autophagy, mRNA translation, ribosome biogenesis as well as cell growth, survival, size and pro-

liferation. In contrast to *TORC2*, *TORC1* is rapamycin sensitive (rapamycin is an immunosuppressive macrolide, which is produced of the bacterium *Streptomyces hygroscopicus* from the Easter Island Rapa Nui). Rapamycin inhibits *TORC1* by forming a complex with FKBP12, which is a FK506 binding protein. Therefore FKBP12 is not able to bind to the C-terminal FRB (FKBP12 rapamycin binding) region of *TOR* protein.
TORC2 influences the cell cycle-dependent proliferation of the actin cytoskeleton. (Hay et al. 2004; Kapahi et al. 2010; McEwan et al. 2011; Wullschleger et al. 2006)

The activity of *TOR* is regulated upstream via growth factors. The binding of insulin or insulin-like-growth factor (IGF) leads to a recruitment of *PI3K* and *Akt* (=*PKB*; homologue of *SCH9*), which is a serine/threonine kinase. By phosphorylating *Akt*, TSC complex (tuberous sclerosis complex) is inactivated. *TSC* is a negative regulator of mTOR (mammalian TOR), as it is a GTPase activating protein (GAP) for the small GTPase Rheb, which is able to activate mTOR. However; *S. cerevisiae* does not possess homologues for TSC complex and Rheb. Therefore it is suggested that the activation of *TOR* in yeast is amino acid induced. (Hay et al. 2004; Wullschleger et al. 2006)

TORC1 has two downstream effectors, *SCH9* and *Tap42* (see Figure 1.4). *SCH9* is a protein kinase, which is homologue of the mammalian *S6K* and *Akt*. *Tap42* regulates the *PP2A*. Under nutrient rich conditions the activated *TORC1* phosphorylates *Tap42*. The phosphorylated *Tap42* binds the catalytic subunit of *PP2A*. Both *SCH9* and the Tap42-PP2A dimer are negative regulators of autophagy. (Urban et al. 2007; Zabrocki et al. 2002)

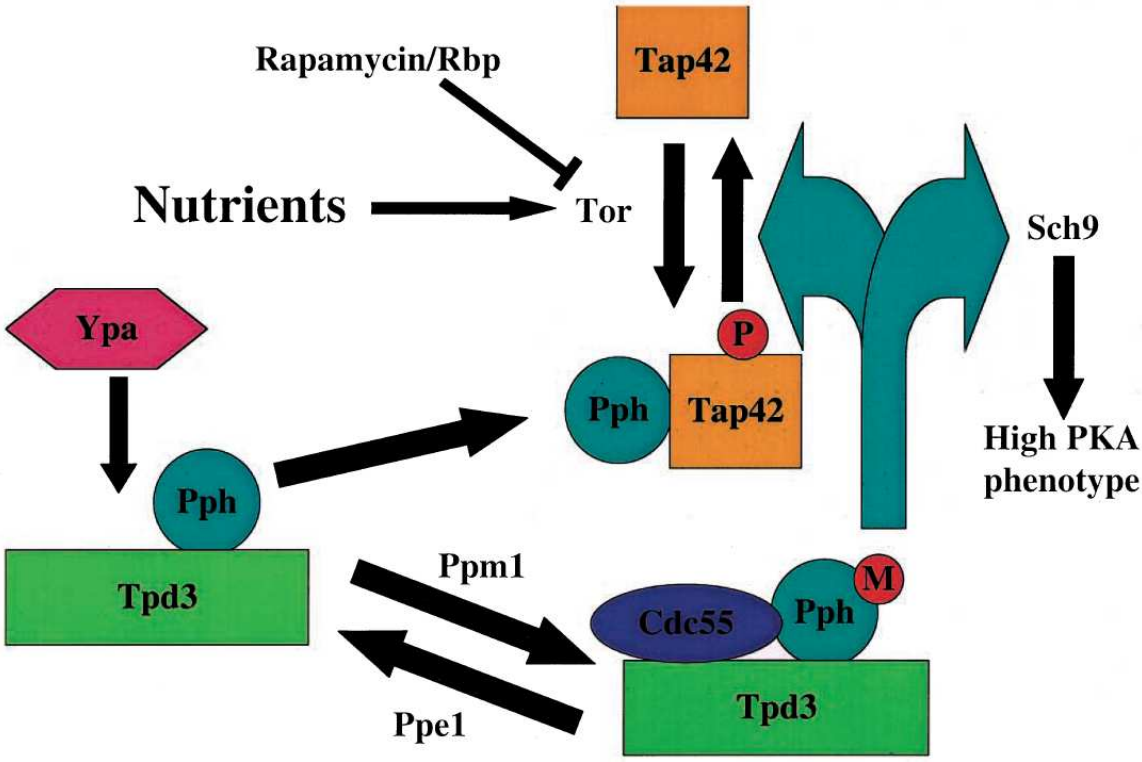

Figure 1.4: TOR signalling pathway. The major regulatory component of autophagy is the TOR complex. Under nutrient rich conditions *TORC1* is active and inhibits autophagy induction. Under nutrient starvation or rapamycin treatment *TORC1* is inactive and allows an increase of autophagic activity. The trimeric form of the *PP2A* consists of the catalytic subunit, and a regulatory subunit. The catalytic subunit is encoded by *Pph* and *Tpd3* and the regulatory subunit is encoded by *CDC55* or *RTS1*. The association of *CDC55* or *RTS1* depends on the methylation of *Pph*. This methylation is catalysed by *Ppm1* and the demethylation by *Ppe1*. The demethylated *Pph* binds to *Tap42* depending on the phosphorylation of *Tap42*. This phosphorylation is probably performed by the *TOR* kinase. Inhibition of *TOR* leads to a dephosphorylation of *Tap42* and a dissociation of *Tap42* from *Pph*. It is supposed that *SCH9* is a substrate of Pph and that active *PP2A* dephosphorylates *SCH9*, which leads to an inactivation of the enzyme. (Zabrocki et al. 2002)

Another pathway for the regulation of autophagy is *RAS*/*PKA* (cAMP dependent protein kinase A) pathway. Ras proteins are small GTP-binding proteins. There are two types of this protein, Ras1p and Ras2p. Under nutrient rich conditions they interact with the adenylate cyclase. This causes an increase of the intracellular cAMP levels, which next activates *PKA*. Activated *PKA* inhibits autophagy via a phosphorylation of Atg13p like *TOR*. (Budovskaya et al. 2004; McEwan et al. 2011)

TOR and *RAS*/*PKA* signalling pathways, lead to an inactivation of the serine/kinase *Rim15*, which positively regulates the downstream stress response transcription factors *Gis1* and *Msn2*/*4*. Both *Gis1* and *Msn2*/*4* are known to be involved in cellular protection. Under caloric restriction it has been already demonstrated that the *TOR/SCH9/Rim15/Gis1* and *RAS/PKA/Rim15/Msn2/4* pathways are involved in life

span extension and stress resistance. These effects occur in long lived mutants lacking a part of these two pathways. (Fontana et al. 2010; Kapahi et al. 2010; Wei et al. 2009) *SNF1* (a serine/threonine kinase) and its mammalian homologue *AMPK* (5'AMP-activated protein kinase) are positive regulators of autophagy. *SNF1*/*AMPK* is activated during nutrient starvation, environmental stress or rapamycin treatment. The activation of *SNF1*/*AMPK* leads to an increase of the AMP/ATP ratio, which is resulting in an increased cellular energy level.
Activated *AMPK* phosphorylates *TSC2*. The activated *TSC2* then inhibits *TORC1*. Further it is known that *SNF1* phosphorylates the stress response transcription factor *Msn2* and thus inhibiting its nuclear accumulation. (Hedbacker et al. 2009; Kapahi et al. 2010)

1.4 The fungal vacuole

The fungal vacuole, which is the analogue of the lysosome, is the most acidic compartment of the cell. The major functions of it are the macromolecular degradation, regulation of the pH homeostasis, osmoregulation, ion and metabolite storage and detoxification. The vacuole possess vacuolar hydrolases like the aminopeptidase Co and I, the repressible alkaline phosphatase, the carboxypeptidase S and Y, dipeptidyl aminopeptidase B, α-manosidase, proteinase A and B and RNAse.
The vacuole does not only possess an important role under "normal" conditions, it has also a central role under stress conditions like ionic and osmotic shock caused by nutrient starvation. (Hughes et al. 2012; Klionsky et al.1990; Li et al. 2009; Martínez-Muñoz et al. 2008)

The fungal vacuole possesses a pH between 5 and 6,5 depending on the growth conditions. The v-ATPases (vacuolare proton-translocating ATPases) are required for maintaining the acidic pH of the vacuole and further of the vacuolar and cellular pH homeostasis. The v-ATPases are proton pumps, which can synthesize or hydrolyse ATP. For the transport of H^+ and Na^+ they need energy, which they belong out of ATP hydrolysis. The v-ATPases are multiple enzymes consisting out of a peripheral and an integral membrane subunit (see Figure 1.5). The peripheral membrane complex, V_1, include an ATP hydrolysis site. The integral membrane complex, V_0, contains a proton pore. The V_1 complex consists out of eight subunits, which are encod-

ed by different *VMA* genes: A (*VMA1*), B (*VMA2*), C (*VMA5*), D (*VMA8*), E (*VMA4*), F (*VMA7*), G (*VMA10*) and H (*VMA13*). In contrast to the V_1 complex, the V_0 complex consists out of six subunits: a (*VPH1* or *STV1*), c (*VMA3*), c' (*VMA11*), c'' (*VMA16*) and d (*VMA6*). (Li et al.2009; Kane et al.1999, Kane 2006; Martínez-Muñoz et al. 2008)

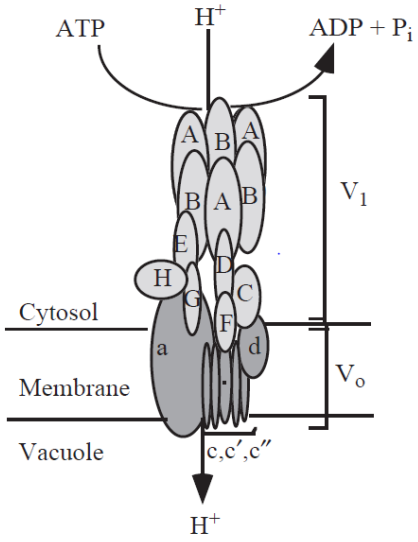

Figure 1.5: Structural design of the v-ATPase in yeast. The v-ATPase consists out of a peripheral membrane V_1 complex containing ATP hydrolysis site and integral membrane V_0 complex containing a proton pore. V_1 is encoded by A (*VMA1*), B (*VMA2*), C (*VMA5*), D (*VMA8*), E (*VMA4*), F (*VMA7*), G (*VMA10*) and H (*VMA13*) subunits and V_0 by a (*VPH1* or *STV1*), c (*VMA3*), c' (*VMA11*), c'' (*VMA16*) and d (*VMA6*). The proton pump transports H^+ and Na^+ by the hydrolyse of ATP into ADP + P_i. (Kane et al.1999)

It is already known that the vacuole and its acidic pH are important for different cellular processes. For example during autophagy the autophagosome fuses with the vacuole and the autophagic body is released into the vacuole, where they are degraded. For the disintegration of the autophagic bodies, the acidic pH is necessary. The resulting amino acids are released into the cytosol, where they are available for the novel protein synthesis. (Li et al. 2009; Nakamura et al. 1996)

Further it was shown in replicative aged yeast, that the vacuolar pH is increased and that this effect is correlated with mitochondrial dysfunction and a disruption of the neutral amino acid storage. Moreover results of caloric restriction (CR) indicate that life span extension upon CR limits age induced mitochondrial dysfunction by the increase of the vacuolar pH. (Hughes et al. 2012)

1.5 Methionine

Methionine is a sulphur amino acid, which is important in different cellular processes:

1. Methionine is the initial amino acid in the protein biosynthesis. (Cellarier et al. 2003, Dominique et al. 1997)
2. S-adenosylmethionine, which is formed out of methionine, is needed as a precursor for the synthesis of the polyamines spermine and spermidine. These polyamines are pivotal for nuclear and cell division. (Cellarier et al. 2003, Minguet et al. 2008)
3. Further S-adenosylmethionine is a methyl donor for the methylation of DNA. (Cellarier et al. 2003, Krijt et al. 2009)
4. Methionine is the precursor of glutathione. Glutathione is a tripeptide, which consists of glutamate, cysteine and glycine. It protects the cell from oxidative stress by the reduction of oxygen species like peroxides or hyperperoxides. (Cellarier et al. 2003, Penninckx et al. 2002)

Aging is a multifactorial process. One prominent aging theory postulates that aging is a result of oxidative damages of the mitochondrial proteins and DNA caused by mitochondrial ROS (reactive oxygen species). It is already known that caloric restriction (CR) leads to a decrease of mitochondrial ROS and oxidative damages of the mitochondrial proteins and DNA. This effect also occurs under methionine restriction without CR based on a decrease in the oxidative photosystem complex I, II, III and IV. (Pamplona et al. 2006, Sanz et al. 2006)

A recent study indicates that methionine restriction in budding yeast leads to a decrease in necrotic cell death and a ROS production and further promotes longevity and increases autophagy. (Ruckenstuhl et al. 2014)

It is further known that CR prolongs the life span of different model organisms. Research in male Fischer 344 rats indicates that methionine restriction increases their life span of at least 30%. Further they are light in weight, although they consume more total calories per body weight compared to the control rats. (Orentreich et al. 1992)

This life prolonging effect is observed in mice under totally restriction of cysteine and cystine or with low methionine levels too. Additionally lower levels of serum IGF-I, insulin, glucose and thyroid hormone have been observed. The levels of liver mRNA for MIF (macrophage migration inhibitory factor) are increased. Further methionine

restricted mice indicates age related changes in T-cell subset and they develop slower lens turbidity. (Miller et al. 2005, Sun et al. 2009)
Methionine is the precursor of glutathione (GSH). GSH is important for maintaining protein function and structure, for the regulation of protein synthesis, protein degradation and immune function. Additionally GSH is an antioxidant that detoxifies endo- and exogenous compounds like free radicals, xenobiotics or lipid peroxides. A decrease of GSH levels lead to a specific diseases including diabetes, AIDS, cataracts and alcoholic liver diseases and cell damage. It is suggested that GSH is important in the aging process, as the amount of GSH decreases during aging. During aging methionine restricted male F344 rates indicate an increased blood GSH level and a conservation of GSH in the tissue. (Richie et al.1994)
It also has been shown that tumour cells have an absolute requirement for methionine. In contrast to “normal” cells, methionine starvation leads to a regression of a variety of animal tumours. (Cellarier et al. 2003)

Saccharomyces cerevisiae reduces sulphate from the environment, which is used for the synthesis of organic sulphur metabolites (see Figure 1.6) like methionine, S-adenosylmethionine or cysteine. The enzymes of this metabolism are encoded by different *MET* genes.
The first step of the sulphur metabolism is the activation of sulphate, which is divided into two reactions. In the first reaction sulphate activation is convert into adenylyl sulphate by ATP sulfurylase and in the second reaction into phosphoadenylyl sulphate by adenylyl sulphate kinase.
In the next step phosphoadenylyl sulphate is reduced in sulphite and afterwards into sulphide.
In the next reaction homocysteine is synthesised. However, there are three possibilities for this reaction:

1. From O-acetyl homoserine and sulphide by the homocysteine synthase
2. Cysteine to cystathionine catalysed by cystathionine γ-synthase and then to homocysteine by cystathionine β-lyase
3. From adenosylmethionine catalysed by homocysteine methyl transferase.

O-acetyl homoserine, which is synthesised out of homoserine by homoserine transacetylase, is important for synthesis of both homocysteine from cysteine and homo-

cysteine from sulphide. Homocysteine is necessary in the transsulfuration pathway and the methyl cycle.
Yeast possesses two transsulfuration pathways: the forward one for the synthesis of cysteine out of homocysteine and the reverse one to convert cysteine into homocysteine.
Methionine is synthesised in the methyl cycle out of homocysteine by homocysteine methyl transferase. In the next step methionine is converted into S-adenosylmethionine by S-adenosylmethionine synthase. S-adenosylhomocysteine is synthesised out of S-adenosylmethionine through a demethylation, which can be afterwards converted into homocysteine by S-adenosylhomocysteine hydrolase. (Chan et al. 2003; Lafaye et al. 2005; Thomas et al. 1997)

To study methionine restriction three different strains were used for this work. They are all the *Saccharomyces cerevisae* strain By4741 mating type a. The first strain has no deletion in the methionine syntheses pathway genes and can build methionine either from aspartate or from cysteine. A methionine supply from environment is not necessary. The second strain has a deletion in *MET2* gene. *MET2* codes for homoserine-trans-acetylase, which catalyzes the acetylation of homoserine. O-acetylhomoserine is needed to build cystathione from cysteine. Homocysteine synthase (*MET15*) cannot synthesize homocysteine and therefore is not able to synthesize methionine. The third strain has a deletion in the *MET15* gene. This means that methionine is just synthesized from aspartate. These strains were used to test if different methionine concentrations have an influence on chronological aged *Saccharomyces cerevisae* cells.

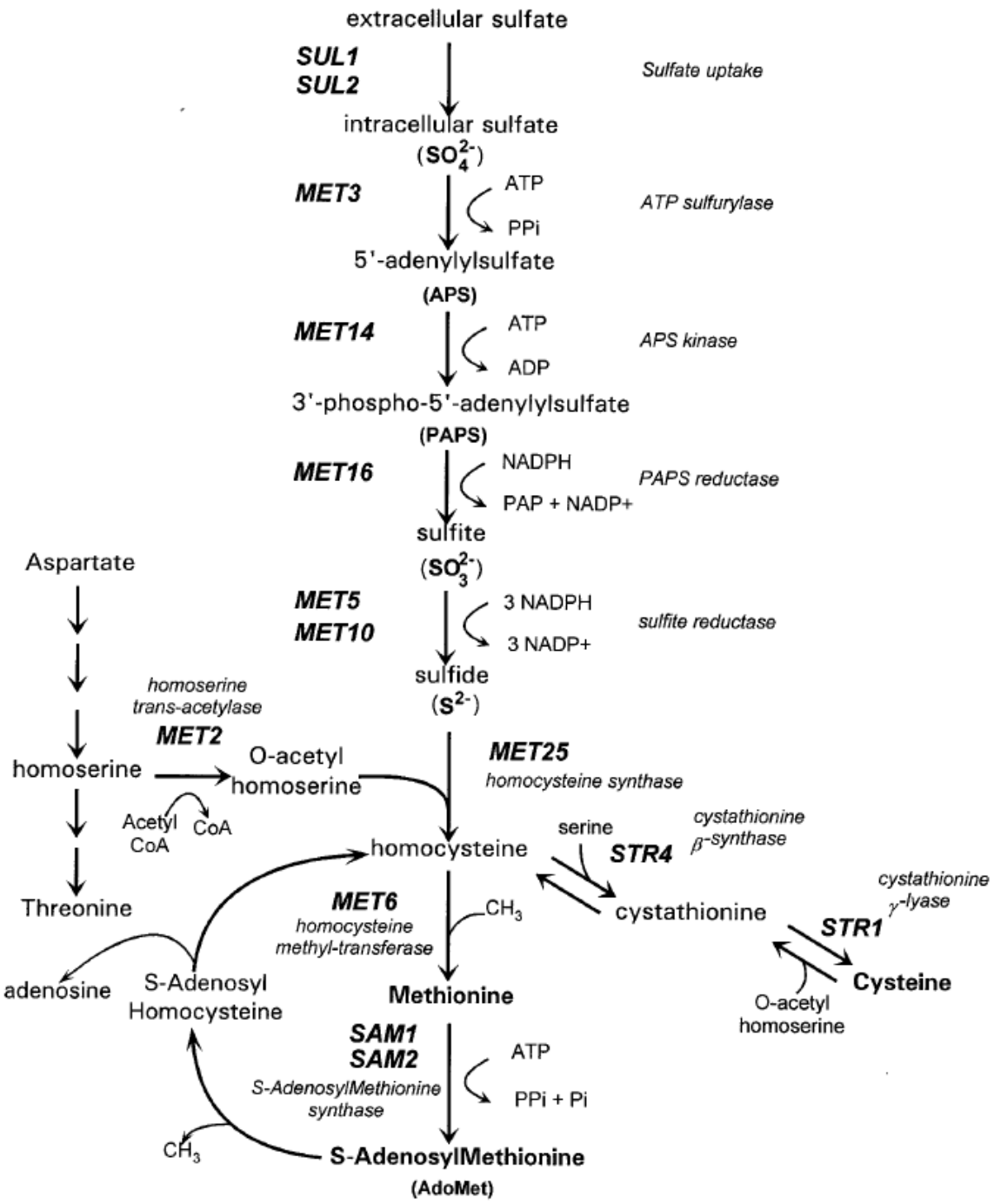

Figure 1.6: Sulphur amino acid biosynthesis in S. cerevisiae. (Dominique et al. 1997)

1.6 Different growth behaviour of a methionine auxotrophic strain with different methionine concentrations

Within her diploma thesis Lisa Klug performed a chronological shift-aging experiment with which she verified that the methionine auxotrophic strain *Bya MET15 Δmet2* shows an enhanced survival under methionine limitation of 10% (3 mg/l). In contrast to this a complete limitation or 500% (150 mg/l) of methionine led to rapid cell death. She could further detect that when shifted in media containing 10% (3 mg/l) or 0% methionine the cells showed nearly no apoptotic or necrotic cell death marker. These data correspond with the survival data of the strain with 10% methionine. However, the cells, which were growing under complete methionine restricted conditions, were dead within the first few days. She considered that autophagy triggers rapid cell death under complete methionine restriction and leads to a better survival in the cells shifted in media with 10% methionine.

2. Materials

2.1 Strains

All used strains, including their genotypes and plasmids, which have been used for this work, are listed in Table 2.1.

Table 2.1: Overview of the used *S. cerevisiae* strains including their genotype, plasmid and origin

Name	Genotype	Plasmid	Origin
BY4741 MET15 (WT)	Mat a; his3Δ1; leu2Δ0; ura3Δ0		Euroscarf
BY4741 MET15 *Δmet2*	Mat a; his3Δ1; leu2Δ0; ura3Δ0; met2::kanMX		Fröhlich lab
BY4741 MET15 chr. Atg8-GFP	Mat a; his3Δ1; leu2Δ0; ura3Δ0; chr. Atg8-GFP		Fröhlich lab
BY4741 MET15 *Δmet2* chr. Atg8-GFP	Mat a; his3Δ1; leu2Δ0; ura3Δ0; met15Δ0; chr. Atg8-GFP		Fröhlich lab
BY4741 *Δmet15* chr. Atg8-GFP	Mat a; his3Δ1; leu2Δ0; ura3Δ0; met2::kanMX; chr. Atg8-GFP		Fröhlich lab
BY4741 MET15 *Δmet2* VPH1-mCherry	Mat a his3Δ1 leu2Δ0 MET15 ura3Δ0; met2::kanMX VPH1-mCherry		Fröhlich lab
BY4741 MET15 *Δmet2* VPH1-mCherry *Δatg5*	Mat a his3Δ1 leu2Δ0 MET15 ura3Δ0; met2::kanMX VPH1-mCherry; ∆atg5::URA3		Fröhlich lab
BY4741 MET15 VPH1-mCherry *Δatg15*	Mat a his3Δ1 leu2Δ0 MET15 ura3Δ0; VPH1-mCherry; ∆atg15::HIS3		Fröhlich lab

BY4741 MET15 *Δmet2 Δcdc55*	Mata his3Δ1 leu2Δ0 MET15 ura3Δ0; met2::kanMX4; cdc55::HIS3		Fröhlich lab
BY4741 MET15 *Δmet2 Δtor1*	Mat a his3Δ1 leu2Δ0 MET15 ura3Δ0 met2::kanMX4; tor1::HIS3		Fröhlich lab
BY4741 MET15 *Δmet2 Δsch9*	Mat a his3Δ1 leu2Δ0 MET15 ura3Δ0; met2::kanMX4; sch9::HIS3		Fröhlich lab
BY4741 MET15 *Δmet2 Δrts1*	Mat a his3Δ1 leu2Δ0 MET15 ura3Δ0; met2::kanMX4; rts1::HIS3		Fröhlich lab
BY4741 MET15 *Δmet2*	Mat a; his3Δ1; leu2Δ0; ura3Δ0; met2::kanMX	pESC-HIS-Vector	Fröhlich lab
BY4741 MET15 *Δmet2*	Mat a; his3Δ1; leu2Δ0; ura3Δ0; met2::kanMX	pESC-HIS-VMA1	Fröhlich lab
BY4741 MET15 *Δmet2*	Mat a; his3Δ1; leu2Δ0; ura3Δ0; met2::kanMX	pESC-HIS-VPH2	Fröhlich lab
BY4741 MET15	Mat a; his3Δ1; leu2Δ0; ura3Δ0; chGFP-ATG8::natNT2		Fröhlich lab
BY4741 MET15	Mat a; his3Δ1; leu2Δ0; ura3Δ0; chGFP-ATG8::natNT2; ppm1::HIS3		Fröhlich lab
BY4741 MET15	Mat a; his3Δ1; leu2Δ0; ura3Δ0; chGFP-ATG8::natNT2; pph21::HIS3		Fröhlich lab

BY4741 MET15 *Δmet2 Δlys2 Δarg4*	Mat a; his3Δ1; leu2Δ0; ura3Δ0; met2::kanMX; lys2Δtetrad; Δarg4:: hpb NT1		This Work
BY4741 MET15 *Δmet2 Δlys2 Δrts1 Δarg4*	Mat a; his3Δ1; leu2Δ0; ura3Δ0; met2::kanMX; lys2Δtetrad; rts1::HIS3; arg4::hpb NT1		This Work
BY4741 MET15 *Δmet2 Δlys2 Δarg4 Δsch9*	Mat a; his3Δ1; leu2Δ0; ura3Δ0; met2::kanMX; lys2Δtetrad; arg4::hpbNT1; sch9::leu		This Work
BY4741 MET15 *Δmet2 Δlys2 Δrts1 Δarg4 Δsch9*	Mat a; his3Δ1; leu2Δ0; ura3Δ0; met2::kanMX; lys2Δtetrad; rts1::HIS3; arg4::hpbNT1; sch9::leu		This Work
BY4741 MET15 *Δmet2 Δlys2 Δarg4 Δsch9*	Mat a; his3Δ1; leu2Δ0; ura3Δ0; met2::kanMX; lys2Δtetrad; arg4::hpbNT1; sch9::leu	pJU676	This Work
BY4741 MET15 *Δmet2 Δlys2 Δrts1 Δarg4 Δsch9*	Mat a; his3Δ1; leu2Δ0; ura3Δ0; met2::kanMX; lys2Δtetrad; rts1::HIS3; arg4::hpbNT1; sch9::leu	pJU676	This Work
BY4741 MET15 *Δmet2 Δhac1*	Mat a; his3Δ1; leu2Δ0; ura3Δ0; met2::kanMX; hac1::ura3		This Work
BY4741 MET15 *Δmet2 Δire1*	Mat a; his3Δ1; leu2Δ0; ura3Δ0; met2::kanMX; ire1::ura3		This Work

2.2 Plasmids

Table 2.2: Plasmids, their description and source used for this work

Name	Description	Source
pESC	pESC- *HIS3*	Stratagene
pESC VMA1	pESC- *HIS3 containing VMA1*	Fröhlich lab
pESC VPH2	pESC- *HIS3 containing VPH2*	Fröhlich lab
pFA6a	pFA6a-hphNT1	Euroscarf; JANKE, C. et al: A versatile toolbox for PCR-based tagging of yeast genes: new fluorescent proteins, more markers and promoter substitution cassettes. Yeast (2004) 21, 974 – 962
pUG72	pUG73-*URA3*	Euroscarf; GÜLDNER, U. et al: A second set of loxP marker cassettes for Cre-mediated multiple gene knockouts in budding yeast. Nucleic Acids Research (2002) 30, e23
pUG73	pUG73- *LEU2*	Euroscarf; GÜLDENER, U. et al: A second set of loxP marker cassettes for Cre-mediated multiple gene knockouts in budding yeast. Nucleic Acids Research (2002) 30, e23
pJU676	pRS416; *URA3 SCH9-5HA*	LOEWITH, R. et al: Mitochondrial genomic dysfunction causes dephosphorylation of Sch9 in the yeast *Saccharomyces cerevisiae.* Eukaryotic Cell (2011) Vol. 10, No. 10, p. 1367–1369

2.3 Primer

All primers from Table 2.3 have been received from MWG Biotech, Germany. The lyophilisates have been dissolved in a specific volume of ddH2O from Fresenius, so that a final concentration of 100 pmol/µl was reached. The Primers were stored at -20°C.

Table 2.3: Name and sequence of primers used for this work

Name	**Sequence (5‘ → 3‘)**
ARG4_fw_hy	GAAGAGCTCAAAAGCAGGTAACTATATAACAAGACTAAGGCAAAC
ARG4_rev_hy	AAGTACCAGACCTGATGAAATTCTTGCGCATAACGTCGCCATCTG
ARG4 control	ACGTTCCTCCCTCTCTCTAAT
KanR5’B	CAAGACTGTCAAGGAGGG
SCH9_fw	AAAATTTACTCTTTTGGCAACTGTTTATAAGAAGAATAAGTCTGA
SCH9_rev	CAAGAGGAGCGATTGAGAAATCATATTTCGAATCTTCCACTGACA
SCH9_control	CGATAACGGTTCTTTCTGCATAT
HAC1_fw	ACAACCTCCTCCTCCCCCACCTACGACAACAACCGCCAC-TCAGCTGAAGCTTCGTACGC
HAC1_bwd	ACGAGAAAAAAAAAATTATACCCTCTTGCGATTGTCTGCAT-AGGCCACTAGTGGATCTG
HAC1 control	GAAAAACAACACCAAGCTGC
IRE1_fw	ACAGCATATCTGAGGAATTAATATTTTAGCACTTTGAAAACA-GCTGAAGCTTCGTACGC
IRE1_bwd	ATAATCAACCAAGAAGAAGCAGAGGGGCATGAACATGGCA-TAGGCCACTAGTGGATCTG
IRE1 control	GCTGCGTAGTGTGAAATATATTG
URA3 control	GTTCATCATCTCATGGATCTGCA

2.4 Media

Table 2.4 shows the media, which have been used for this work. All the used media were prepared with deionised water and autoclaved at 121°C for 25 minutes. 10x stocks for the amino acids were sterilized separately and added to the minimal media after autoclaving. For shift experiments glucose (2%), YNB (yeast nitrogen base and ammonium sulphate, 10x stocks) and amino acids mixtures (10x stocks) were used for the minimal media and autoclaved separately.

Table 2.4: Composition of the used growth media for *S. cerevisiae*

Media	**Composition**
YPD (full media)	1% yeast extract 2% bacto peptone 2% glucose (2% agar-agar)
SMD/SMG (minimal media)	0,17% yeast nitrogen base 0,5% ammonium sulfate 2% glucose/galactose or 1% glucose + 1% galactose or 1,5% glucose + 0,5% galactose or 1,9% glucose + 0,1% galactose 30 mg/l adenine 80 mg/l histidine 200 mg/l leucine 300 mg/l uracile 30 mg/l all other amino acids

2.5 Buffer and solutions

2.5.1 DNA agarose gel electrophoresis

Table 2.5: Solutions and their compositions used for DNA gel electrophoresis

Solution	Components
TAE	40 mM Tris/acetic acid 1 mM EDTA; pH 8,0
Agarose gel	1% Agarose in 1x TAE 0,001% Ehidium bromide
Ethidium bromide	0,001% Fermentas
DNA loading dye (6x)	Fermentas

2.5.2 Casy cell counter

Table 2.6: Solutions and their composition used for CASY cell counter

Solution	Components
CASYTON	0,1 mM EDTA 0,9 mM NaCl isotonic salt solution

2.5.3 Chemical lyses

Table 2.7: Solutions and their composition used for chemical lyses

Solution	Components
Lysis buffer CP	1,85M NaOH 7,5% β-mercaptoethanol
TCA	55% trichloroacetic acid in ddH_2O
Finale sample buffer (FSB, 1x)	0,1% bromophenol blue 10% glycerol 2% SDS 100 mM β-mercaptoethanol 50 mM Tris/HCl, pH 6,8
Tris solution	2 M Tris

2.5.4 SDS PAGE and Western Blot

Table 2.8: Solutions and their composition used for SDS PAGE and Western Blot

Solution	Components
Electrophoresis buffer	192 mM Glycine 25 mM Tris-HCl, pH 8,3 0,2 % sodium dodecyl sulfate (SDS)
Separating gel	0,1 % ammonium peroxodisulfate (APS) 12,5 % acrylamide 0,4 % N.N'-methylen-bisacrylamide 0,01 % N.N.N'.N'-tetramethylethylenediamide (TEMED) 0,2 % SDS 250 mM Tris-HCl, pH 8,8
Stacking gel	5 % acrylamide 0,1 % ammonium peroxodisulfate (APS) 0,13 % N.N'-methylene-bisacrylamide 0,01 % N.N.N'.N'-tetramethylethylenediamide (TEMED) 0,2 % SDS 250 mM Tris-HCl pH 6,8
Blotting buffer	150 mM glycine 20 mM Tris 20% methanol 0,05% SDS
TBS (-T)	150 mM NaCl 10 mM Tris/HCl; pH 7,6 (0,02 % Triton-X 100)
TST	150 mM NaCl 10 mM Tris-HCl, pH 7,4 0,1 % Tween20
Blocking solution	1% milk powder in 1xTBS
PVDF Transfer membrane	Milipore, USA
ECL™ Western Blotting Detection reagents	GE Healthcare-Amersham

X-ray films	Sterling Diagnostics, USA

2.5.5 Antibodies

Table 2.9: Primary and secondary antibodies and their dilution used in this work

Antibody	Dilution
Primary antibodies	
α-GFP	1:5000 in TBS + 1% milk powder
α-GAPDH	1:20000 in TST + 1% milk powder
Secundary antibodies	
α-mouse	1:10000 in 1xTBS + 1% milk powder
α- mouse	1:10000 in 1xTST + 1% milk powder

2.5.6 Quinacrine and PI double staining

Table 2.10: Solutions and their composition used for quinacrine and PI double staining

Solution	Components
HEPES	1 M HEPES-KOH, pH 7,6
HEPES Buffer	100 mM HEPES 2% glucose
Quinacrine	200mM quinacrine
Propidiumiodid (PI)	100µg/ml in ddH_2O

2.5.7 Yeast transformation

Table 2.11: Solutions and their composition used for yeast transformation

Solution	Components
Lithium acetate	100 mM Lithium acetate 10 mM Tris/HCl, pH 7,5 1 mM EDTA, pH 8,0
PEG solution	40% polyethylenglycole 4000 100 mM Lithium acetate 10 mM Tris/HCl, pH 7,5 1 mM EDTA, pH 8,0
Carrier DNA	10 mg/ml Herring sperm-DNA

2.5.8 Chemicals and enzymes

Table 2.12: Chemicals and enzymes and their source used in this work

Chemicals, Enzymes	Source
Phusion® High Fidelity DNA Polymerase (2U/µl)	Finnzymes
Taq polymerase (5U/µl)	Fermentas
Thermo Pol Reaction Buffer (10x)	New England Biolabs
dNTPs	Fermentas

2.5.9 Standards

Table 2.13: Standards and their source used in this work

Name	Source
Lambda DNA/EcoRI+HindIII Marker	Fermentas
PageRuler^{TM} Prestained Protein Ladder	Fermentas

2.5.10 Equipment

Table 2.14: Equipment used in this work

Equipment	Source
Analytical balance	Sartorius
Autoclave	Systec
Cell counter CASYTM	Schärfe Systems
Centrifuge	Hermle Z400K
Centrifuge (table top)	Heraeus Biofuge fresco
Colony counter	Scanalyzer Colonycounter Digital m
Electroblotting power supply	Biorad Power Pac300
Electrophoresis chamber	Thermo EC
Electroporator	EC Electroporator
Fluorescence microscope	Zeiss
Freezer	Thermo Forma
Incubator	Unitron
Magnetic stirrer	Heidolph
pH-meter	Methrom
Photometer	Genesys
Pipettes	Socorex
Thermocycler	GeneAmp PCR System
Thermomixer	Eppendorf Thermostat plus
Tips, tubes	Eppendorf
Vortex	Scientific Industries
Waterbath	GFL
Water distillation	GFL Dest 2208

3. Methods

3.1 General molecular biological methods

3.1.1 Agarose gel electrophoresis

1% agarose gels were used for the agarose gel electrophoresis. Therefore agarose powder was dissolved in 1x TAE (40mM Tris/acetic acid pH8; 0,1 mM EDTA) in a microwave. During the cool down phase 0,001% Ethidium bromide was added in a gel tray before the gel got totally polymerized.
The samples were mixed with a 6x DNA loading dye and were loaded together with a standard control (Lambda/*Eco*RI+*Hind*III). For the electrophoresis 0,5x TAE was used as running buffer. Depending on the size of the gel 70 V were used for small gel and 90 V for large ones.

3.1.2 Polymerase chain reaction (PCR)

For the knockout of genes a polymerase chain reaction was performed, using the corresponding forward and reverse primer (see Table 3.1). The program for the knockout PCRs is shown in Table 3.2.

Table 3.1: Components for the Hygromycin PCR and the regular PCR

Volume [µl]	Component
Hygromycin PCR	
1	Phusion High Fidelity DNA Polymerase (2 U/µl)
5	10x buffer (50 mM Tris/HCl, pH 9,2 ; 22,5 mM $MgCl_2$; 160 mM NH_4SO_4; 20% DMSO; 1% Triton-X100)
8,75	dNTPs
3,2	Primer fwd (1:10 diluted)
3,2	Primer rev (1:10 diluted)
1	pFA6a-hphNT1
28,35	ddH_2O

regular PCR	
0,3	Taq DNA Polymerase (5 U/µl)
6	10x Thermo Pol Reaction Buffer
6	dNTPs
3	Primer fwd (1:20 diluted)
3	Primer rev (1:20 diluted)
12	pUG73/pUG72
30	ddH_2O

Table 3.2: PCR program for the Hygromycin PCR and the regular PCR

Temperature [°C]	**Time [minutes]**
Hygromycin PCR	
97	3 (hot start)
97	1
54	0:30 — 10x
68	2:40
97	1
54	0:30 — 20x
68	2:40 + 20 sec/cycle
regular PCR	
94	2
94	0:30
58	0:30 — 35x
72	3
72	15

3.1.3 Yeast transformation

For the yeast transformation 30 ml YPD were inoculated with OD_{600} of 0,2 of ONC. After incubating it at 28°C a OD_{600} of 0,6 was reached. The cells were harvested at 3500 rpm for 6 minutes. The cells were washed with 10 ml ddH_2O first and with a 10 ml Lithiumacetate solution afterwards. The cells were re-suspended in 300 µl Lithiumacetate solution and incubated for 28 minutes at 30°C. After that 50 µl of these cells, 300 µl PEG solution and 5 µl Herring sperm-DNA (10 mg/ml; fresh denatured at

95°C for five minutes) were mixed. For the plasmid transformation 1 µl of the plasmid was directly added and the solution was vortexed for 30 seconds. For the knock out transformation solution of the yeast cells, PEG and Herring sperm-DNA were vortexed for 30 seconds and afterwards 30 µl of the PCR containing the insert was added. This mix was incubated at 28°C for 30 minutes and at 42°C for 20 minutes. The cells were harvested and re-suspended in 100 µl ddH_2O. In a next stept the cells were plated on selective media and the plates were incubated at 28°C for two to four days. However, for the transformation with hygromycin or leucine knockout cassettes, the cells were plated onto YPD plates. After incubation at 28°C overnight the plates were replica-plated on selective media and then incubated at 28°C for two to four days.

3.1.4 Colony PCR

To verify positive clones of a transformation of *S. cerevisiae* the colony PCR was used. The cell material of the clones was used as template and had been resolved directly in the PCR sample tubes. The following PCR product was analysed by agarose gel electrophoresis.
Components and programmes used for the colony PCR are described in Table 3.3 and Table 3.4.

Table 3.3: Components for the colony PCR

Volume [µl]	Component
0,1	Taq DNA Polymerase (5 U/µl)
2	10x Thermo Pol Reaction Buffer
2	dNTPs
1	Primer fwd (1:20 diluted)
1	Primer rev (1:20 diluted)
14	ddH_2O

Table 3.4: Colony-PCR program for the regular colony PCR and the leucine colony PCR

Temperature [°C]	Time [minutes]	
Regular colony PCR		
94	6	
94	0:30	
58	1	10x
72	2	
72	7	
Leucine colony-PCR		
95	6	
95	0:45	
50	0:45	35x
72	1:30	
72	10	

3.2 Cell biological methods

3.2.1 Clonogenicity assay

In the clonogenicity assay the survival rate of strains was measured by plating the cells on agar plates.

Therefore a dilution of 1:100 and 1:10000 of the cell culture with ddH_2O was done. From the 1:100 dilution a 1:10000 dilution with CASYTON was produced to measure the cell count of the culture with a CASY® cell counter. The CASY® cell counter can detect particles from a size of 1,5 to 15 µm. Based on the resulting cell/ml count, 500 cells of the 1:10000 with ddH_2O were plated onto YPD agar plates and incubated at 28°C for two days. The survival of the culture can be calculated by counting the colony forming units (cfu) with the LemnaTec colony counter.

3.2.2 Aging shift

The yeast strain was incubated at 28°C in 5 ml SMD (separately autoclaved) with all amino acids in a shaking incubator (145 rpm) overnight. On the next day a main culture was inoculated with a cell count of 5 x 10^5 cells of the overnight culture (ONC) in SMD (separately autoclaved) with all amino acids in 250 ml flasks. This culture was

incubated at 28°C in a shaking incubator for 24 hours. The cells were harvested in sterile falcon tubes at 3500 rpm for four minutes. The pellet was washed with SMD -met (SMD without methionine), SMD –his –met (SMD without histidine and methionine), SMD -leu (SMD without leucine) or SMD –arg –lys -met (SMD without arginine, lysine and methionine). Afterwards the cells were re-suspended in SMD –met, SMD –his –met, SMD –leu or SMD –arg –lys –met. 10 ml of this culture was divided into baffled flasks. In the culture with SMD -met different methionine concentrations (0 mg/l, 3 mg/l or 30 mg/l) were added. The cells were incubated at 28°C and 145 rpm in a shaking incubator.

3.2.3 Quinacrine staining

A cell count of $2*10^7$ were harvested and washed with 450 µl YPD with 100 mM HEPES (pH 7,6). The cell pellet was re-suspended in YPD with 100 mM HEPES (pH 7,6) and with 200 mM quinacrine. The cells were incubated under shaking at 30°C for ten minutes and five minutes on ice. The cells were washed three times with 500 µl cold HEPES buffer (100 mM; pH 7,6) with 2% D-glucose. After the third washing step the pellet was re-suspended in 50 µl cold HEPES buffer (100 mM; pH 7,6) with 2% D-glucose. The samples remained on ice until being microscoped within one hour.

3.2.4 Quinacrine/PI double staining

A cell count of $2*10^7$ were harvested and washed with 450 µl YPD with 100 mM HEPES (pH 7,6). The cell pellet was re-suspended in YPD with 100 mM HEPES (pH 7,6) and with 200 mM quinacrine. The cells were incubated under shaking at 30°C for ten minutes and five minutes on ice. The cells were washed two times with 500 µl cold HEPES buffer (100 mM; pH 7,6) with 2% D-glucose. The cell pellet was re-suspended in 500 µl cold HEPES buffer (100 mM; pH 7,6) with 2% D-glucose and 0,5 µl PI (propidium iodide; 100 µg/ml) was added and incubated on ice in the dark for ten minutes. The cells were washed once with 500 µl cold HEPES buffer (100 mM; pH 7,6) with 2% D-glucose and the pellet was were re-suspended in 50 µl cold HEPES buffer (100 mM; pH 7,6) with 2% D-glucose. The samples remained on ice until being microscoped within one hour.

3.2.5 Fluorescence microscopy

For the fluorescence microscopy of the quinacrine and PI stained cells ~2 µl of the pellet with supernatant were transferred on a microscope slide and covered with a cover glass. For the quinacrine fluorescence the eGFP filter was used with an exposure time of one second. For the PI fluorescence the ds Red filter was used at an exposure time of 200 milliseconds. The microscopy was performed with objective lens having a 40 time magnification and 2,0 numerical aperture in immersol oil at room temperature.

For the fluorescence microscopy of the Atg8-GFP expressing cells 100 µl of the cell culture were harvested. ~2 µl of the pellet with suppernatant were placed on a microscope slide and covered with a cover glass. For the GFP-fluorescence the eGFP filter was used with an exposure time of five second. The microscopy was performed with objective lens having a 63 time magnification and 1,25 numerical aperture in immersol oil at room temperature.

3.3 Biochemical methods

3.3.1 Chemical lysis

3 OD_{600} units were harvested of the cell culture and washed once with 1 ml ddH_2O. The pellet was re-suspended in 150 µl lysis buffer (fresh prepared) and incubated on ice for ten minutes. 150 µl 55% TCA were added additionally and the cells were incubated on ice for ten minutes. The samples were centrifuged at 10000 g and 4°C for ten minutes. The pellet was re-suspended in 100 µl 1xFSB loading buffer. If necessary untitrated Tris base was added until the indicator showed a blue colour. The cells were heated at 95°C for five minutes and stored at -20°C or were used directly for SDS-PAGE.

3.3.2 SDS-Polyacrylamide gel electrophoresis

For the SDS-PAGE a cross-linked denaturizing polyacrylamide gel was used to separate proteins, based on their mobility in an electric field. The migration of the proteins on the polyacrylamide gel is dependent on their molecular weight.

The gel consists of acrylamide monomers, ammonium peroxosulfate (used as a radical chain initiator), N,N'-methylenebisacrylamide (used as a cross linker) and TEMED

(used as a catalyser for polymerisation). The gel consists of an upper stacking gel (5% acrylamide) and a lower running gel (12,5% acrylamide).
For the electrophoresis a Tris-Glycin-SDS running buffer was used. For the stacking gel the electrophoresis was running at 12 mA and for the running gel at 18 mA. For the determination of the molecular weight of the protein bands in the Western Blot analysis 3 µl of Page Ruler^{TM} Prestained Protein Ladder standard was used.

3.3.3 Western Blot

In Western Blot analysis protein expression is detected via antibody-tag-binding. Therefore the proteins were transferred from the polyacrylamide gel to a PVDF membrane (Millipore). Before that the membrane was activated in methanol and washed with water. The transfer was performed in a tank-blot system (Trabs-Blot^{TM} Cell; BioRad) with CAPS transfer buffer at 220 mA for 60 minutes. The blotted membrane was blocked with 1% milkpowder in TBS at 4°C overnight or for 30 minutes with 3% milkpowder in TBS at room temperature under shaking to inhibit unspecific bindings. The membrane was incubated with the primary antibody under shaking at room temperature for one hour. The membrane was washed with TBS-T three times for five minutes before it was incubated with the secondary antibody under shaking at room temperature for one hour. The blot was washed for another three times with TBS-T for five minutes each. For the detection of the protein expression the ECL-System (chemiluminescence) of Amersham Biociences was used. With this reaction mix the membrane was incubated for one minute and exposed on an X-ray film for one, five and 30 minutes, depending on the intensity of the signal.

3.4 Statistic

For the calculation of the significance the T-TEST (one-side distribution/two samples with same variance) of Microsoft Excel was used and the significant results were indicated with asterisks (*: $p<0,05$; **: $p<0,01$; ***: $p<0,001$). The data are representing the mean ± SEM of one representative experiment.

For the statistical analysis of the quinacrine and PI stained cells about 500 cells of each sample at each point of time were counted with ImageJ. Of the quinacrine images the vacuole stained cells (only cells with acidic vacuole, not with acidic cytoplasm), bright cells and partially or cytoplasmatic bright stained cells were counted and from the PI images all PI positive cells. The percentage of the stained cells had been calculated out of the total cell count.

4. Results

4.1 Methionine restriction leads to an increased autophagy

To verify previous results that methionine restriction leads to an enhanced autophagy a Western Blot analysis was performed. Therefore *Bya MET15 chr. Atg8-GFP, Bya Δmet15 chr. Atg8-GFP* and *Bya MET15 Δmet2 chr. Atg8-GFP* were used to detect autophagy.

The Atg8-GFP construct is necessary for the detection of the autophagosome. During autophagy the autophagosome is transported to the vacuole and gets degraded. The Atg8-GFP construct and the free GFP can be detected with a α-GFP antibody. Autophagy is monitored based on the resulting signal of free GFP.

For the Western Blot analysis samples were taken on days one, two and three after inoculating in SMD with all amino acids. The experiment was performed together with Silvia Dichtinger.

Figure 4.1 shows the result of the Western Blot analysis. It indicates that the autophagy is strongly enhanced in the *Bya Δmet15 chr. Atg8-GFP* and *BY4741 MET15 Δmet2 chr. Atg8-GFP* strain compared to the *Bya MET15 chr. Atg8-GFP* strain.

On day one there was nearly no free GFP detectable in the *Bya MET15 chr. Atg8-GFP* strain. The amount of free GFP increased in this strain every day, whereas the amount of the free GFP stayed nearly the same in the two other strains. The highest signal of free GFP was detected in the *Bya Δmet15 chr. Atg8-GFP* strain. Christoph Ruckenstuhl could confirm this result with an ALP-assay and fluorescence microscopy in his paper “Lifespan extension by methionine restriction requires autophagy-dependent vacuolar acidification”.

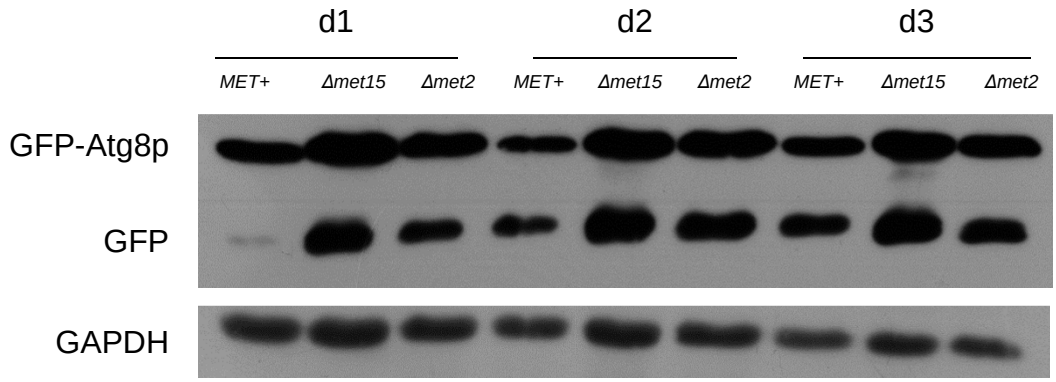

Figure 4.1: Methionine restriction leads to an increased autophagy. The ONC of *Bya MET15 chr. Atg8-GFP*, *Bya MET15 Δmet2 chr. Atg8-GFP* and *Bya Δmet15 chr. Atg8-GFP* were inoculated in SMD with all amino acids with an OD600 0,05 and incubated at 28°C. On day one, two and three samples were taken. A chemical lyses was performed. The samples were loaded on a SDS gel and a Western Blot analysis was done. The free GFP has a molecular weight of ~30 kDa and the Atg8-GFP construct ~48 kDa. The molecular weight of the bands was evaluated with a standard, PageRulerTM Prestained Protein Ladder. The expression of the free GFP and the Atg8-GFP construct were detected with a α-GFP antibody. As loading control a α-GAPDH antibody was used.

4.2 Complete methionine restriction in a shift-aging induces vacuolar acidification followed by cytoplasmic acidification

It is already known through Christoph Ruckenstuhl`s work that the intracellular pH drops eventually in *Bya MET15 Δmet2*, which were shifted in media without methionine in contrast to cells, which were shifted in SMD with 3 mg/l or 30 mg/l methionine and in SMD without leucine.

To validate the experiment of the pH measurement and determine the effect on vacuolar pH, the cells were stained with quinacrine, as quinacrine stains the acidic compartments of a cell. So the stain has the possibility to diffuse across the cell membranes. Therefore it was possible to visualize different phenotypes of cells. Furthermore to visualize the vacuole membrane a *Bya MET15 Δmet2 vph1-mCherry* strain has been used, as *VPH1* is a subunit of the vacuolar-ATPase V0 domain. This experiment was performed first by Iryna Entfellner.

The results of the microscopy are shown in Figure 4.2. On day one and three most of the cells, which were shifted to media without or 3 mg/l methionine, showed a vacuolar staining. The amount of the bright cells increased every day. However the bright cells indicated differences: some were completely bright, some showed only a cytoplasmatic staining and some were partially stained. In the dsRed images (show the Vph1-mCherry tag of the vacuole) of the cells shifted in SMD with 0 mg/l methionine,

the vacuole of those cells, which show a cytoplasmatic or partially staining in the eGFP images (show the acidic compartments of the cell) were visible. In contrast to that, the cells, which were completely bright, did not show a vacuole.

Some of the cells, which were shifted to media with 30mg/l methionine, were bright or cytoplasmatic stained from the beginning. On day three it was not possible to visualize the vacuole and there were lots of bright cells, partially and cytoplasmatic stained cells. From day five the number of the bright cells decreased.

In both shifts (3 or 30 mg/l methionine) the vacuolar membrane of the cells, which were bright in the eGFP images, was not visible in the dsRed pictures.

Comparing all three shift-experiments, the *Bya MET15 Δmet2 vph1-mCherry* strain shifted to media with 0 mg/l methionine showed most count of bright cells, which means most of the cells with acidic cytoplasm.

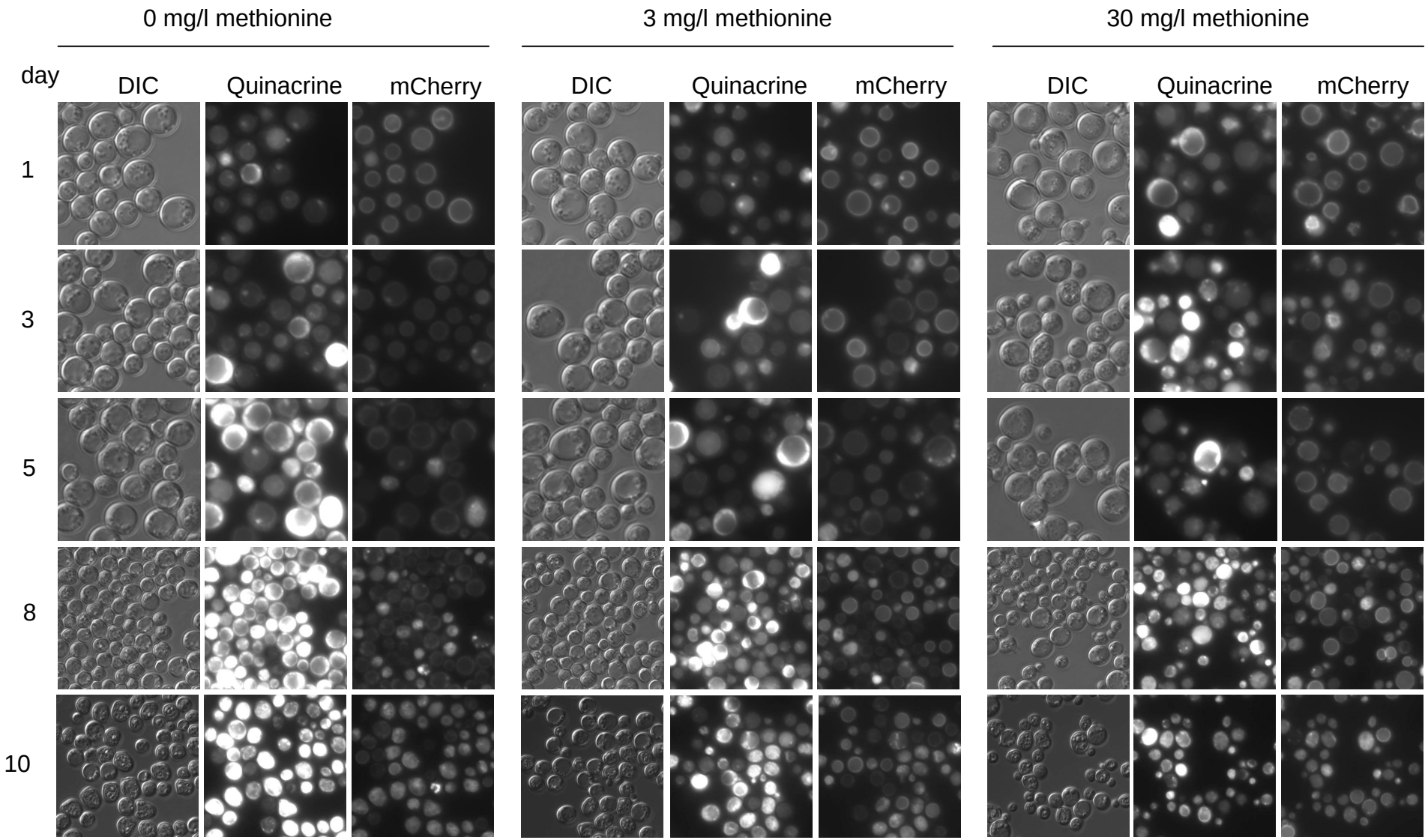

Figure 4.2: Methionine restriction induces vacuolar, and subsequently, cytoplasmic acidification. Quinacrine staining of a *Bya MET15 Δmet2 vph1-mCherry* strain. The ONC of the strain was inoculated in SMD with all amino acids to a cell count if 5*105 cells and incubated at 28°C. After for 24 hours the cells were shifted into SMD without, 3 mg/l or 30 mg/l methionine. On day one, three, five, eight and ten samples were taken and stained with quinacrine. For the quinacrine images the eGFP filter (1000 ms) and for the vph1-mCherry tag the dsRed filter (3000 ms) were used.

A statistical analysis of the microscopy images of the vacuole stained cells (only acidic vacuole, not acidic cytoplasm), the bright cells and of the cells with a bright cytoplasm or which are partially bright had been carried out (see Figure 4.3). The percentage was calculated out of the total cell count from each measurement time point. The results of the statistical analysis showed that the percentage of the vacuole stained cells was highest in the cells after the shift into SMD with 0 mg/l methionine (~80%) in contrast to the cells shifted into SMD with 3 mg/l (~55%) or 30 mg/l methionine (~35%) on day one.

In the shift without methionine, there were nearly no bright or cytoplasmatic and partially stained cells on the first day. The number of the bright or cytoplasmatic and partially stained cells increased every day. At day five there were nearly no vacuole stained cells. About 30% bright cells and 60% cytoplasmatic and partially stained cells remained. The cytoplasmatic and partially bright cells started to decrease, whereas the bright cells still increased. On day ten all types of the bright cells showed a cell count between 35% and 40%.

In the shift experiment with 3 mg/l methionine there were less than 10% bright or cytoplasmatic and partially stained cells on the first day. The cells with acidic vacuoles had a cell count of about 55%. From the first day the cell count of the acidic vacuoles decreased and the count of the cytoplasmatic and partially bright cells increased. On day ten there were about 10% vacuole stained cells, about 5% bright cells and about 35% cytoplasmatic and partially stained cells.

The treatment with 30mg/l methionine showed: On day one 10% or less of the cells were bright or cytoplasmatic and partially stained. Day three indicated between 15 and 20% bright and vacuole stained cells and 30% cytoplasmatic and partially stained cells. Day five showed only about 10% bright and vacuole stained cells. 35% of the cells were cytoplasmatic and partially stained. All stained cells decreased from the fifth day on. On day ten there were nearly no vacuole stained cells or cytoplasmatic and partially bright cells left. About 15% were totally bright stained.

A. 0 mg/l methionine

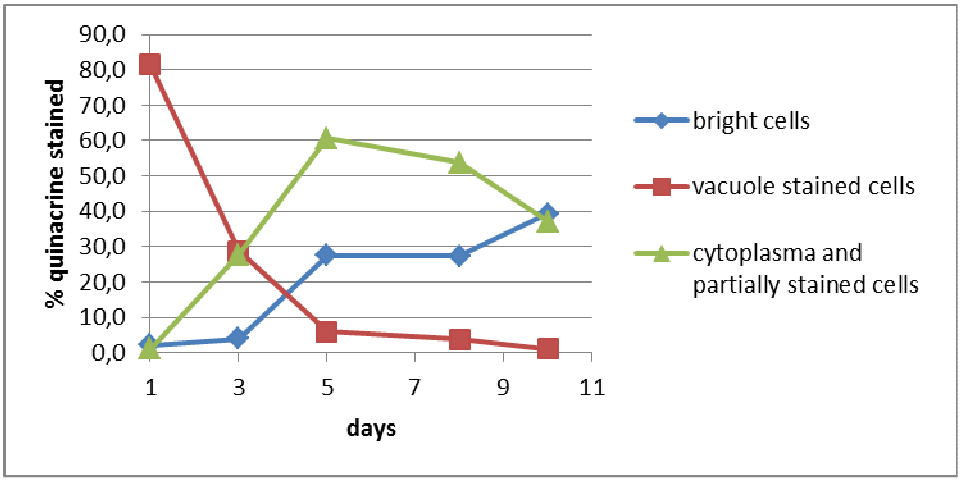

B. 3 mg/l methionine

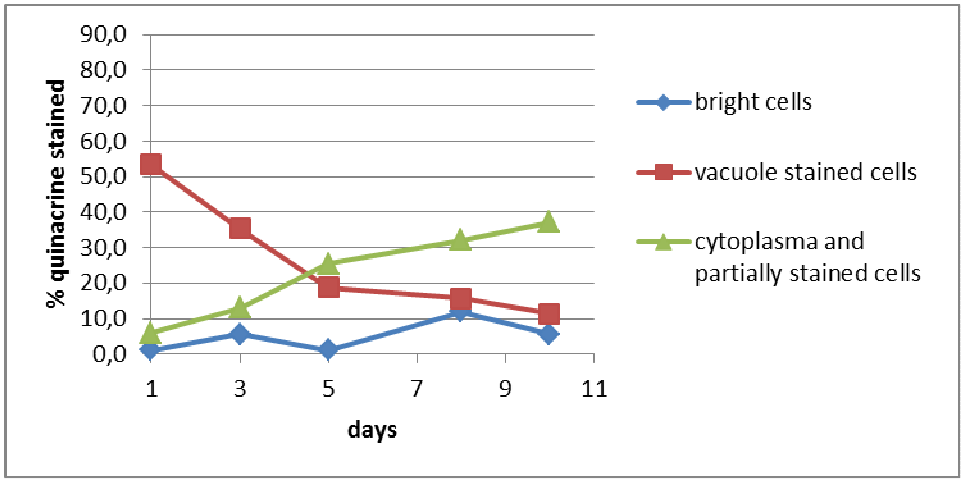

C. 30 mg/l methionine

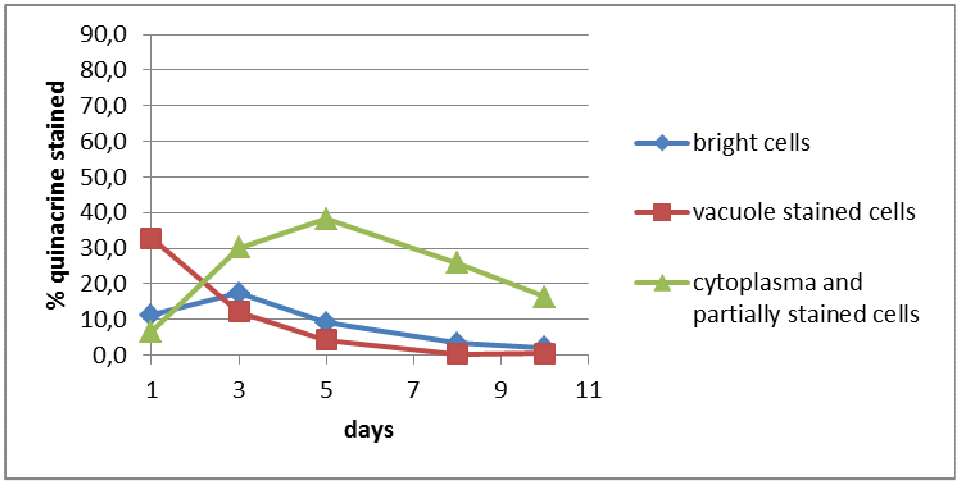

Figure 4.3: Methionine restriction causes vacuolar acidification followed by a cellular acidification. Statistical analysis of the microscopy images of the quinacrine stained *Bya MET15+ Δmet2 vph1-mCherry* after a shift into SMD with **A.** 0 mg/l, **B.** 3 mg/l or **C.** 30 mg/l methionine. The red curve represents the percentage of the acidic vacuoles, the blue curve of the complete bright cells and the green curve of the cells with a bright cytoplasm or which are partially bright out of the total cell count from each measurement time point. The cells have been counted with ImageJ.

To prove, if the bright cells were necrotic, the cells were double stained with quinacrine and PI (see Figure 4.4). In the shift without or 3 mg/l methionine the bright cells are not necrotic/PI stained. In these two shifts the necrotic cells showed complete, but weak bright cytoplasmatic quinacrine staining. In the shift with 30mg/l methionine no bright cells are PI positive on day one. However, on the other days more bright cells became PI positive.

There were more PI positive cells after the shift with 30 mg/l methionine than after the shift without or with 3 mg/l methionine.

It seemed that methionine restriction had a positive influence on the vacuolar acidification, which might be autophagy dependent.

It could be that the cytoplasmatic and partially stained cells occur because the vacuole was not intact anymore or that the vacuole was intact but pumps in the membranes or the vacuole did not function anymore, which might occur because of an increased autophagy.

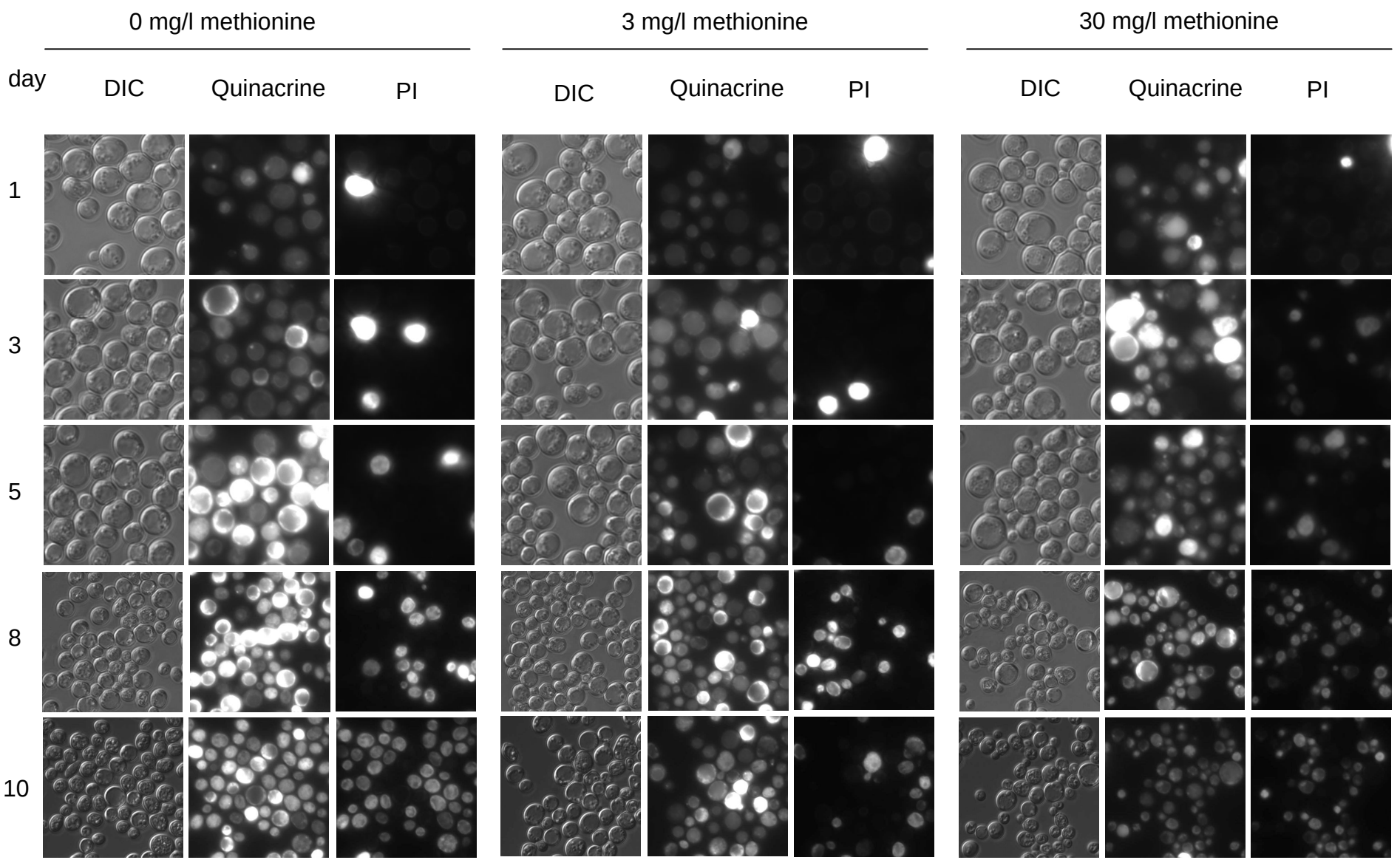

Figure 4.4: Bright cells do not show a PI positive phenotype under methionine restriction. Quinacrine and PI double staining of a *Bya MET15 Δmet2 vph1-mCherry* strain. The ONC of the strain were inoculated in SMD with all amino acids to a cell count of $5*10^5$ cells and incubated at 28°C. After 24 hours the cells were shifted into SMD without, 3 mg/l or 30 mg/l methionine. On day one, three, five, eight and ten samples were taken and stained with quinacrine and PI. For the quinacrine images the eGFP filter (1000 ms) and for the PI images the dsRed filter (200 ms) were used.

4.3 Vacuolar acidification is autophagy dependent

It is already known that the vacuole is the downstream target of autophagy. To test if the higher vacuolar acidification *Bya MET15 Δmet2 vph1-mCherry* strain under methionine restriction was autophagy dependent, a shift experiment was performed *Bya MET15 Δmet2 vph1-mCherry Δatg5* strain. *ATG5* is an autophagy related gene and essential for autophagy.

Comparing the microscopy images from Figure 4.2 and Figure 4.5 it was possible to see that *Δmet2* strain with the *ATG5* knock out showed not only an acidic vacuole but also an acidic cytoplasm after quinacrine staining on the first day. The dsRed pictures indicated that less cells did have an intact vacuole membrane.

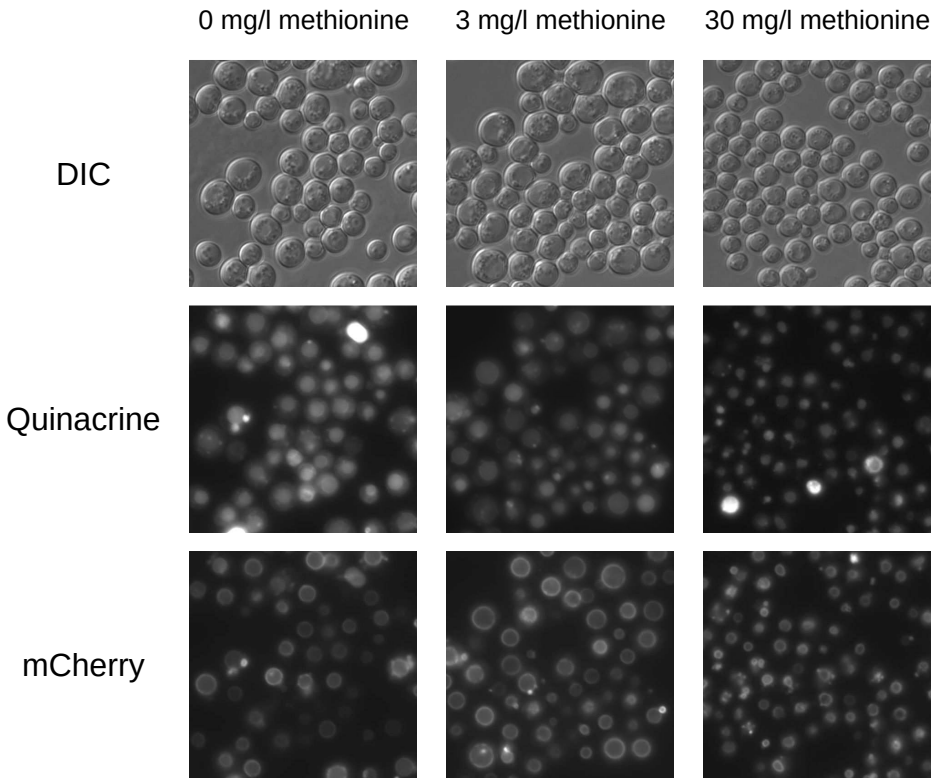

Figure 4.5: Vacuolar acidification is autophagy dependent. Quinacrine staining of a *Bya MET15 Δmet2 vph1-mCherry Δatg5* strain. ONC of the strain was inoculated in SMD with all amino acids to a cell count if $5*10^5$ cells and incubated at 28°C. After 24 hours the cells were shifted into SMD without, 3 mg/l or 30 mg/l methionine. On day one samples were taken and stained with quinacrine. For the quinacrine images the eGFP filter (1000 ms) and for the vph1-mCherry tag the dsRed filter (3000 ms) were used.

A further statistical analysis of the microscopy images of the vacuole stained cells (only acidic vacuole, not acidic cytoplasm) was done comparing the *Bya MET15 Δmet2 vph1-mCherry* strain with the *Bya MET15 Δmet2 vph1-mCherry Δatg5* strain

(see Figure 4.6). The percentage was calculated out of the total cell count from day one. The results of the statistical analysis of the *Bya MET15 Δmet2 vph1-mCherry* strain showed that the percentage of the vacuole stained cells after the shift into SMD with 0 mg/l methionine is ~80%, into SMD with 3 mg/l ~55% and 30 mg/l methionine ~35%. In contrast to these results the *Bya MET15 Δmet2 vph1-mCherry Δatg5* strain showed after the shift into SMD with 0 mg/l methionine less than five percent acidic vacuoles and after the shift with 3 mg/l or 30 mg/l methionine about 35%. These results indicated that autophagy was essential for the enhanced vacuolar acidification under methionine restriction.

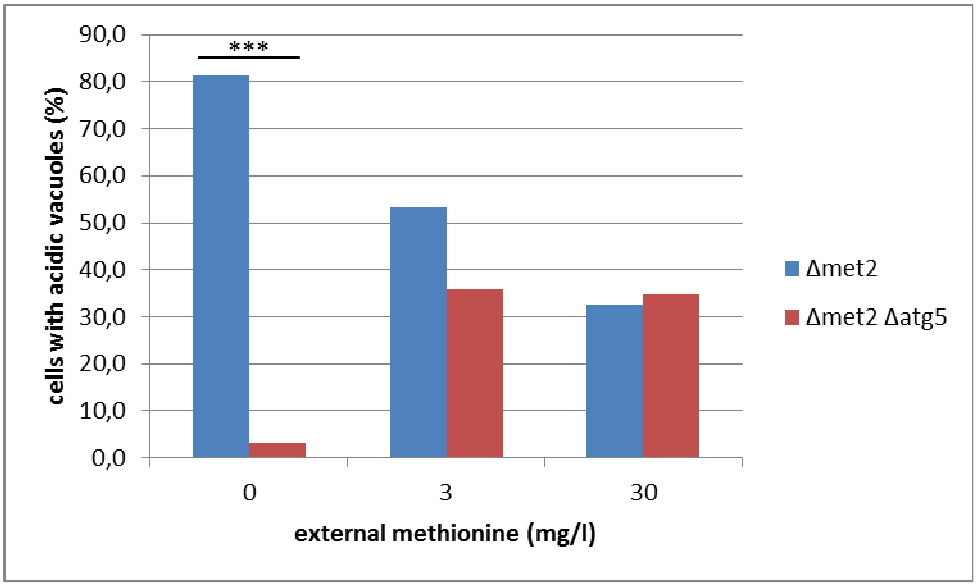

Figure 4.6: Vacuolar acidification is autophagy dependent. Statistical analysis of the microscopy images of the quinacrine stained *Bya MET15 Δmet2 vph1-mCherry and Bya MET15 Δmet2 vph1-mCherry Δatg5* after a shift into SMD with 0 mg/l, 3 mg/l or 30 mg/l methionine. The red bar represents the percentage of the acidic vacuoles of the *Bya MET15 Δmet2 vph1-mCherry Δatg5* and the blue bar represents the percentage of the acidic vacuoles of the *Bya MET15 Δmet2 vph1-mCherry* from day one. The cells had been counted with ImageJ. The differences between the *Bya MET15 Δmet2 vph1-mCherry and Bya MET15 Δmet2 vph1-mCherry Δatg5* strain in media without methionine were significant with p<0,001 (***).

4.4 Overexpression of *VMA1* and *VPH2* increase the vacuolar acidification under methionine restriction

VMA1, which is a subunit of the v-ATPase and *VPH2*, necessary for v-ATPase assembly, are known to be required for the vacuolar acidification. Therefore we overexpressed both these components of the vacoular ATPases in a pESC-*HIS*-Vector system to prove if this overexpression led to an enhanced vacuolar acidification.

Figure 4.7 shows the microscopy images of a *Bya MET15 Δmet2 pESC-HIS-*V*ector, Bya MET15 Δmet2 pESC-HIS-VMA1* and *Bya MET15 Δmet2 pESC-HIS-VPH2* strain after the quinacrine staining from the first day.

Most of the cells showed an acidic vacuole and some cells additionally indicated acidic cytoplasm. Furthermore there were nearly no bright cells.

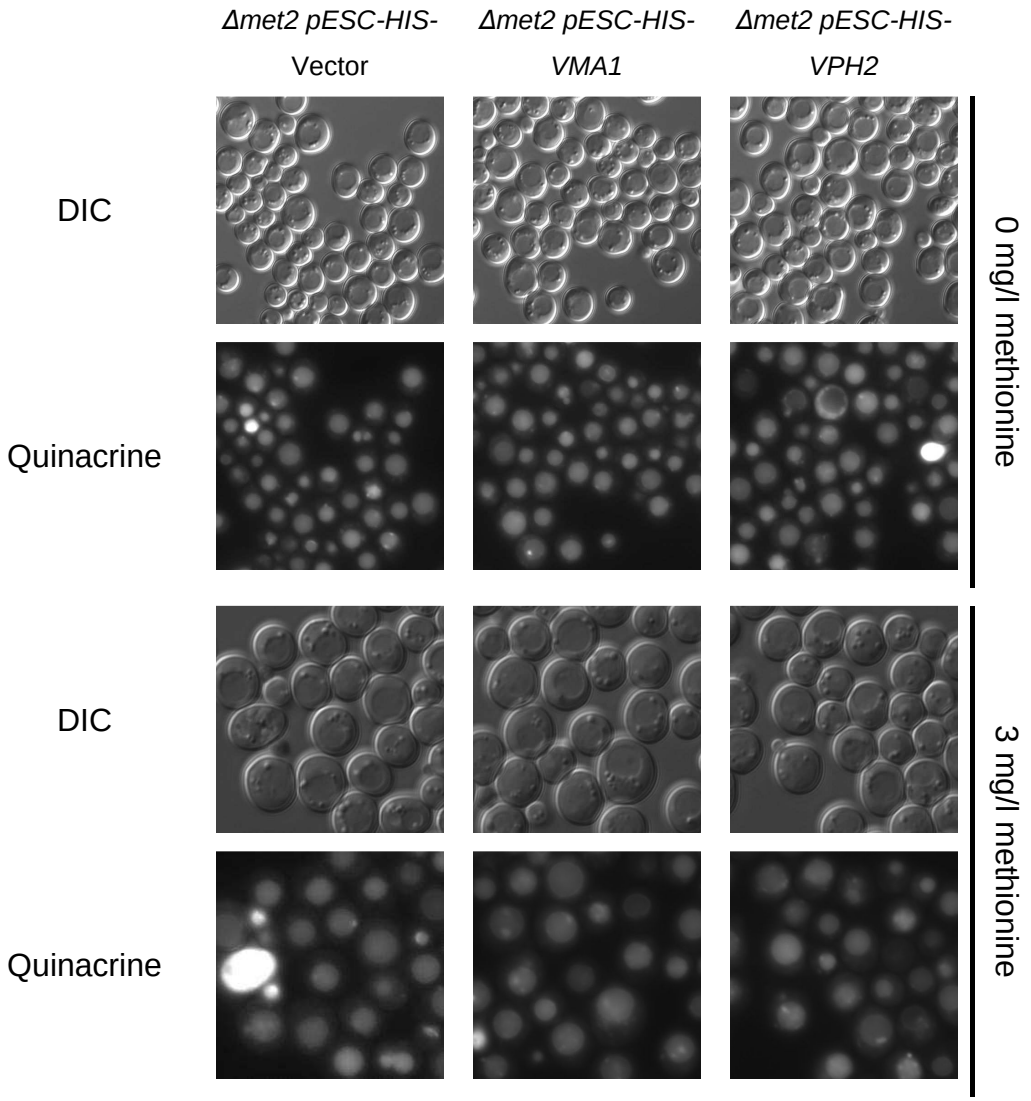

Figure 4.7: Overexpression of *VMA1* and *VPH2* increase the vacuolar acidification under methionine restriction. Quinacrine staining of *a Bya MET15 Δmet2 pESC-HIS-Vector, Bya MET15 Δmet2 pESC-HIS-VMA1* and *Bya MET15 Δmet2 pESC-HIS-VPH2* strain. The ONC of the strain was inoculated in SMD-His to a cell count if $5*10^5$ cells and incubated at 28°C. After for 24 hours the cells were shifted into SMG-His with 0 mg/l or 3 mg/l methionine. The cells were shifted into SMG to induce the promotor activity as the pESC-*HIS* plasmid contains a galactose promotor. On day one samples were taken and stained with quinacrine. For the quinacrine images the eGFP filter (1000 ms) was used. The data represent the mean +/- SEM (n=3) of one representative experiment.

Figure 4.8 shows a statistical analysis of the microscopy images of the vacuole stained cells (only acidic vacuole, not acidic cytoplasm). The percentage had been calculated out of the total cell count from day one. The results of the statistical analysis of *Bya MET15 Δmet2 pESC-HIS*-Vector, *Bya MET15 Δmet2 pESC-HIS-VMA1* and *Bya MET15 Δmet2 pESC-HIS-VPH2* indicated about 10% more acidic vacuoles in the overexpression strains in media without methionine. In the shift experiment with 3 mg/l methionine the overexpression of *VMA1* or *VPH2* exhibited about 15% more vacuole stained cells compared to the vector. Comparing both shift experiments the cells in the media with 0 mg/l methionine possess more acidic vacuoles (*Bya MET15 Δmet2 pESC-HIS*-Vector: ~67%; *Bya MET15 Δmet2 pESC-HIS-VMA1*: ~76%; *Bya MET15 Δmet2 pESC-HIS-VPH2*: ~75%) than the cells in SMD with 3 mg/l methionine (*Bya MET15 Δmet2 pESC-HIS*-Vector: ~50%; *Bya MET15 Δmet2 pESC-HIS-VMA1*: ~67%; *Bya MET15 Δmet2 pESC-HIS-VPH2*: ~64%).

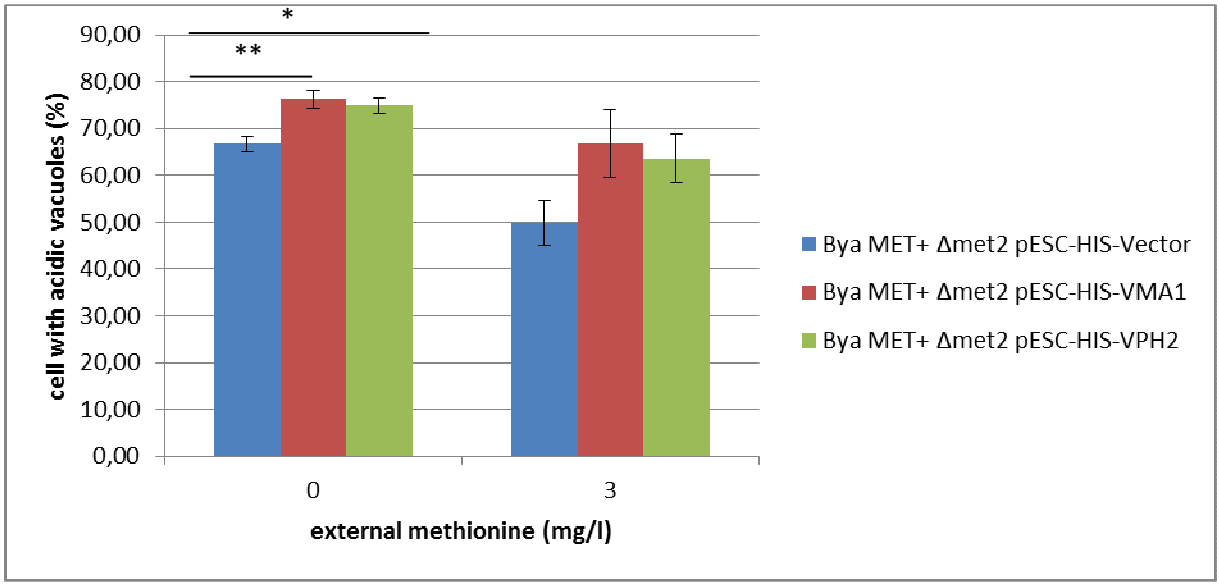

Figure 4.8: Overexpression of *VMA1* and *VPH2* increase the vacuolar acidification under methionine restriction. Statistical analysis of the microscopy images of the quinacrine stained *Bya MET15 Δmet2 pESC-HIS*-Vector, *Bya MET15 Δmet2 pESC-HIS-VMA1* and *Bya MET15 Δmet2 pESC-HIS-VPH2* after a shift into SMD with 0 mg/l or 3 mg/l methionine. The blue bar represents the percentage of the acidic vacuoles of the *Bya MET15 Δmet2 pESC-HIS-Vector*, the red bar represents the percentage of the acidic vacuoles of the *Bya MET15 Δmet2 pESC-HIS-VMA1* and the green one of the *Bya MET15 Δmet2 pESC-HIS-VPH2* strain from day one. The cells had been counted with ImageJ. The differences in media without methionine were significant with $p<0,05$ (*) between *Bya MET15 Δmet2 pESC-HIS-Vector* and *Bya MET15 Δmet2 pESC-HIS-VPH2* and with $p<0,01$ (**) between *Bya MET15 Δmet2 pESC-HIS-Vector* and *Bya MET15 Δmet2 pESC-HIS-VMA1.* The data are representing the mean ± SEM (n=3) of one representative experiment.

4.5 Deletion of *CDC55,* the regulatory subunit of PP2A and the protein kinases *SCH9* and *TOR1* leads to an increased survival in a methionine auxotrophic *Δmet2* strain shifted to media without methionine

The TOR (target of rapamycin) signalling pathway is known to cause cell cycle arrest, down regulation of protein synthesis and to inhibit autophagy under nutrient rich conditions. To prove the role of the protein kinases of the TOR signalling pathway, a shift aging experiment with deletion mutants of *CDC55*, *SCH9* or *TOR1* in a *Δmet2* strain was performed. The cells were cultured in SMD with all amino acids at 28°C and shifted in SMD without or 30 mg/l methionine after 24 hours. 500 cells were plated on YPD agar plates at different time points.

In both SMD without or with 30 mg/ml methionine all three knock out strains (*Δmet2 Δcdc55, Δmet2 Δtor1, Δmet2 Δsch9*) show a better survival compared to the methionine auxotrophic *Δmet2* strain. In SMD without methionine the highest effect showed the *Δmet2 Δcdc55* strain with 10% better survival compared to the *Δmet2* strain. The *Δmet2 Δtor1* and the *Δmet2 Δsch9* strain indicated an increased survival less than 10%. (Figure 4.9 A)

In contrast to the results of the cells shifted in 0 mg/l methionine, the *Δmet2 Δtor1* and the *Δmet2 Δsch9* strain caused an increased survival about 15% compared to the *Δmet2* strain and the *Δmet2 Δcdc55* strain less than 10% in media with 30 mg/l methionine. (Figure 4.9 B)

A. 0 mg/l methionine

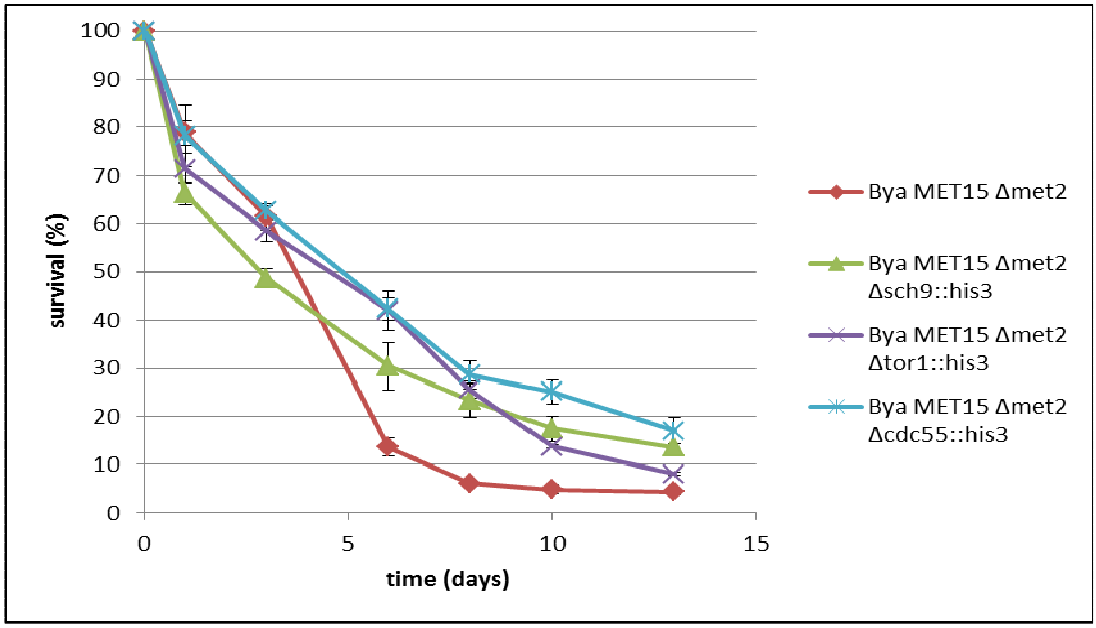

B. 30 mg/l methionine

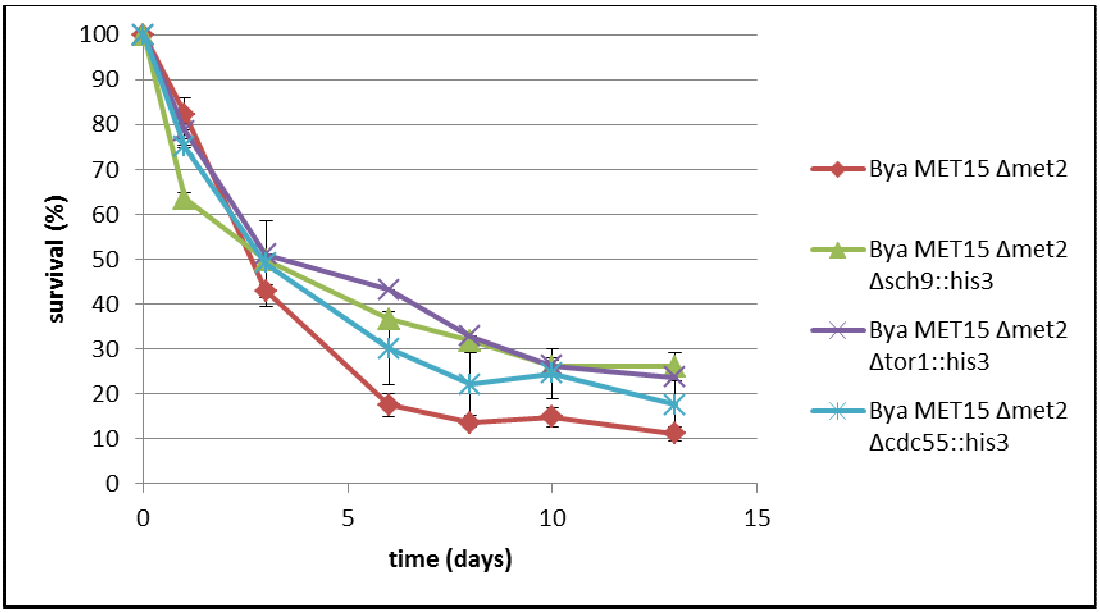

Figure 4.9: Deletion of the regulatory subunit *CDC55* of PP2A and the protein kinases *SCH9* and *TOR1* leads to a better survival compared to the *Δmet2* strain when shifted in media with 0 or 30 mg/l methionine. The ONC of the strain were inoculated in SMD with all amino acids to a cell count of $5*10^5$ cells and incubated at 28°C. After 24 hours the cells were shifted into SMD with **A.** 0 mg/l or **B.** 30 mg/l methionine. The lifespan of the shifted chronological aged cells was determined through clonogenic cell survival assay. The data are representing the mean ± SEM (n=4 to 6) of one representative experiment.

These results lead to the conclusion, that Cdc55p, Tor1p and Sch9p have a negative effect on the cell survival under both conditions SMD without and with 30 mg/ml methionine.

4.6 Deletion of the methyltransferase of the PP2A (*ppm1*) shows autophagic activity only on day one of a chronological aging

The protein phosphatase 2A (PP2A) is required for the regulation of the *TOR* kinase, as it interacts with *Tap42* and *SCH9* and therefore inhibits autophagy. To test if a deletion of the methyltransferase *PPM1*, which is needed to activate PP2A, or *PPH21* (part of the catalytic subunit of PP2A) in a *Δmet2* strain led to a better survival compared to wild type, a clonogenicity assay was performed. A knock out of *PPM1* potentially leads to a complete inactivation of the PP2A, whereas a deletion of *PPH21* might have only marginal effects due to still functional *PPH22*.

Figure 4.10 shows the results of the clonogenicity assay. In the first three days both knock outs (*Bya MET15 chr. Atg8-GFP Δppm1* and *Bya MET15 chr. Atg8-GFP Δpph21*) indicated a better survival compared to the wild type strain. From day three the cell counts of *Bya MET15 chr. Atg8-GFP Δppm1* decreased. On day eight nearly all cells were dead. *Bya MET15 chr. Atg8-GFP Δpph21* showed a better survival compared to *Bya MET15 chr. Atg8-GFP* till day eight. From day eight till day twelve the two strains nearly indicated the same survival.

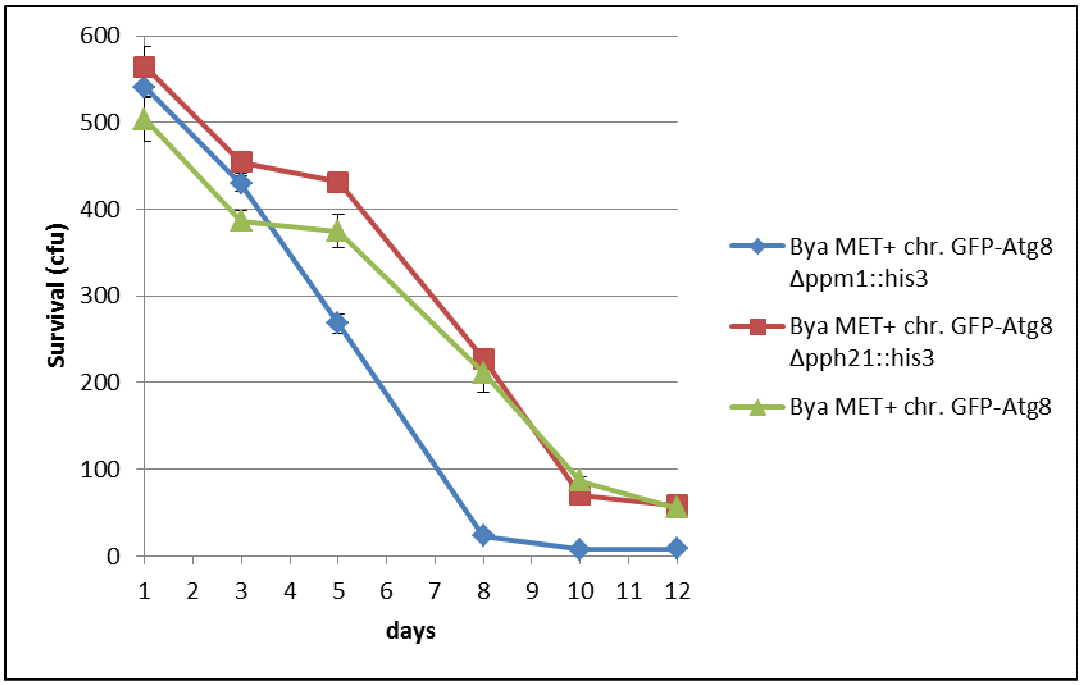

Figure 4.10: Deletion of the catalytical subunite of PP2A (*pph21*) and the methyltransferase *ppm1* of the PP2A in a *Δmet2* back ground does not show a better survival compared to the Δmet2 strain in a chronological aging experiment. The ONC of the strain were inoculated in 10 ml SMD with all amino acids to an OD_{600} of 0,05 and incubated at 28°C. The lifespan of the chronological aged cells was determined through clonogenic cell survival assay. The data are representing the mean ± SEM (n= 6) of one representative experiment.

To test if the deletion of *PPM1* and *PPH21* leads to an enhanced autophagy a Western Blot analysis was performed. Therefore a *Bya MET15 chr. Atg8-GFP, Bya MET15 chr. Atg8-GFP Δppm1* and *Bya MET15 chr. Atg8-GFP Δpph21* were used to detect autophagy.

For the Western blot analysis samples were taken on days one, two, three and five after inoculating in SMD with all amino acids. Figure 4.11 shows the result of the Western Blot analysis. The results of *Bya MET15 chr. Atg8-GFP* indicated the same, which was shown in Figure 4.1: The amount of free GFP increased in this strain every day till day three. On day five the amount of the free GFP started to decrease, however, the signal was stronger as on day one.

In contrast to this result *Bya MET15 chr. Atg8-GFP Δppm1* indicated only a free GFP signal on day one. The induction of free GFP was only a little higher than in the wild type strain. Because the GAPDH control is higher too this could come from differences in amount of loaded protein. From day two on, no free GFP signal was detectable, although ~500 cfu formed in the clonogenicity assay (see Figure 4.10).

Bya MET15 chr. Atg8-GFP Δpph21 showed nearly the same amount of free GFP in the first three days. On day one the free GFP signal was higher than in *Bya MET15 chr. Atg8-GFP* and on day two and three nearly the same. However, this signal decreased on day five.

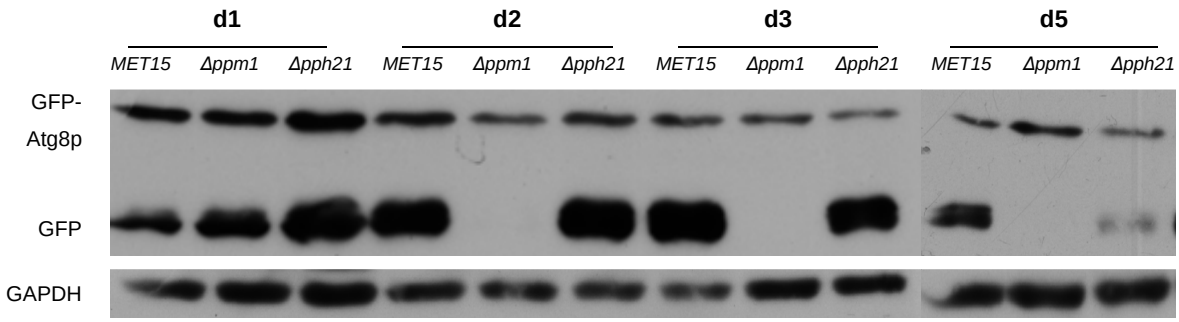

Figure 4.11: *Ppm1* knock out strain indicates autophagic activity only on day one. The ONC of *Bya MET15 chr. Atg8-GFP*, *Bya MET15 chr. Atg8-GFP Δppm1* and *Bya MET15 chr. Atg8-GFP Δpph21* strains were inoculated in SMD with all amino acids with an OD_{600} 0,05 and incubated at 28°C. On day one, two, three and five samples were taken. A chemical lyses was performed. The samples were loaded on a SDS gel and a Western blot analysis was done. The free GFP has a molecular weight of ~30 kDa and the Atg8-GFP construct ~48 kDa. The molecular weight of the bands was evaluated with a standard, PageRulerTM Prestained Protein Ladder. The expression of the free GFP and the Atg8-GFP construct were detected with a α-GFP antibody. As loading control a α-GAPDH antibody was used.

To confirm the results of the Western blot analysis, a fluorescence microscopy of the Atg8-GFP expressing cells was performed. The Atg8-GFP protein showed punctuate (autophagosome) or/and vacuolar localization (delivery of the protein into the vacuole).

The results of the microscopy (see Figure 4.12) corresponded with the results of the Western Blot analysis. On day one *Bya MET15 chr. Atg8-GFP* indicated some autophagosomes and Atg8p were localized in the vacuole. In contrast to this *Bya MET15 chr. Atg8-GFP Δppm1* and *Bya MET15 chr. Atg8-GFP Δpph21* showed enhanced vacuolar localization of the protein compared to the wild type strain. The delivery of Atg8p into the vacuole in *Bya MET15 chr. Atg8-GFP* increased every day till day three and decreased on day five. *Bya MET15 chr. Atg8-GFP Δppm1* only indicated some autophagosomes from the second day. *Bya MET15 chr. Atg8-GFP Δpph21* showed high levels of vacuolar localization of Atg8p in the first three days. This level decreased on day five.

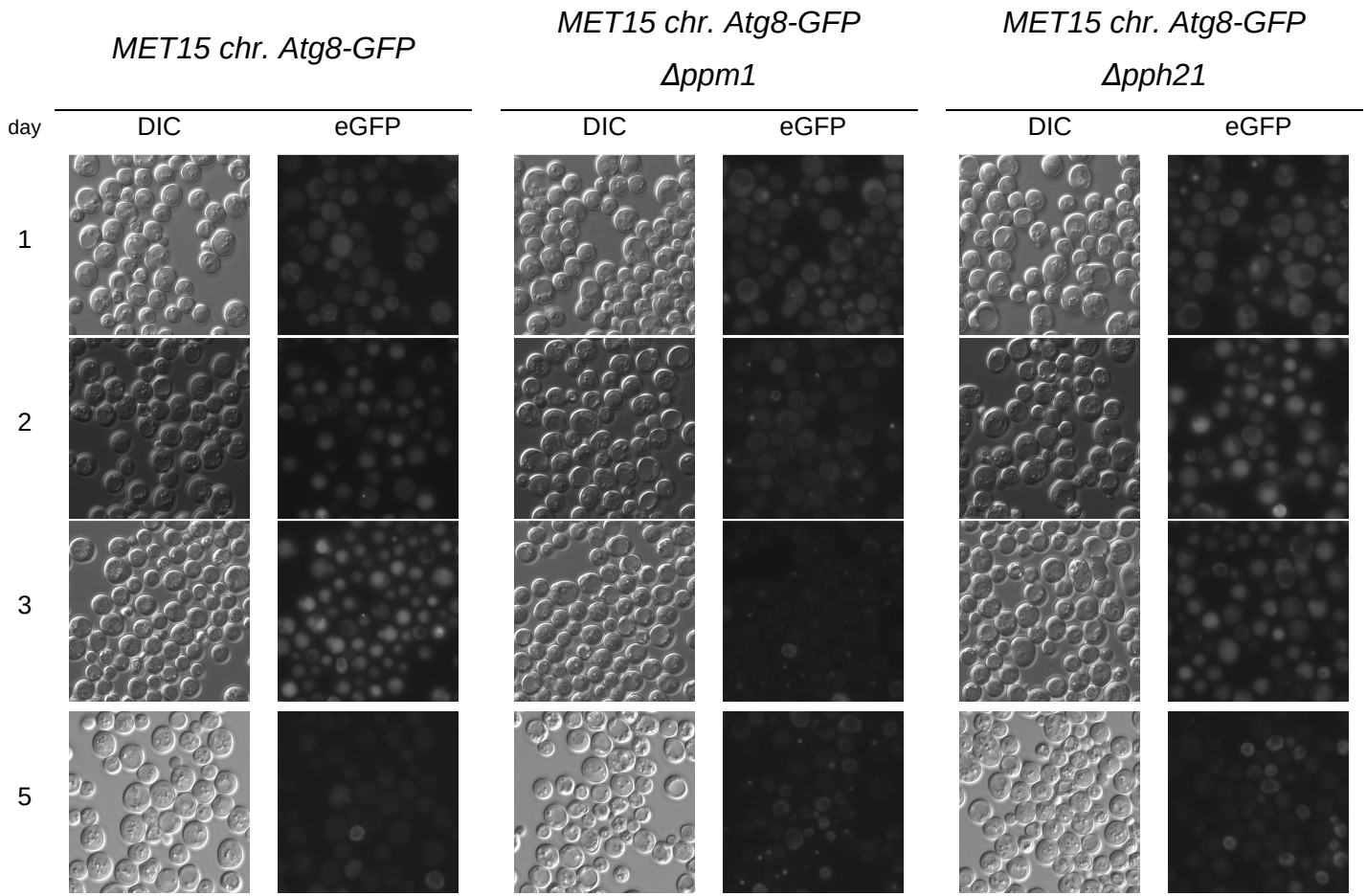

Figure 4.12: *Ppm1* knock out strain indicates autophagic activity only on day one. The ONC of *Bya MET15 chr. Atg8-GFP*, *Bya MET15 chr. Atg8-GFP Δppm1* and *Bya MET15 chr. Atg8-GFP Δpph21* strains were inoculated in SMD with all amino acids with an OD_{600} 0,05 and incubated at 28°C. On day one, two, three and five samples were taken. For the fluorescence images the eGFP filter (5000 ms) was used.

4.7 Deletion of *ppm1* in a *Δmet2* back ground indicates a time delay in the acidification of the cytoplasm compared to a *Δmet2* strain under complete methionine restriction in a shift-aging

SCH9 is part of the TOR signaling pathway and inhibits autophagy under nutrient rich conditions. It is already known that it is phosphorylated by *TORC1*. However, recent studies indicated that the *PP2A* also might regulate *SCH9*, by controlling the phosphorylation state of *SCH9*.

To test if a *Bya MET15 Δmet2 Δppm1 and Bya MET15 Δmet2 Δsch9* showed similar vacuolar acidification levels like the *Bya MET15 Δmet2,* a quinacrine and PI double staining was performed in an aging shift experiment with 0 mg/l methionine (see Figure 4.13) or 0 mg/l leucine (see Figure 4.14).

Comparing the results of the three strains of the aging shift experiment with 0 mg/l methionine it was possible to see that in the first three days there were nearly no differences in the three strains. On day one most of the cells showed an acidic vacuole and there were nearly no PI positive cells. Day three indicated some bright cells (completely, cytoplasmatic or partially stained). However, most of the cells showed an acidic vacuole. *Bya MET15 Δmet2 Δsch9* revealed more PI positive cells than the other two strains. On day five in the quinacrine images of *Bya MET15 Δmet2* showed lots of bright cells (complettly, cytoplasmatic or partially stained). Some further cells were PI positive. Most of the cells of *Bya MET15 Δmet2 Δppm1* possessed an acidic vacuole and only some an acidic cytoplasm. There were nearly no PI positive cells. *Bya MET15 Δmet2 Δsch9* indicated some bright cells and vacuole stained cells. However, there were cells, which were completely, but only weakly stained and most of these cells were PI positive.

On day eight and ten the bright cells in the *Bya MET15 Δmet2* strain started to decrease and the amount of the PI positive cells started to increase. The bright cells began to correspond with the PI positive cells. Most of the cells of *Bya MET15 Δmet2 Δppm1* indicated an acidic cytoplasm. However, there remained also some cells with an acidic vacuole. Nearly no cells were PI positive. Most of the cells of the *Bya MET15 Δmet2 Δsch9* showed complete, but weak staining. There were still some bright cells, which partly corresponded with the PI positive cells. Finally it can be said, that *Bya MET15 Δmet2 Δppm1* showed a delay in the acidification of the

cytoplasm compared to the *Bya MET15 Δmet2* strain and this delay did not occur in *Bya MET15 Δmet2 Δsch9* under methionine restriction.

In contrast to this experiment, most of the cells which were shifted into media without leucine showed an acidic vacuol and there were nearly no PI positive cells on day one. On day three most of the cells of the *Bya MET15 Δmet2* strain were bright (completely, cytoplasmatic or partially stained). The PI positive cells started to increase and these cells corresponded with the bright cells. There were nearly no cells with an acidic vacuole. *Bya MET15 Δmet2 Δppm1* and *Bya MET15 Δmet2 Δsch9* showed fewer bright cells compared to *Bya MET15 Δmet2.* There remained cells with an acidic vacuole. Only some cells were PI positive. From day five till day ten most of the cells of *Bya MET15 Δmet2* and *Bya MET15 Δmet2 Δsch9* showed a complete, but weak staining. There were nearly no bright cells. Most of the cells were PI postive.

On day five in the quinacrine images of the *Bya MET15 Δmet2 Δppm1* strain most of the cells showed an acidic cytoplasm and some cells with an acidic vacuole remained. On day eight and ten most of the cells were bright (completely, cytoplasmatic or partially stained). There were some PI positive cells, which corresponded with the complete bright cells.

In conclusion it can be said, that the delay in the acidification of the cytoplasm of *Bya MET15 Δmet2 Δppm1* compared to *Bya MET15 Δmet2* remained under leucine restriction, however, not as well as under methionine restriction. It is already known from Lisa Klug´s master thesis that this different type of cell death, which occurs under methionine restriction, appears also under leucine restriction, however, not in that high amount.

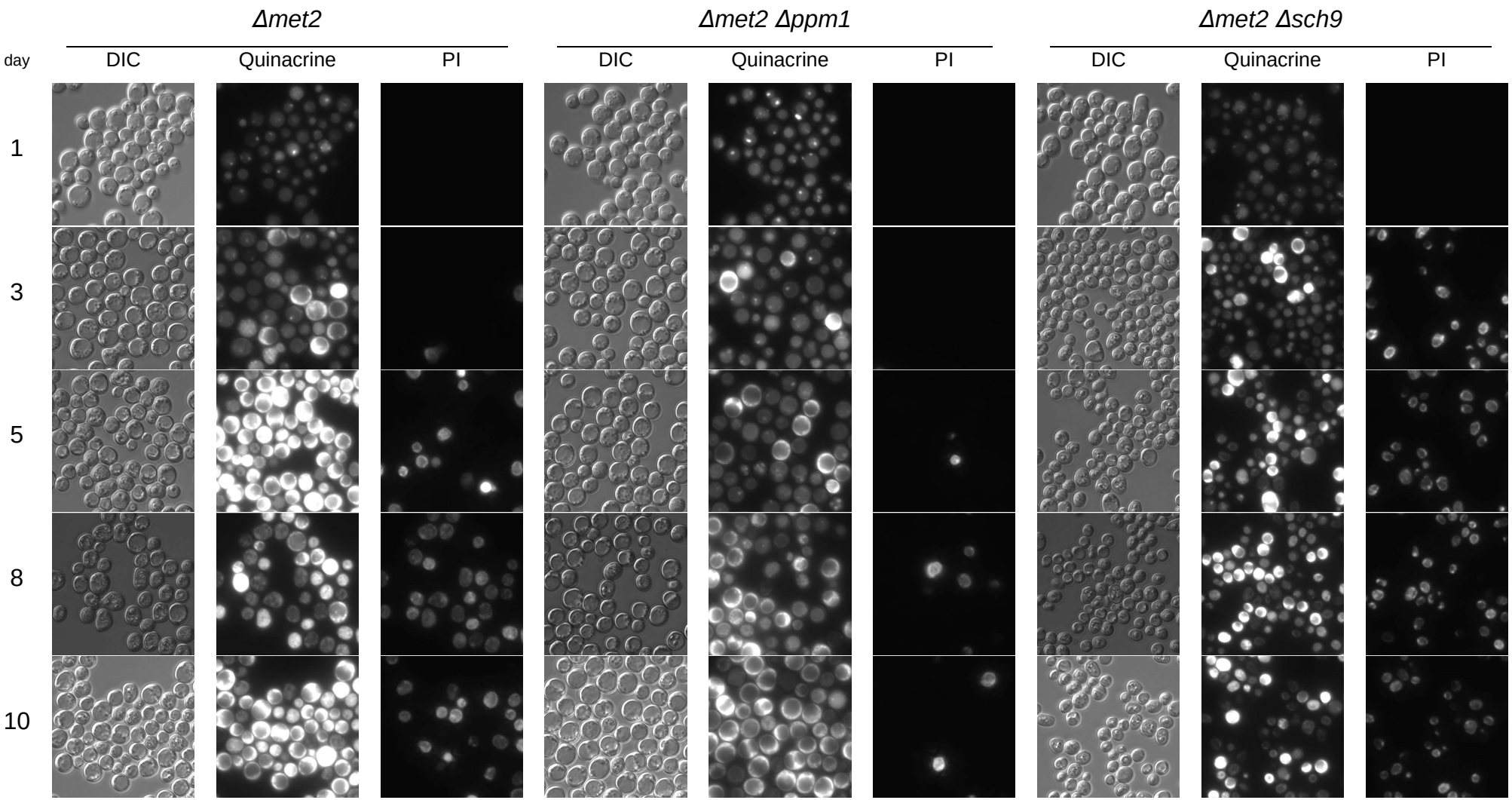

Figure 4.13: Deletion of *ppm1* in a *Δmet2* back ground indicates a time delay in the acidification of the cytoplasm compared to a *Δmet2* strain under complete methionine restriction during a shift-aging. Quinacrine and PI double staining of a *Bya MET15 Δmet2, Bya MET15 Δmet2 Δppm1* and *Bya MET15 Δmet2 Δsch9*. The ONC of the strain were inoculated in SMD with all amino acids to a cell count of $5*10^5$ cells and incubated at 28°C. After 24 hours the cells were shifted into SMD 0 mg/l methionine. On day one, three, five, eight and ten samples were taken and stained with quinacrine and PI. For the quinacrine images the eGFP filter (1000 ms) and for the PI images the dsRed filter (200 ms) were used.

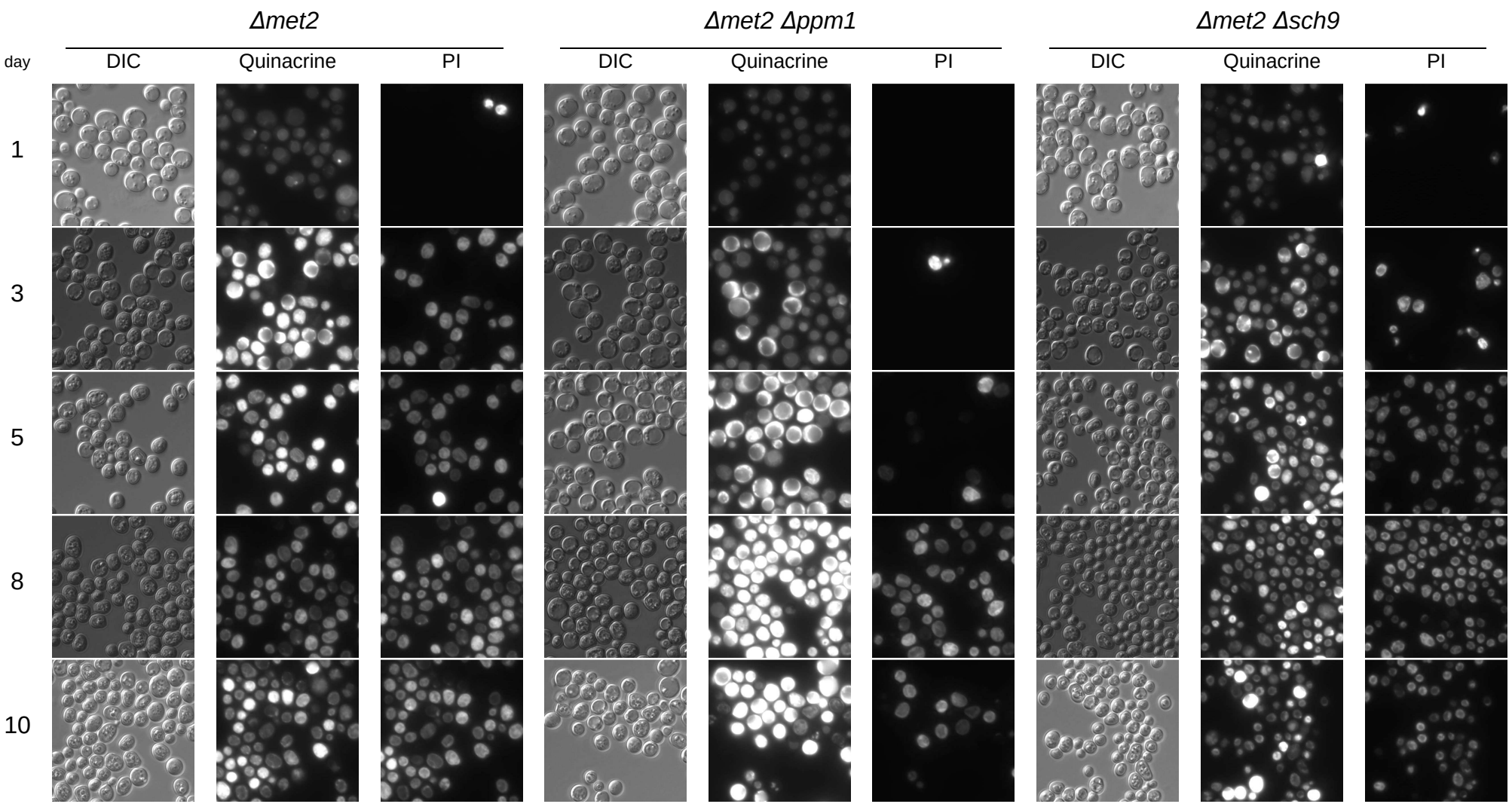

Figure 4.14: Deletion of *ppm1* in a *Δmet2* back ground indicates a time delay in the acidification of the cytoplasm compared to a *Δmet2* strain in media without leucine. Quinacrine and PI double staining of a *Bya MET15 Δmet2, Bya MET15 Δmet2 Δppm1* and *Bya MET15 Δmet2 Δsch9*. The ONC of the strain were inoculated in SMD with all amino acids to a cell count of $5*10^5$ cells and incubated at 28°C. After 24 hours the cells were shifted into SMD 0 mg/l leucine. On day one, three, five, eight and ten samples were taken and stained with quinacrine and PI. For the quinacrine images the eGFP filter (1000 ms) and for the PI images the dsRed filter (200 ms) were used.

A statistical analysis of the microscopy images of the vacuole stained cells (only acidic vacuole, not acidic cytoplasm), the bright cells, the cells with a bright cytoplasm or the ones which were partially bright and the PI positive cells were carried out (see Figure 4.15). The percentage was calculated out of the total cell count from each measurement time point.

The results of the statistical analysis showed that the percentage of the vacuole stained cells were highest in the cells after the shift into SMD with 0 mg/l methionine (*Bya MET15 Δmet2* and *Bya MET15 Δmet2 Δppm1* ~60%; *Bya MET15 Δmet2 Δsch9:* ~35%) in contrast to the cells shifted into SMD with 0 mg/l leucine (*Bya MET15 Δmet2* and *Bya MET15 Δmet2 Δsch9* ~20%; *Bya MET15 Δmet2 Δppm1:* ~60%) on day one. Only *Bya MET15 Δmet2 Δsch9* indicated cytoplasmatic and partially bright cells and PI positive cells (~10%).

In the shift without methionine the number of the cells with an acidic vacuole of *Bya MET15 Δmet2, Bya MET15 Δmet2 Δppm1* and *Bya MET15 Δmet2 Δsch9* decreased every day. On day five *Bya MET15 Δmet2* and *Bya MET15 Δmet2 Δppm1* showed only about 10% of cells with an acidic vacuole. In contrast to this the *Bya MET15 Δmet2 Δsch9* indicated a vacuolar staining of about 15 to ~20% till day ten. This staining remained till day ten. *Bya MET15 Δmet2* possessed nearly no acidic vacuoles from day eight. In contrast to this result, *Bya MET15 Δmet2 Δppm1* indicated about five percent vacuole stained cells on day ten. *Bya MET15 Δmet2* showed an increase of the cytoplasmatic and partially stained cells till day five (~70%). Then the amount of cytoplasmatic and partially bright stained cells started to decrease till day ten (~55%). The amount of cytoplasmatic and partially bright cells of *Bya MET15 Δmet2 Δppm1* and *Bya MET15 Δmet2 Δsch9* increased to 10% till day five. Afterwards there was a strongly rise to ~75% of these cells of *Bya MET15 Δmet2 Δppm1* till day ten. In contrast to this the amount of the cytoplasmatic and partially stained cells of *Bya MET15 Δmet2 Δsch9* increased only to about 35% till day ten. *Bya MET15 Δmet2* showed an increase in the bright cells to 10% from day three till day five. Afterwards the amount of the bright cells decreased. *Bya MET15 Δmet2 Δsch9* showed about five percent bright cells from day three till day eight. This amount increased till ~15%. Through the whole time period *Bya MET15 Δmet2 Δppm1* indicated nearly no bright cells. From the first cells the PI positive cells increased in all three

strains. On day ten *Bya MET15 Δmet2* showed about 35%, *Bya MET15 Δmet2 Δppm1* ~15% and *Bya MET15 Δmet2 Δsch9* about 50% PI positive cells.
In the shift experiment with 0 mg/l leucine the number of the cells with an acidic vacuole decreased in *Bya MET15 Δmet2, Bya MET15 Δmet2 Δppm1* and *Bya MET15 Δmet2 Δsch9* every day. *Bya MET15 Δmet2* indicated nearly no acidic vacuoles from day three. The amount of the vacuolar stained cells of *Bya MET15 Δmet2 Δppm1* decreased from about ~55% to ~10% till day five. From day eight there were nearly no cells with an acidic vacuole left. *Bya MET15 Δmet2 Δsch9* showed about 20% cells with acidic vacuole in the first three days. Day five indicated nearly no cells with a vacuolar staining. The amount of the cells with cytoplasmatic and partially staining increased to ~45% in *Bya MET15 Δmet2* till day three. This amount remained till day five. Afterwards the cells with cytoplasmatic and partially staining decreased to about 15% till day ten. *Bya MET15 Δmet2 Δppm1* showed an increase of the cytoplasmatic and partially bright cells to ~55% till day five. On day ten about 50% of these cells were left. In the first three days *Bya MET15 Δmet2 Δsch9* showed an increase from ~10 till ~30% of the cells with cytoplasmatic and partially staining. From day five till day ten the amount remained about 25%.
The amount of the bright cells of *Bya MET15 Δmet2* increased to nearly 20% till day five and decreased to ~15% till day ten. *Bya MET15 Δmet2 Δppm1* indicated nearly no bright cells till day five. The amount of the bright cells increased to nearly 30% till day eight and decreased to ~20% till day ten. *Bya MET15 Δmet2 Δsch9* showed an increase of the bright cells to about five percent from the first day till day ten.
From the first cells the PI positive cells increased in all three strains. On day ten *Bya MET15 Δmet2* showed about 65%, *Bya MET15 Δmet2 Δppm1* ~40% and *Bya MET15 Δmet2 Δsch9* about 75% PI positive cells.

Comparing the results of the statistical analysis of the aging shift experiment in media with 0 mg/l methionine or leucine they indicated that in both experiments, there was a delay in the acidification of the cytoplasm compared to the *Bya MET15 Δmet2* of the *Bya MET15 Δmet2 Δppm1*. However, this effect was not so high in cells in media without leucine. A delay in the acidification of the cytoplasm was also shown *Bya MET15 Δmet2 Δsch9* under methionine restriction, but this effect was reduced compared to *Bya MET15 Δmet2 Δppm1* and did not arise under leucine restriction.

A. 0 mg/l methionine; *Δmet2*

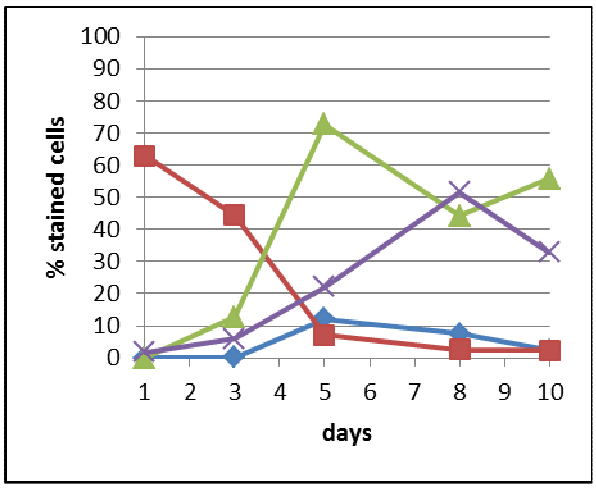

B. 0 mg/l leucine; *Δmet2*

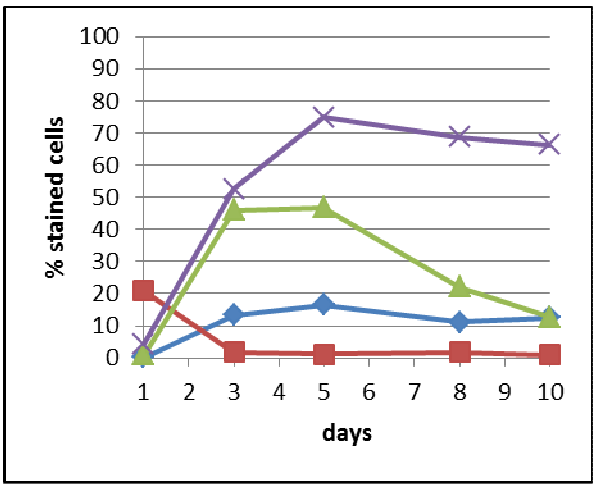

C. 0 mg/l methionine; *Δmet2 Δppm1*

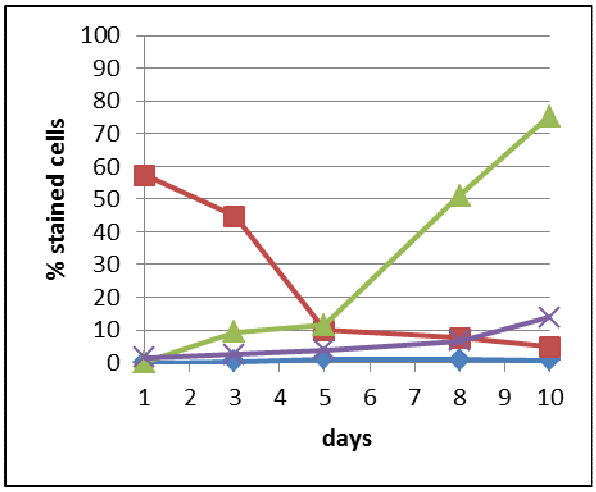

D. 0 mg/l leucine; *Δmet2 Δppm1*

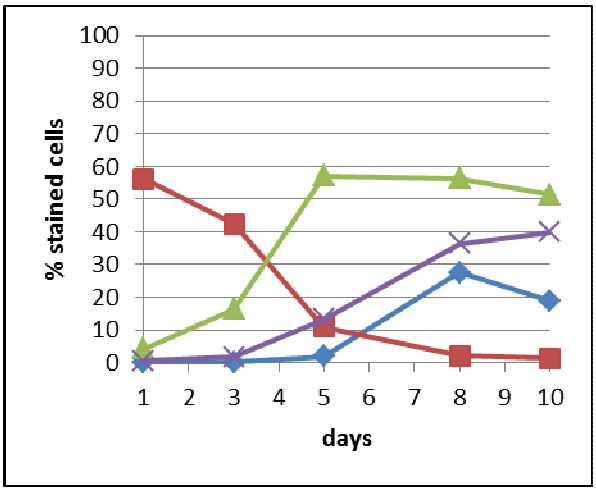

E. 0 mg/l methionine; *Δmet2 Δsch9*

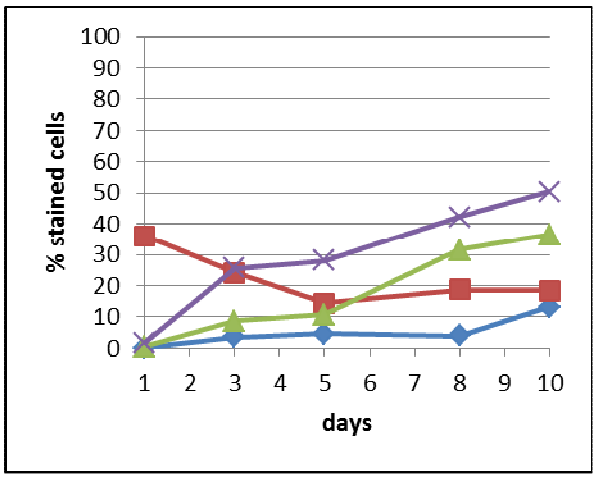

F. 0 mg/l leucine; *Δmet2 Δsch9*

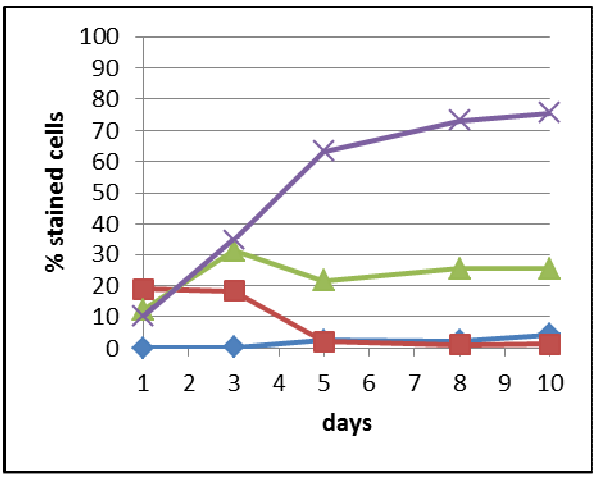

Figure 4.15: Deletion of *ppm1* in a *Δmet2* back ground indicates a time delay in the acidification of the cytoplasm compared to a *Δmet2* strain under methionine restriction. Statistical analysis of the microscopy images of the quinacrine stained *Bya MET15 Δmet2, Bya MET15 Δmet2 Δppm1* and *Bya MET15 Δmet2 Δsch9* after a shift into SMD with 0 mg/l methionine or 0 mg/l leucine. The red curve represents the percentage of the acidic vacuoles, the blue curve of the complete bright cells, the green curve of the cells with a bright cytoplasm or which are partially bright and the violet curve the PI positive cells out of the total cell count from each measurement time point. The cells have been counted with ImageJ.

Further a quinacrine and PI double staining and a statistical analysis in a shift experiment with 0 mg/l methionine or leucine was performed of a *Bya MET15 Δmet2 Δrts1* strain (see attachment). *RTS1* is the regulatory subunit of the PP2A. The acidic vacuoles remained under methionine restriction in contrast to the leucine restriction. However, this rescue effect of the *Δrts1* clones was instable, when the cells were stored at -80°C.

To prove if the delay in the acidification of the cytoplasm *Bya MET15 Δmet2 Δppm1* occured too after a shift experiment in media with 30 mg/l methionine, a quinacrine and PI double staining was performed in an aging shift experiment with 0 mg/l methionine (see Figure 4.16) or 30 mg/l methionine (see Figure 4.17).

Comparing the results of the microscopy images of the cells treated with 0 mg/l or 30 mg/l methionine, nearly all cells of *Bya MET15 Δmet2* and *Bya MET15 Δmet2 Δppm1* showed an acidic vacuole in media without methionine on day one. In contrast to this *Bya MET15 Δmet2* in media with 30 mg/l methionine indicated some bright cells and cells with an acidic cytoplasm. In both experiments there were nearly no PI positive cells. On day three both experiments indicated cells with an acidic vacuole and only some bright cells or partially and cytoplasm stained cells.
On day six the quinacrine images of *Bya MET15 Δmet2* showed lots of bright cells (complettly, cytoplasmatic or partially stained) under methionine restriction. Some further cells were PI positive. Most of the cells of *Bya MET15 Δmet2 Δppm1* possessed an acidic vacuole and only some an acidic cytoplasm. There were nearly no PI positive cells. On day eight and ten most of the cytoplasmatic or partially stained cells changed to completely bright cells of *Bya MET15 Δmet2*. Most of these bright cells corresponded with the PI positive cells. On day eight *Bya MET15 Δmet2 Δppm1* indicated an increase of the cells with an acidic cytoplasm. There were also cells left with an acidic vacuole and nearly no PI positive cells occure. On day ten most of the cells were cytoplasmatic or partially stained and some cells were completely bright. Only a few cells were PI positive.
In contrast to this the microscopy images of the cells cultured in media with 30 mg/l methionin showed only a view vacuole stained cells and most of the cells were bright (completely, cytoplasmatic or partially stained) in *Bya MET15 Δmet2* and *Bya MET15 Δmet2 Δppm1* from day six till day ten. Nearly all of these bright cells were PI positive.

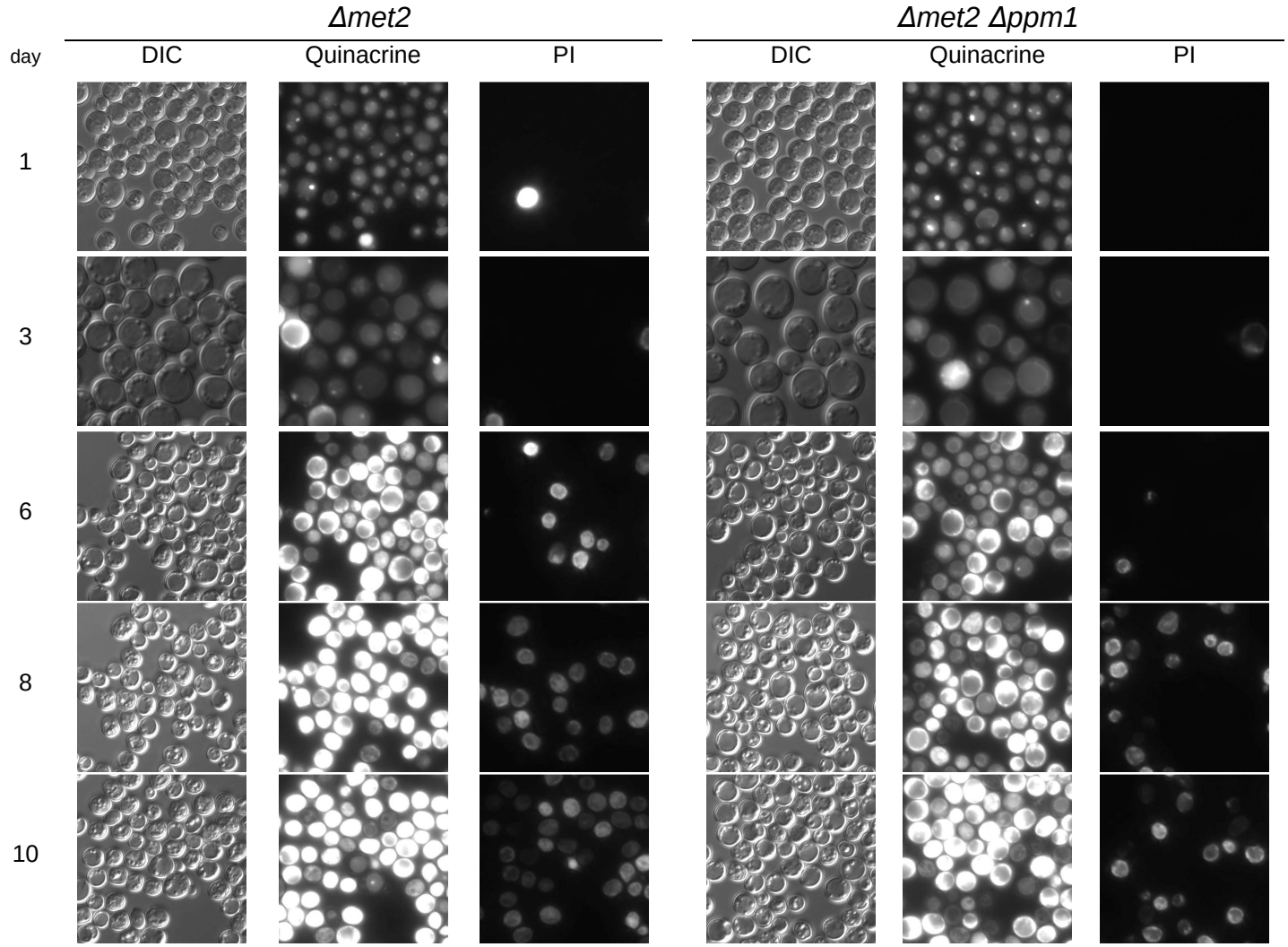

Figure 4.16: Deletion of *ppm1* in a *Δmet2* back ground indicates a time delay in the acidification of the cytoplasm compared to a *Δmet2* strain under methionine restriction. Quinacrine and PI double staining of a *Bya MET15 Δmet,* and *Bya MET15 Δmet2 Δppm1*. The ONC of the strain were inoculated in SMD with all amino acids to a cell count of $5*10^5$ cells and incubated at 28°C. After 24 hours the cells were shifted into SMD 0 mg/l methionine. On day one, three, six, eight and ten samples were taken and stained with quinacrine and PI. For the quinacrine images the eGFP filter (1000 ms) and for the PI images the dsRed filter (200 ms) were used.

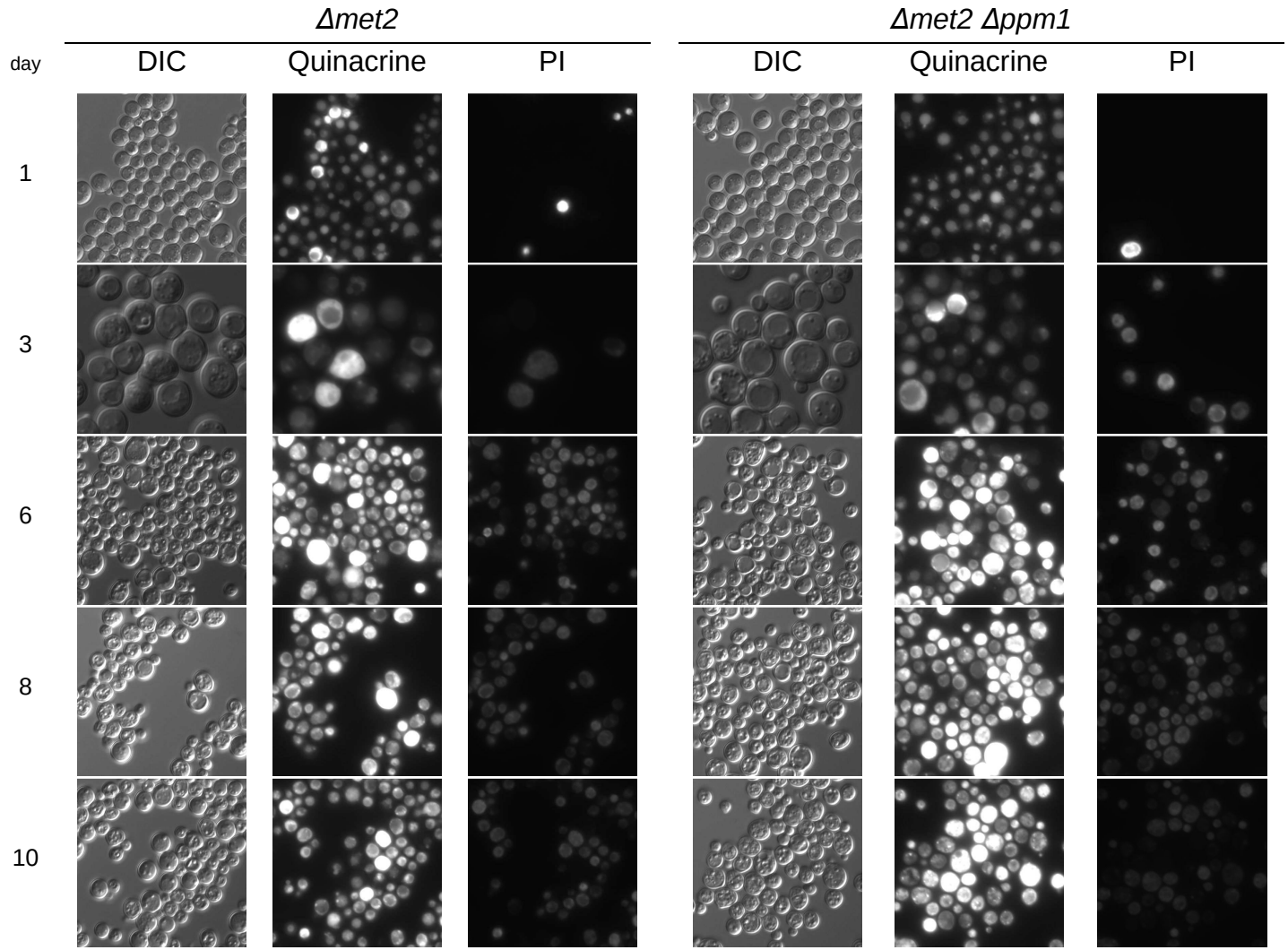

Figure 4.17: Deletion of *ppm1* in a *Δmet2* back ground indicates an earlier acidification of the cytoplasm compared to a *Δmet2* strain in media with 30 mg/l methionine. Quinacrine and PI double staining of a *Bya MET15 Δmet,* and *Bya MET15 Δmet2 Δppm1*. The ONC of the strain were inoculated in SMD with all amino acids to a cell count of $5*10^5$ cells and incubated at 28°C. After 24 hours the cells were shifted into SMD 30 mg/l methionine. On day one, three, six, eight and ten samples were taken and stained with quinacrine and PI. For the quinacrine images the eGFP filter (1000 ms) and for the PI images the dsRed filter (200 ms) were used.

A statistical analysis of the microscopy images of the vacuole stained cells (only acidic vacuole, not acidic cytoplasm), the bright cells, of the cells with a bright cytoplasm or which are partially bright and the PI positive cells was carried out (see Figure 4.18) by the two shift experiments. The percentage was calculated out of the total cell count from each measurement time point.

The results of the statistical analysis showed that the percentage of the vacuole stained cells was highest in the cells after the shift into SMD with 0 mg/l methionine (*Bya MET15 Δmet2* ~65%, *Bya MET15 Δmet2 Δppm1* ~70%) in contrast to the cells shifted into SMD with 30 mg/l methionine (*Bya MET15 Δmet2* and *Bya MET15 Δmet2 Δppm1:* ~60%) on day one. Cells in both treatments indicated nearly no bright cells (completely, cytoplasmatic or partially stained) or PI positive cells.

Under methionine restriction the count of the cells with an acidic vacuole of *Bya MET15 Δmet2* decreased continuously till day ten (nearly no cells with a vacuolar staining). The amount of cytoplasmatic or partially bright cells increased up to ~55% till day six. From day six till day ten the count of these cells decreased to less than ~30%. The bright cells and the PI positive cells increased up to ~50% till day ten. Comparing the curves of the bright and the PI positive cells, it seems that the bright cells correlated with the PI positive cells. Under methionine restriction cytoplasmatic or partially stained cells of *Bya MET15 Δmet2 Δppm1* increased up to ~70% from the first day till day ten. Till day six nearly no bright cells occurred. The amount of the bright cells increased to ~10% from day six till day ten. The PI positive cells increased to about 25% from day one till day ten. The amount of cells with an acidic vacuole was stable at about 70% on the first three days. From day three till day ten the count decreased till there were nearly no cells with a vacuolar staining left.

In the media with 30 mg/l methionine the amount of the cells with an acidic vacuole of *Bya MET15 Δmet2* decreased to about 10% till day six. The count of this phenotype remained at this level till day ten. The cytoplasmatic or partially bright cells increased up to 40% till day eight and decreased to ~30% till day ten. In the first three days there were nearly no bright cells. The amount of the bright cells rose up to ~20% till day six and decreased to ~10% till day ten. On day ten there were about 70% PI positive cells. The count of the cells with an acidic vacuole of *Bya MET15 Δmet2 Δppm1*

decreased continuously till day eight, where nearly no cells with a vacuolar staining were left. The amount of the cytoplasmatic or partially bright cells increased up to ~35% till day six and remained at this level till day eight. From day eight till day ten the cytoplasmatic or partially bright cells rose up to ~45%. In the first three days there were nearly no bright cells. The amount of the bright increased up to ~25% till day eight and decreased to ~10% till day ten. From the first day till day ten the amount of the PI positive cells rose up to 80%.

Comparing the results of the statistical analysis of the aging shift experiment in SMD with 0 mg/l methionine or 30 mg/l methionine with the aging shift experiment in the media with 0 mg/l methionine or leucine, a delay in the acidification of the cytoplasm occured in the Bya *MET15 Δmet2 Δppm1* strain shifted in media with 0 mg/l methionine or leucine compared to the *Bya MET15 Δmet2.* This delay did not occur after a shift in SMD with 30 mg/l methionine. *Bya MET15 Δmet2 Δppm1* cultured in media 30 mg/l methionine indicated similar results in the statistical analysis like *Bya MET15 Δmet2* in SMD with 30 mg/l methionine.

A. 0 mg/l methionine; *Δmet2*

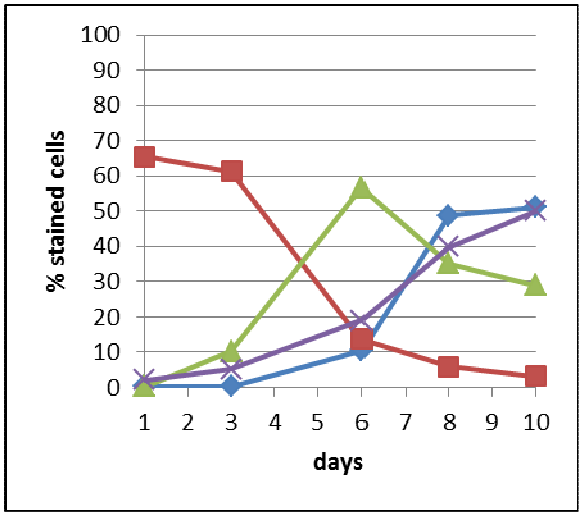

B. 30 mg/l methionine; *Δmet2*

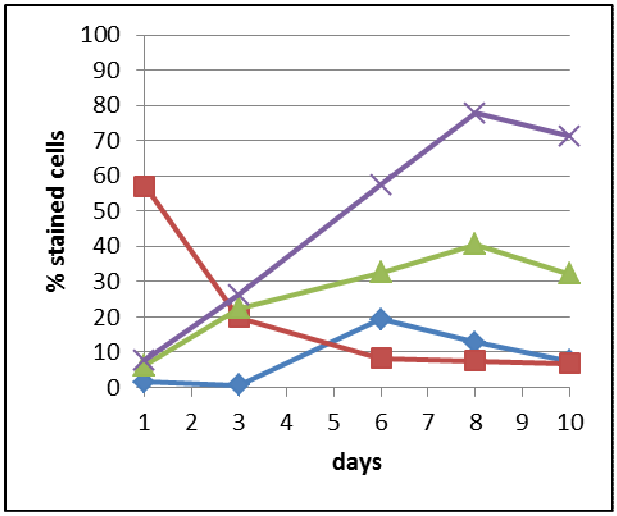

C. 0 mg/l methionine; *Δmet2 Δppm1*

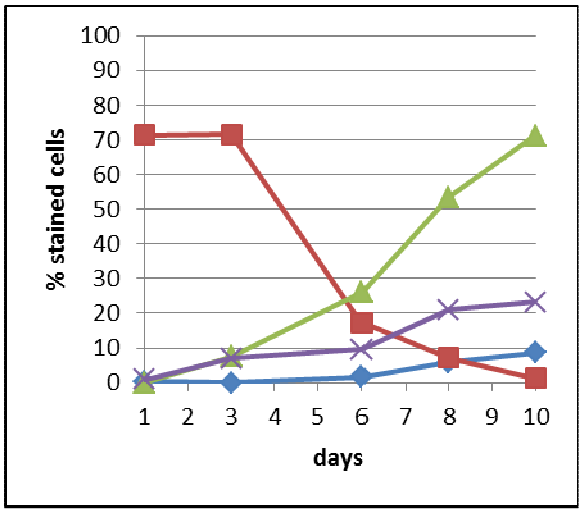

D. 30 mg/l methionine; *Δmet2 Δppm1*

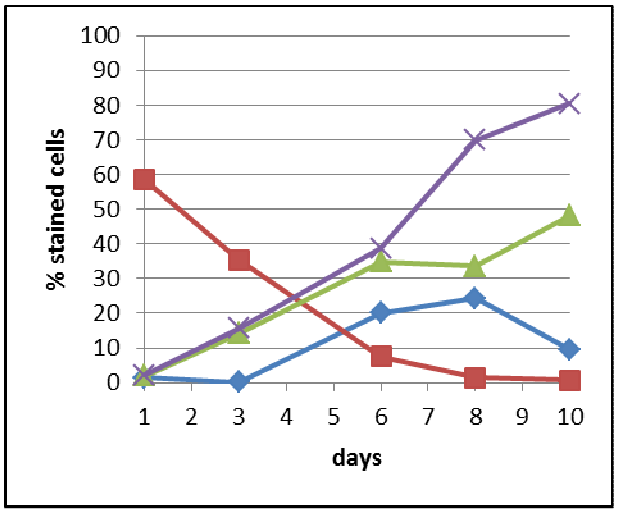

Figure 4.18: Deletion of *ppm1* in a *Δmet2* back ground indicates a time delay in the acidification of the cytoplasm compared to a *Δmet2* strain under methionine restriction. Statistical analysis of the microscopy images of the quinacrine stained *Bya MET15 Δmet2* and *Bya MET15 Δmet2 Δppm1* after a shift into SMD with 0 mg/l or 30 mg/ methionine. The red curve represents the percentage of the acidic vacuoles, the blue curve of the complete bright cells, the green curve of the cells with a bright cytoplasm or which are partially bright and the violet curve the PI positive cells out of the total cell count from each measurement time point. The cells have been counted with ImageJ.

4.7.1 Overexpression of *VMA1* and *VPH2* did not induce an increased cell death under complete methionine restriction

To prove if an overexpression-induced increase of vacuolar acidification lead to an increased cell death under methionine restriction a shift aging experiment was performed. Therefore *Bya MET15 Δmet2 pESC-HIS*-Vector, *Bya MET15 Δmet2 pESC-HIS-VMA1* and *Bya MET15 Δmet2 pESC-HIS-VPH2* were shifted into media with 0 mg/l or 3 mg/l methionine after 24 hours.

In both shifts (0 mg/l or 3 mg/l methionine) it seems that the overexpression of *VMA1* shows a better survival compared to the *Bya MET15 Δmet2 pESC-HIS*-Vector and *Bya MET15 Δmet2 pESC-HIS-VPH2* shows nearly the same survival compared to the control (see Figure 4.19)

A. 0mg/l methionine

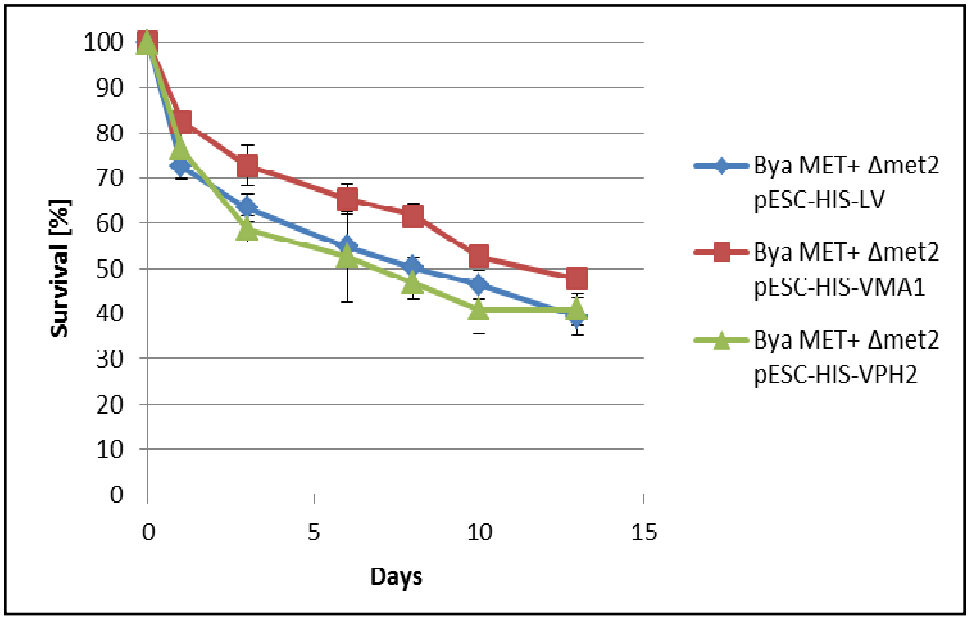

B. 3mg/l methionine

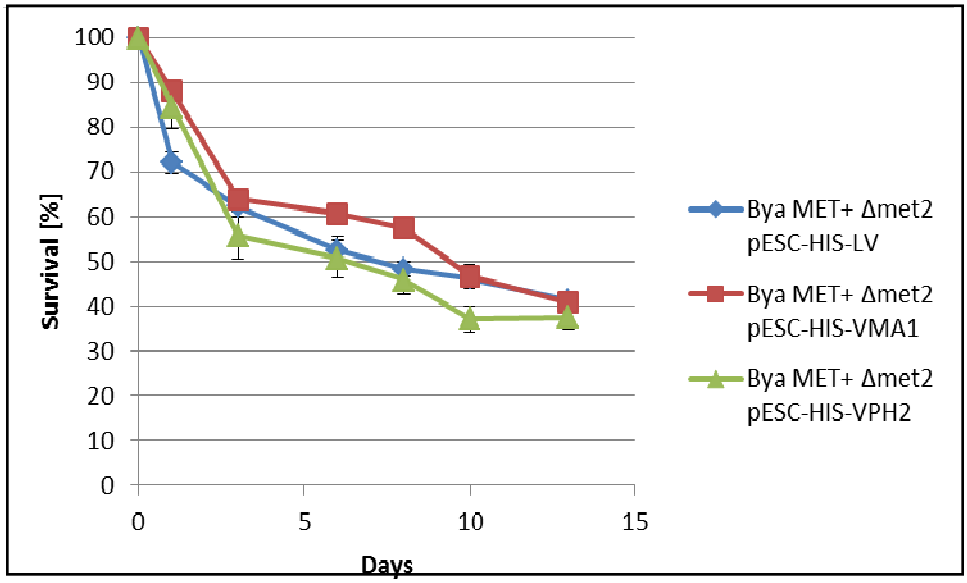

Figure 4.19: Overexpression of *VMA1* and *VPH2* did not induce an increased cell death under methionine restriction. The ONC of the strain were inoculated in SMD-HIS to a cell count of $5*10^5$ cells and incubated at 28°C. After 24 hours the cells were shifted into SMG-HIS with **A.** 0 mg/l or **B.** 3 mg/l methionine. The lifespan of the shifted chronological aged cells was determined through clonogenic cell survival assay. The cells were shifted into SMG to induce the promotor acivity as the pESC-HIS plasmid contains a galactose promotor. The data are representing the mean ± SEM (n= 6) of one representative experiment.

4.7.2 ER stress is not included in the cell death induced under complete methionine restriction

It is already known that *HAC1* and *IRE1* are involved in ER stress signalling. Therefore knock outs of *HAC1* and *IRE1* in a *Δmet2* strain were performed to prove if ER stress is involved in the cell death mechanism induced under complete methionine restriction. So *Bya MET15 Δmet2 Δhac1* and *Bya MET15 Δmet2 Δire1* were shifted into media with 0 mg/l or 30 mg/l methionine after 24 hours.

From day six it seemed that in both shift experiments *Bya MET15 Δmet2 Δhac1* indicated a regrowth and *Bya MET15 Δmet2 Δire1* and *Bya MET15 Δmet2* did not really show changes in the survival from this day on. (see Figure 4.20).

The shift experiment with 0 mg/l methionine *Bya MET15 Δmet2 Δhac1* and *Bya MET15 Δmet2 Δire1* indicated small positive effect in the survival compared to *Bya MET15 Δmet2.*

In contrast to this the shift experiment with 30 mg/l methionine only *Bya MET15 Δmet2 Δhac1* showed small positive effect in the survival compared to *Bya MET15 Δmet2.*

A. 0 mg/l methionine

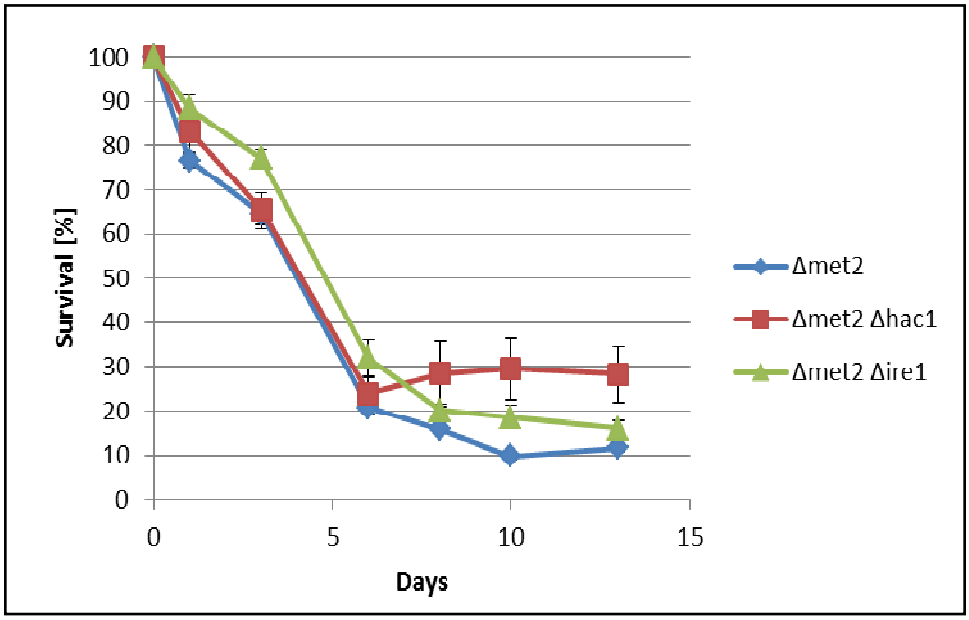

B. 30 mg/l methionine

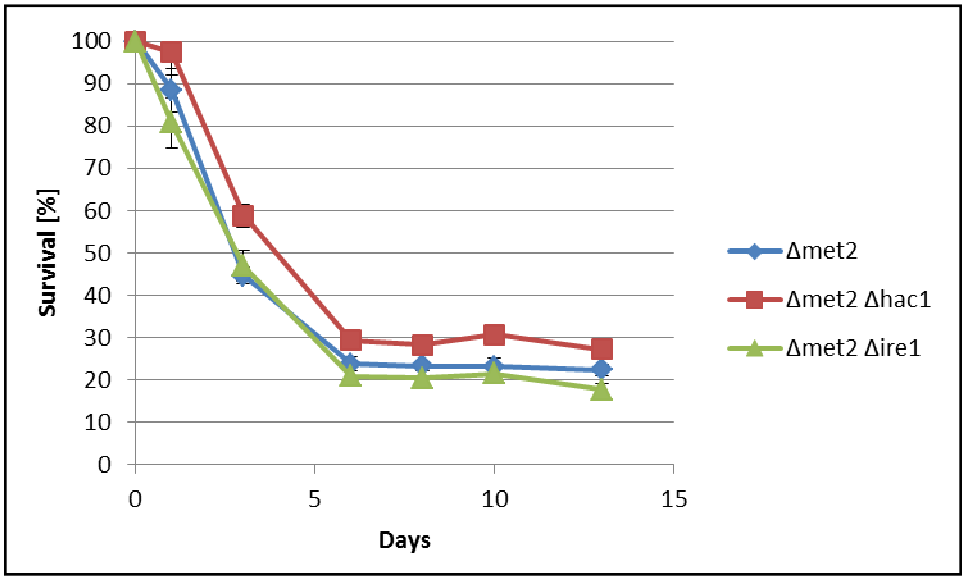

Figure 4.20: ER stress is not included in the cell death induced under complete methionine restriction. The ONC of the strain were inoculated in SMD with all amino acids to a cell count of $5*10^5$ cells and incubated at 28°C. After 24 hours the cells were shifted into SMD with **A.** 0 mg/l or **B.** 30 mg/l methionine. The lifespan of the shifted chronological aged cells was determined through clonogenic cell survival assay. The data are representing the mean ± SEM (n=4 to 6) of one representative experiment.

5. Discussion

A Western Blot analysis together with previous data indicated that the methionine auxotroph strains (*Δmet2* and *Δmet15*) showed an enhanced autophagy compared to a methionine-prototroph strain (*MET+*). In his paper “Lifespan extension by methionine restriction requires autophagy dependent vacuolar acidification” Christoph Ruckenstuhl verified that this enhanced autophagy is correlating with a chronological life span extension under methionine restriction. By experimenting with *ATG* knockouts he could further show that this effect is autophagy dependent, as the effect of lifespan extension under methionine restriction did only occur very limited in these knock outs.

Quinacrine fluorescence microscopy and their statistical analyses of the *Δmet2* strain pointed out that there was a higher acidification of the vacuole under methionine restriction. This enhancement was autophagy dependent, as a knockout of *ATG5* in a *Δmet2* strain led to a decrease of the vacuolar acidification. The microscopy images of the quinacrine staining of the *Δmet2 Δatg5* strain showed that the cells do not only possess a vacuole staining, they further had a cytoplasmatic staining. An overexpression of *VMA1* or *VPH2*, which are both part of the v-ATPase and are important for the vacuolar pH homeostasis, led to an increased acidification of the vacuole. The v-ATPases are the vacuolar proton pumps and are H^+ ATPases that obtain their energy from ATP hydrolysis to transport H^+ through the membrane. (Martínez-Muñoz et al. 2008; Kane 2006; Hirata et al. 1990) Further it was shown in *Schizosaccharomyces pombe* that an overexpression of *VMA1* leads to a maintenance of the acidification of the vacuole and an increased chronological lifespan. (Stephan et al. 2013)

A deletion of *VPH2* led to a decrease of the chronological life span under methionine restriction (Ruckenstuhl et al. 2014). Other studies showed that the vacuolar acidification is necessary for the degradation of the autophagic bodies (Nakamura et al. 1996). Hughes and Gottschling (2012) demonstrated that the vacuolar pH is linked with the mitochondrial function. They further showed that the overexpression of *VMA1* or *VPH2* supressed age-induced mitochondrial dysfunction and enhanced vacuolar acidification in budding yeast.

These data suggest that methionine restriction enhances the vacuolar acidification and that this enhancement is autophagy dependent.

The TOR (target of rapamycin) signalling pathway is known to inhibit autophagy when active. The protein phosphatase 2A (*PP2A*) is required for the TOR kinase activity. Under nutrient rich conditions *TOR* is active and phosphorylates *Tap42*. The phosphorylated *Tap42* binds the catalytic subunit of *PP2A*. Under starvation *TOR* is inactive and *Tap42* is dephosphorylated. Therefore *PP2A* dissociates of *Tap42* and is methylated. A further component of the TOR signalling pathway is *SCH9*. It can interact with *Tap42* too. When *PP2A* is associated with *Tap42*, *SCH9* is phosphorylated. (Zabrocki et al. 2002) However, *TOR* is able to phosphorylate *SCH9.* (Bielinski et al. 2007)

Deletion of *CDC55* (part of the regulatory subunit of PP2A), *SCH9* or *TOR1* in a *Δmet2* strain showed an increased survival compared to the *Δmet2* strain under both conditions in SMD without or with 30 mg/ml methionine.

It has been reported that *TORC1* and *SCH9* are involved in the regulation of longevity, stress resistance and genomic stability. It was further indicated that the TOR signalling pathway is involved in the regulation of the protein kinase Rim15p and Msn2/4p. An inactivation of *TORC1* leads to an inactivation of *SCH9*. This causes a phosphorylation of Rim15p. The phosphorylated Rim15p activates Mns2/4p and Gis1p, which are stress response transcription factors and mediators for life span extension. This leads to an induction of autophagy. (Wei et al. 2009, Yorimitsu et al. 2007)

Further it was indicated that the *PP2A* regulates the phosphorylation of *S6K* and *Akt*, which are both homologous of SCH9. (Bielinski et al. 2007, Andrabi et al. 2007)

Bielinski et al. (2007) showed in *Drosophila* that a deletion of the catalytic subunit of *PP2A* leads to an increase of the phosphorylation of *SCH9*. However, a knock out of the regulatory subunit of *PP2A* or *Tap42* did not enhance the phosphorylation of *SCH9*. So it can be concluded that *PP2A* is important for the dephosphorylation of *SCH9*.

The results of Andrabi et al. (2007) suggested that Akt is not only a pro survival but also a pro death protein. This depends on the function of PP2A and the signals of the environment.

Taking these results together, it seems that the better survival of the knock outs of the TOR pathway is caused by an induction of autophagy.

A Western Blot analysis and fluorescence microscopy indicated in *Bya MET15 chr. Atg8-GFP Δppm1* a free GFP signal, and thus autophagic activity, only on day one. In contrast to this *Bya MET15 chr. Atg8-GFP Δpph21* showed a higher free GFP signal compared to the wild type strain on day 1 and nearly the same was detected on day two and three. However, this signal decreased on day five.

Ruckenstuhl et al. (2014) speculated that there could be another mechanism in autophagy regulation, beside the PP2A dependent one: a methionine independent mechanism, where high acetate levels could possibly block autophagy on day one. *MET15* indicated ~80% higher acetate levels as *Δmet2* and *Δmet15* on this day. On day two, *MET15* showed nearly the same acetate levels as *Δmet2* and lower levels as *Δmet15.*

In a chronological survival assay a *Bya MET15 chr. Atg8-GFP Δppm1* strain did not show a better survival compared to the *Bya MET15* strain. The deletion of *PPH21* indicated only a positive effect in the survival in the first eight days.

It has already been shown that methionine is a repressor of autophagy. Further the cell growth is promoted, because of a SAM (S-adenosylmethionine) mediated methylation of *PP2A* by the methyltransferase *PPM1*. It is suggested that a demethylation of *PP2A* leads to a dephosphorylation of substrates that lead to an enhancement of autophagy. Additionally it is shown that the methylation of *PP2A* depends on the intracellular SAM and methionine levels. Therefore *PP2A* is a sensor of the metabolic state and is able to trigger the appropriate cellular response. (Sutter et al. 2013)

The deleted *PPH21* can be replaced by *PPH22*. However, it was discovered that not all of the *PPH21* functions were replaced. *PPM1* methylates the catalytic subunit of *PP2A.* So in the knockout of *PPH21, PPM1* is not able to methylate *PPH21*, which might lead to a lower methylation of *PP2A*, which leads to the enhanced autophagy in *Bya MET15 chr. Atg8-GFP Δpph21.*

It has been already shown that a deletion of *PPM1* leads to an increase of ~50% of the association of the catalytic subunit of PP2A with Tap42. (Wu et al. 2000) This findings could be the reason why *Bya MET15 chr. Atg8-GFP Δppm1* showed only autophagic activity on day one.

Further I was able to verify that shifting *Δmet2* cells in media without methionine led additionally to the vacuolar acidification to an acidification of the cytoplasm after prolonged incubation. Therefore these cells might be dead, although they do not show necrotic cell death marker. As methionine restriction in a *Δmet2* strain led to an in-

creased autophagy, it might be that the cytoplasmatic acidification is caused by to high autophagy levels, which might lead to a disturbance of the cytosolic and vacuolar pH homeostasis and thus to cell death.

The results indicate that there is a chronological order of the phenotypes of this cell death mechanism under complete methionine restriction. First the cells showed an acidic vacuole. Afterwards the cells indicated a bright cytoplasm and the vacuoles were not stained anymore. Next the whole cells got bright/acidic. Only some of these bright cells were PI positive. The count of the PI positive cells increased. The bright cells were most likely dead (by comparing to clonogenic survival data), presumably because of an acidification of the cytoplasm. However, the plasma membrane remained stable and therefore the cells were not PI positive. It seems that methionine is necessary for the destabilization of the plasma membrane or that methionine is involved in a methylation pathway, which is utilized for the destabilization of the plasma membrane.

It is thought that an overexpression of *VMA1* or *VPH2*, which are necessary for the vacuolar acidification, might lead to an increased cell death compared to the control strain. However, in our setup the cells did not show an increased cell death under complete methionine restriction as expected. The *VPH2* overexpression showed nearly the same survival as the control strain and it seems that overexpression of *VMA1* indicated a small positive effect in the survival. Nevertheless, we do not know if this effect occurs under normal cell death conditions too. Fang et al. (2013) showed that *PPP2R2B*, which is the brain specific regulatory subunit B of *PP2A*, is involved in autophagic cell death induced under starvation and ER stress. However, the knockout of *IRE1* and *HAC1* in a *Δmet2* background did only show a small positive effect in the survival compared to the *Δmet2* strain. Therefore we can conclude that ER stress is not involved in the cell death induced by high acidification of the cell.

Concluding it can be stated that methionine restriction enhances the autophagy mediated acidification of the vacuole and therefore promotes lifespan extension in budding yeast. On the other hand high autophagy levels under complete methionine restriction might trigger a specific cell death mechanism, in which PP2A and Sch9p are involved.

Further experiments should determine the role of PP2A, Tap42p and Sch9p in autophagy under methionine restriction to possibly decipher this specific cell death mechanism.

6. Attachment

A. 0 mg/l methionine

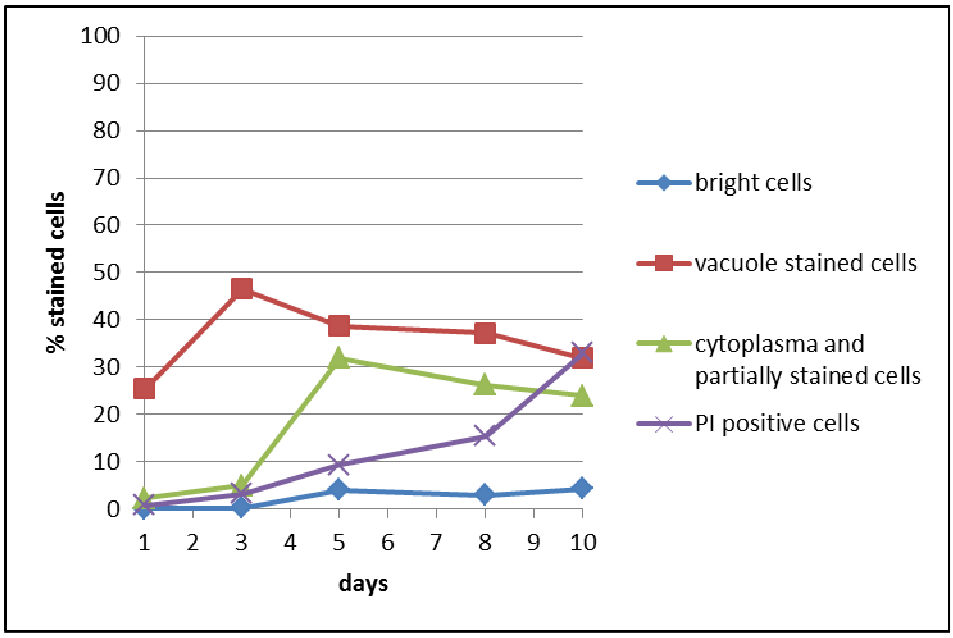

B. 0 mg/l leucine

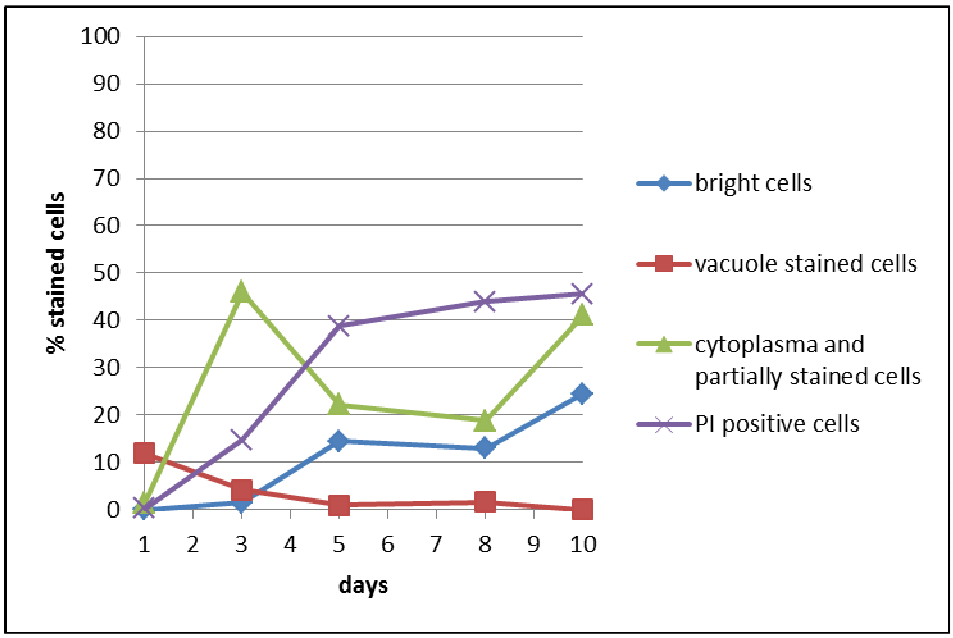

Figure 6.1: Deletion of *rts1* in a *Δmet2* back ground indicates an extended vacuolar acidification in media with 0 mg/l methionine (A) compared to media with 0 mg/l leucine (B). Statistical analysis of the microscopy images of the quinacrine stained *Bya MET15 Δmet2 Δrts1* after a shift into SMD with 0 mg/l methionine or 0 mg/l leucine. The red curve represents the percentage of the acidic vacuoles, the blue curve of the complete bright cells, the green curve of the cells with a bright cytoplasm or which are partially bright and the violet curve the PI positive cells out of the total cell count from each measurement time point. The cells have been counted with ImageJ.

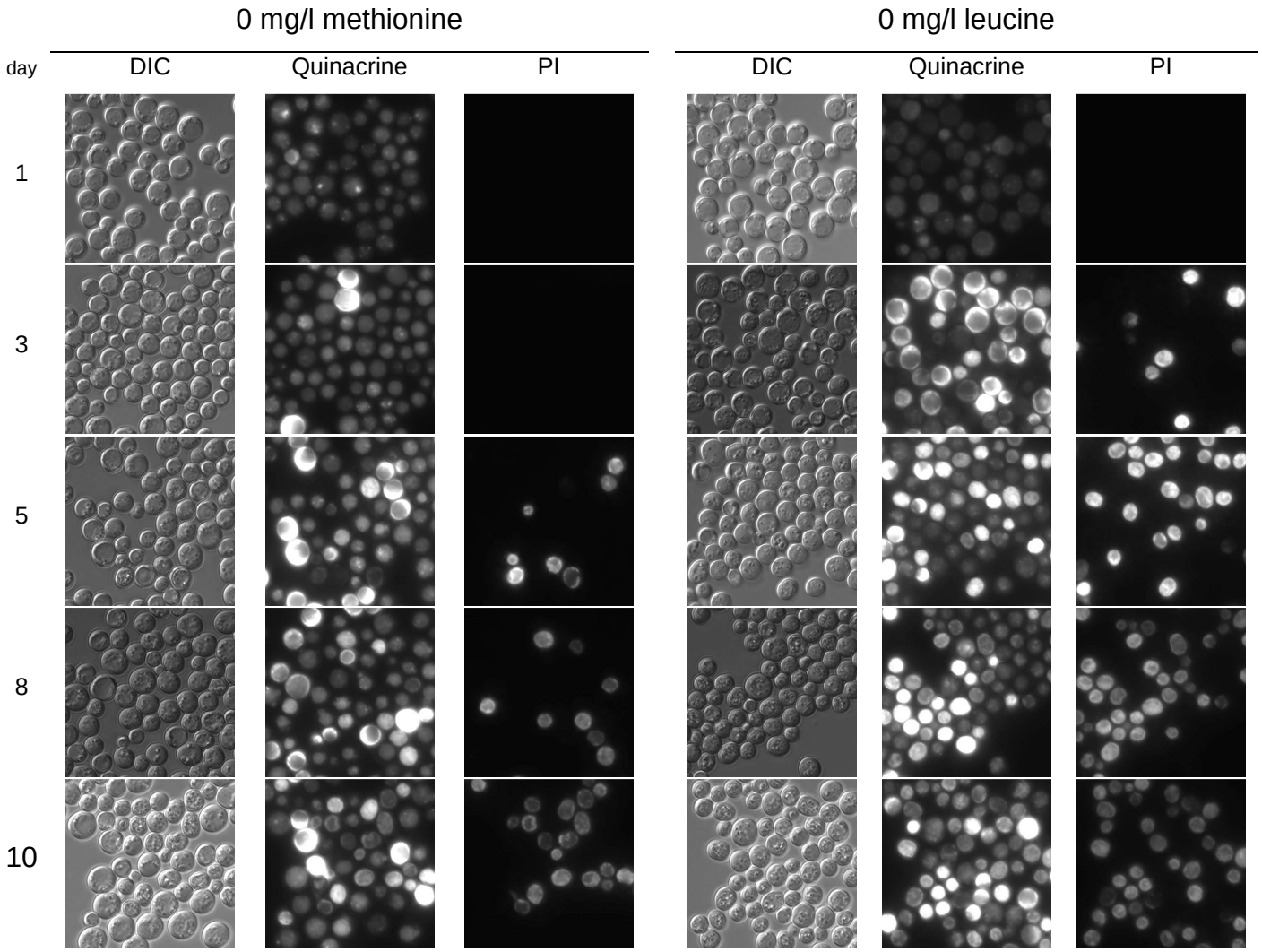

Figure 6.2: Deletion of *rts1* in a *Δmet2* back ground indicates an extended vacuolar acidification in media with 0 mg/l methionine compared to media with 0 mg/l leucine. Quinacrine and PI double staining of *Bya MET15 Δmet2 Δrts1*. The ONC of the strain were inoculated in SMD with all amino acids to a cell count of $5*10^5$ cells and incubated at 28°C. After 24 hours the cells were shifted into SMD 0 mg/l methionine or 0 mg/l leucine. On day one, three, five, eight and ten samples were taken and stained with quinacrine and PI. For the quinacrine images the eGFP filter (1000 ms) and for the PI images the dsRed filter (200 ms) were used.

7. Abbreviations

µg	Microgram
µl	Microliter
AIF	Apoptosis inducing factor
AMP	Adenosine monophosphate
AMPK	5'AMP activated kinase
Ams1	α-mannosidase
Ape1	Aminopeptidase 1
Atg	Autophagy related
ATP	Adenosine triphosphate
cAMP	cyclic adenosine monophosphate
bp	Base pair
BSA	Bovine serume albumin
CAPS	N-cyclohexyl-3-aminopropanesulfonic acid
cfu	Colony forming units
CR	Caloric restriction
Cvt	Cytoplasm to vacuole targeting
ddH2O	Double destilled water
DIC	Differential interference contrast microscopy
DNA	Deoxyribonucleic acid
dNTP	Desoxy nucleotide triphosphate
dsRED	RED fluorescing protein drFP583 from *Discosoma*
EDTA	Ethylenediaminetetraacetic acid
ECL	Enhanced chemiluminescence
eGFP	enhanced green fluorescent protein
ER stress	Endoplasmic reticulum stress
GAP	GTPase activating protein
GAPDH	Glyceraldehyde 3-phosphate dehydrogenase
GFP	Green fluorescent protein
GSH	Glutathione
GSSG	Glutathione-disulfide (oxidized form)
GTP	Guanosine triphosphate
HIS	Histidine

IGF-I	Insulin-like growth factor 1
IM	Isolation membrane
kDa	Kilo dalton
mA	Milli ampere
ml	Milliliter
mM	Millimolar
MIF	Macrophage migration inhibitory factor
OD	Optical density
ONC	Overnight culture
PAS	Pre-autophagosomal structure or phagophore assembling site
PBS	Phosphate buffered saline
PCR	Polymerase chain reaction
PE	Phosphatidyl ethanolamine
PEG	Polyethylene glycol
PI	Propidiumiodide
PI3K	Phosphatidylinositol 3-kinase
PKA	Protein kinase A
PKB	Protein kinase B
PP2A	Protein phosphatase 2A
preApe1	Precursor of aminopeptidase 1
ROS	Reactive oxygen species
rpm	Revolutions per minute
SAM	S-adenosyl methionine
SDS	Sodium dodecyl sulfate
SEM	Standard error of the mean
SMD	Synthetic minimal medium with glucose
SMG	Synthetic minimal medium with galactose
Snf1	Sucrose non-fermenting
TAE	Tris acetate EDTA buffer
TBS (T)	Tris buffered saline (with Tween)
TEMED	N,N,N,N’-Tetramethylethylenediamine
TRIS	Tris(hydroxymethyl)aminomethane
TST	Tris saline buffer with Tween
TOR	Target of rapamycin

TORC1	TOR complex 1
TORC2	TOR complex 2
TSC complex	Tuberous sclerosis complex
Ura	Uracil
v-ATPase	Vacuolare proton-translocating ATPass
YPD	Yeast peptone dextrose

8. References

Andrabi, S., Gjoerup, O. V., Kean, J. A., Roberts, T. M., Schaffhausen, B. 2007. Protein phosphatase 2A regulates life and death decisions via Akt in a context-dependent manner. *PNAS 104 (48):19011–19016.* 2007.

Balaban, R. S., Nemoto, S., Finkel, T. 2005. Mitochondria, oxidants, and aging. *Cell.; 120(4):483-95.* 2005.

Bielinski, V. A., Mumby, M. C. 2007. Functional analysis of the *PP2A* subfamily of protein phosphatases in regulating Drosophila S6 kinase. *Exp.Cell Res. 313, 3117–3126.* 2007.

Budovskaya, Y. V., Stephan, J. S., Deminoff, S. J., Herman, P. K. 2005. An Evolutionary Proteomics Approach Identifies Substrates of the cAMP-dependent Protein Kinase. *Proceedings of the National Academy of Sciences of the United States of America 102 (39) (September 27): 13933–13938. doi:10.1073/pnas.0501046102.* 2005.

Cellarier, E., Durando, X., Vasson, M. P., Farges, M. C., Demiden, A., Maurizis, J. C., Madelmont, J. C., Chollet, P. 2003. Methionine dependency and cancer treatment. *Cancer Treatment Reviews 29, 489-499.* 2003.

Chan, S. Y., Appling, D. R. 2003. Regulation of S-Adenosylmethionine Levels in Saccharomyces cerevisiae. *Journal of Biological Chemistry 278, 43051-43059.* 2003.

Fang, K., Li, H. F., Hsieh, C. H., Li, D. Y., Song, D. C., Cheng, W. T., Guo, Z. X. 2013. Differential autophagic cell death under stress with ectopic cytoplasmic and mitochondrial-specific PPP2R2B in human neuroblastoma cells. *Apoptosis 18:627–638.* 2013.

Fontana, L., Partridge, L., Longo, V. D. 2010. Dietary Restriction, Groth Factors and Aging: from yeast to humans. *Science (New York, N.Y.) 328 (5976) (April 16): 321–326.doi:10.1126/science.1172539.* 2010.

Gerson, H., Gerson, D. 2000. The budding yeast, *Saccharomyces cerevisiae*, as a model for aging research: a critical review. *mechanisms of aging and development 120 (2000) 1-22.* 2000.

Hay, N., Sonenberg, N. 2004. Upstream and Downstream of mTOR. *Genes & Development 18 (16) (August 15): 1926–1945. doi:10.1101/gad.1212704.* 2004.

He, C., Klionsky, D. J. 2009. Regulation Mechanisms and Signaling Pathways of Autophagy. *Annu. Rev. Genet. 43, 67-93.* 2009.

Hedbacker, K., Carlson, M. 2008. SNF1/AMPK Pathways in Yeast. *Frontiers in Bioscience : a Journal and Virtual Library 13 (January 1): 2408–2420.* 2008.

Hirata, R., Ohsumk, Y., Nakano, A., Kawasaki, H., Suzuki, K., Anraku, Y. 1990. Molecular structure of a gene,*VMA1*, encoding the catalytic subunit of H-translocating adenosine triphosphatase from vacuolar membranes of *Saccharomyces cerevisiae*. *J. Biol. Chem. 265, 6726–6733.* 1990.

Huang, W., Klionsky, D. J. 2002. Autophagy in yeast: a review of the molecular machinery. *Cell Struct. Funct 27, 409-420.* 2002.

Hughes, A. L., Gottschling, D. E. 2013. An Early-Age Increase in Vacoular pH Limits Mitochondrial Function and Lifespan in Yeast. *Nature. Author manuscript; available in PCM 2013 June 13.* 2013.

Kane, P. M. 2006. The Where, When, and How of Organelle Acidification by the Yeast Vacuolar H+-ATPase. *Microbiol Mol Biol Rev.; 70(1): 177–191.* 2006.

Kane, P. M., Parra, K. J. 2000. Assembly and Regulation of the Yeast Vacuolar H(+)-ATPase. *The Journal of Experimental Biologie 203, 81-87.* 2000.

Kapahi, P., Chen, D., Rogers, A. N., Katewa, S. D., Li, P. W.-L., Thomas, E. L., Kockel, L. 2010. With TOR, Less Is More: A Key Role for the Conserved Nutrient-Sensing TOR Pathway in Aging. *Cell Metabolism 11, 453-465.* 2010.

Klionsky, D. J., Herman, P. K., Emr, S. D. 1990. The Fungal Vacuole: Composition, Function, and Biogenesis. *Microbiological Reviwes, Sept. 1990, p. 266-292.* 1990.

Krijt, J., Dutá, A. & Kozich, V. 2009. Determination of S-Adenosylmethionine and SAdenosylhomocysteine. *J. Chromatogr. B Analyt. Technol. Biomed. Life Sci 877, 2061-2066.* 2009.

Lafaye, A., Junot, C., Pereira, J., Lagniel, G., Tabet, J.-C., Ezan, E., Labarre, J. 2005. Combined Proteome and Metabolite-profiling Analyses Reveal Surprising Insights into Yeast Sulfur Metabolism. *Journal of Biological Chemistry 280, 24723-24730.* 2005.

Levine, B., Klionsky, D. J. 2004. Development by Self-Digestion: Molecular Mechanisms and Biological Functions of Autophagy. *Developmental Cell, Vol. 6, 463–477, .* 2004.

Li, S. C., Kane, P. M. 2009. The Yeast Lysosome-like Vacuole: Endpoint and Crossroads. *Biochim Biophys Acta. 2009 April; 1793(4): 650-663. doi:10.1016/j.bbamer.2008.08.003.* 2009.

Martínez-Muñoz, G. A., Kane, P. 2008. Vacuolar and Plasma Membrane Proton Pumps Collaborate to Achieve Cytosolic pH Homeostasis in Yeast. *J Biol Chem. 283(29):20309-19.* 2008.

McEwan, D. G., Dikic, I. 2011. The Three Musketeers of Autophagy: Phosphorylation, Ubiquitylation and Acetylation. *Trends in Cell Biology 21 (4) (April): 195–201.doi:10.1016/j.tcb.2010.12.006.* 2011.

Miller, R. A., Buehner, G., Chang, Y. Harper, J. M., Sigler, R., Smith-Wheelock, M. 2005. Methionine-deficient diet extends mouse lifespan, slows immune and lens aging, alters glucose, T4, IGF-I and insulin levels, and increases hepatocyte MIF levels and stress resistance. *Aging Cell 4, 119-125.* 2005.

Minguet, E. G., Vera-Sirera, F., Marina, A., Carbonell, J. & Blázquez, M. A. 2008. Evolutionary diversification in polyamine biosynthesis. *Mol. Biol. Evol 25, 2119-2128.* 2008.

Nair, U., Klionsky, D. J. 2005. Molecular Mechanisms and Regulation of Specific and Nonspecific Autophagy Pathways in Yeast. *Journal of Biological Chemistry 280, 41785-41788.* 2005.

Nakamura, N., Matsuura, A., Wada, Y., Ohsumi, Y. 1997. Acidification of Vacuoles Is Required for Autophagic Degradation in the Yeast, Saccaromces cerevisiaae. *J. Biochem121, 338-344.* 1997.

Orentreich, N., Matias, J. R., DeFelice, A., Zimmerman, J. A. 1993. Low methionine ingestion by rats extends life span. *J. Nutr 123, 269-274.* 1993.

Pamplona, R., Barja, G. 2006. Mitochondrial oxidative stress, aging and caloric restriction: the protein and methionine connection. *Biochim. Biophys. Acta 1757, 496-508.* 2006.

Pennickx, M. J. 2002. An overview on gluthione Saccharomyces versus non-conventional yeasts. *FEMS Yeast Research 2 295-305.* 2002.

Plant, P. J., Manolson, M. F., Grinstein, S., Demaurex, N. 1999. Alternative Mechanisms of Vacuolar Acidification in H(+)-ATPase-deficient Yeast. *Journal of Biological Chemistry, vol. 274, no. 52, p. 37270-9.* 1999.

Richie, J. P., Leutzinger, Y.., Parthasarathy, S., Malloy, V., Orentreich, N., Zimmerman, J. A. 1994. Methionine restriction increases blood glutathione and longevity in F344 rats. *FASEB J 8, 1302-1307.* 1994.

Ruckenstuhl, C., Netzberger, N., Entfellner, I., Camona-Gutierrez, D., Kickenweiz, T., Stekovic, S., Gleixner, C., Klug, L., Sorgo, A. G., Eisenberg, T., Büttner, S., Marino, G., Konziel, R., Jansen-Dürr, P., Fröhlich, K.-U., Froemer, G., Madeo, F. 2014. Lifespan Extension by Methionine Restriction Requires Autophagy-Depend Vacuolar Acidification. *PloS Genet 10(5): e1004347. doi:10.1371/journal.pgen.1004347.* 2014.

Sanz, A., Caro, P., Ayala, V., Portero-Otin, M., Pa,plona, R., Barja, G. 2006. Methionine restriction decreases mitochondrial oxygen radical generation and leak as well as oxidative damage to mitochondrial DNA and proteins. *FASEB J 20, 1064-1073.* 2006.

Stephan, J., Franke, J., Ehrenhofer-Murray A. E. 2013. Chemical genetic screen in fission yeast reveals roles for vacuolar acidification, mitochondrial fission, and cellular GMP levels in lifespan extension. *Aging Cell 12, pp574–583.* 2013.

Sun, L., Sadighi Akha, A. A., Miller, R. A., Harper, J. M. 2009. Life-Span Extension in Mice by Preweaning Food Restriction and by Methionine Restriction in Middle Age. *The Journals of Gerontology Series A: Biological Sciences and Medical Sciences 64A, 711-722.* 2009.

Sutter, B. M., Wu, X., Laxman, S., Tu, B. P. 2013. Methionine inhibits autophagy and promotes growth by inducing the SAM-responsive methylation of *PP2A*. *Cell 154, 403–415.* 2013.

Suzuki, K., Ohsumi, Y. 2007. Molecular machinery of autophagosome formation in yeast, Saccharomyces cerevisiae. *FEBS Lett 581, 2156-2161.* 2007.

Tang, F., Watkins, J. W., Bermudez, M., Gray, R., Gaban, A., Portie, K., Grace, S., Kleve, M., Craciun, G. 2008. A life-span extending form of autophagy employs the vacuole-vacuole fusion machinery. *Autophagy 4, 874-886.* 2008.

Teter, S. A., Klionsky. D. J. 2000. Transport of proteins to the yeast vacuole: autophagy, cytoplasm-to-vacuole targeting, and role of the vacuole in degradation. *Semin Cell Dev Biol.; 11(3):173-9.* 2000.

Thomas, D., Surdin-Kerjan, Y. 1997. Metabolism of sulfur amino acids in Saccharomyces cerevisiae. *Microbiol. Mol. Biol. Rev 61, 503-532.* 1997.

Todde, V., Veenhuis, M., van der Klei, I. J. 2009. Autophagy: principles and significance in health and disease. *Biochim. Biophys. Acta 1792, 3-13.* 2009.

Tsujimoto, Y., Shimizu, S. 2005. Another way to die: autophagic programmed cell death. *Cell Death Differ 12, 1528-1534.* 2005.

Urban, J., Soulard, A., Huber, A., Lippman, S., Mukhopadhyay, S., Deloche, O., Wanke, V., Anrather, D., Ammerer, G., Riezmann, H., Broach, J. R., De Virgilio, C., Hall, M. N., Loewith, R. 2007. *Sch9* Is a Major Target of *TORC1* in *Saccharomyces cerevisiae*. *Molecular Cell 26 (5) (June 8): 663–674.doi:10.1016/j.molcel.2007.04.020.* 2007.

Wei, M., Fabrizio, P., Hu, J., Ge, H., Cheng, C., Li, L., Longo, V. D. 2008. Life Span Extension by Calorie Restriction Depends on *Rim15* and Transcription Factors Downstream of Ras/PKA, Tor, and Sch9. *PLoS Genet.; 4(1): e13.* 2008.

Wei, M., Fabrizio, P., Madia, F., Hu, J., Ge, H., Li, L. M., Longo, V. D. 2009. *Tor1/Sch9*-Regulated Carbon Source Substitution Is as Effective as Calorie Restriction in Life Span Extension. *PLoS Genet 5(5): e1000467. doi:10.1371/journal.pgen.1000467.* 2009.

Wu, J., Tolstykh, T., Lee, J., Boyd, K., Stock, J. B., Broach, J. R. 2000. Carboxyl methylation of the phosphoprotein phosphatase 2A catalytic subunit promotes its functional association with regulatory subunits in vivo. *The EMBO Journal Vol. 19 No. 21 pp. 5672-5681.* 2000.

Wullschleger, S., Loewith, R., Hall, M. N. 2006. TOR Signaling in Growth and Metabolism. *Cell 124, 471-484.* 2006.

Yorimitsu, T., Klionsky, D. J. 2005. Autophagy: molecular machinery for self-eating. *Cell Death Differ 12 Suppl 2, 1542-1552.* 2005.

Yorimitsu, T., Zaman, S., Broach, J. R., Klionsky D. J. 2007. Protein Kinase A and *Sch9* Cooperatively Regulate Induction of Autophagy in Saccharomyces cerevisiae. *Mol Biol Cell.; 18(10): 4180–4189.* 2007.

Zabrocki, P., Van Hoof, C., Goris, J., Thevelein, J. M., Winderickx, J., Wera, S. 2002. Protein phosphatase 2A on track for nutrient-induced signalling in yeast. *Molecular Microbiology 43(4), 835-842.* 2002.